博士論文

Risk Assessment and Fatigue Life Prediction of RC Deck by Utilizing Survival Analysis and Full Scale Numerical Simulation

（生存時間解析とフルスケール数値解析を用いた RC 床版のリスク評価と疲労寿命解析）

Fang Jie

房　捷

Department of Civil Engineering

The University of Tokyo

A thesis submitted in partial fulfillment of the requirements for the degree of

Doctor of Engineering

Abstract

Large numbers of bridges were constructed during the periods of high economic growth in Japan. Nowadays, performance degradation have been widely found in reinforced concrete (RC) bridge deck slabs after almost fifty years of usage. In order to maintain these structures and ensure safety, a rational bridge deck slab maintenance system are need. Not only the overall deterioration feature, but also detailed deterioration process and mechanism is essential. As a first step, the Ministry of Land, Infrastructure, Transportation and Tourism (MLIT) announced an inspection system on 1 July 2014, which offers an opportunity for statistical analysis. A method called survival analysis has been used to analyze the bridge inspection data and the fundamental idea comes from medicine (Yamazaki and Ishida, 2015). On the other hand, the study of deterioration process and simulation for individual bridge also carried out at same time. The fatigue loading test under wheel load were conducted by Matsui sensei (Maeda and Matsui, 1984). Then in order to quantify the mechanism of the fatigue failure, instead of the two dimensional beam model, the three-dimensional fatigue simulation of RC slabs under traveling wheel load has been developed (Maekawa et al, 2006).

But still there were some problem existing in the previous study. For survival analysis, part of the results remained ambiguous and inconsistency results have been found in univariate and multivariate analysis. Therefore, appropriate data processing should be conducted in order to clarify the deterioration characteristics of each area and distinguish between high risk areas and low risk areas. For numerical simulation, the fatigue analysis only applied the load on the middle of a simple RC slab plate. In the actual situation, as the loading position changes, the distance between the load and the girder also changes, and it will directly affect the fatigue life. Additionally, since the actual structure is more complicated, the size, shape and boundary condition is totally different comparing with simple plate, the strain and stress distribution, displacement and moment is also different. Therefore, full scale numerical simulation should be used to get more accurate result. Additionally, based on the deterioration process, the limitation of survival analysis should be checked by comparing the result of both methods and the necessary information which can be used to improving the accuracy of inspection and survival analysis to be clarified.

Generally speaking, for the basic definition of survival analysis, one object can only have one survival time and survival state. However, according to the data processing from previous research, if one slab has been inspected multiple times, the continuous inspection record was treated as several independent data which violates the basic law. Therefore, data processing, including data cleaning and data selection should be appropriately conducted. In this research, each continuous observation of individual object was first treated as a datum, and pre-survival time was calculated. Then amount these data, one pre-survival time was selected as the true

survival time. Moreover, univariate and multivariate inconsistencies caused by high correlation between variables are also modified by reducing the correlation of each variables to 0.5.

By conducting data processing and reanalyzing, the deterioration characteristics of different regions were clarified. Reduplicative dynamic traffic load was a major reason for the deterioration of bridge deck slabs in the Tokyo region. Correspondingly, thicker slabs had much greater loading capacity; therefore, a decreased hazard ratio was evident. Existence of water also shows some effects. Water flow is faster for slabs with greater slopes; thus, the hazard ratio tends to be smaller. For East Japan, the traffic volume is not a main deterioration reason since the traffic volume and hazard ratio is relatively small. Through the analysis, the result shows high deterioration risks in the severe winter environment region, including rainy and snowy weather, low temperature, less sunshine hour. Additionally, during the extended snow melting process, the water with a lot of chloride ions penetrates into cracks and accelerates the deterioration process. Rebar is corroded and slab is seriously damaged unless there is appropriate protection and repair work. Using geographical coordinate information, risk scores and environment hazard map were made; distinctions between high-risk and low-risk areas were clearly shown. Especially in the mountainous area of Yamagata Prefecture, combine with the large amount usage of de-icing salt, the deterioration rate is relatively high.

One of the biggest advantages of survival analysis is grasping of the overall situation of the data. However, it cannot give any further prediction. In order to obtain the service life of each individual bridge, numerical simulation is used. According to the actual bridge design drawing, a complete full span finite element model with a length of 30 meters and width of 11 meters has been created. But large model which contained large amount of solid element will consume a lot of computation time. In order to speed up the calculation process, part of the solid elements was retained, and the remaining part was replaced by beam elements.

The result shows that the beam-solid hybrid full scale model can successfully analyze the fatigue life of the RC deck. However, full scale model and simple plate model show inconsistent results under dry and wet condition because of the different boundary condition. Therefore, the usage of full scale model would be more previse. Next, in order to check different deterioration process and mechanism of full scale numerical model, the displacement decreasing trend, the maximum principle strain distribution, horizontal crack generation time and condition are compared between full scale numerical model. Under dry case, the fatigue cycle is greatly increased if the slab thickness was increased. However, under wet case, even though the thickness of the slab has increased a lot, the increasing in fatigue life is very limited. Additionally, in the case of the same thickness of the slab, the fatigue life in a dry and wet case are significantly different. These results are also consistent with the survival analysis results. According to the maximum principle strain distribution, it can be seen that the deterioration of

slab under dry case thought a relative long time period. Since the damage is shown in the surface area, the current inspection can easily detect it and the survival analysis can consider this type of deterioration. However, for wet case, comparing with top surface, the maximum principle strain in the bottom surface showed a delayed trend. According to the road bridge deck maintenance management manual, it is said that the horizontal crack is generated after the acceleration period, which is the late stage of the deterioration. But base on the simulation result, the horizontal crack happened at the initial deterioration through a very short period. It is necessary to carefully consider the acceleration of deterioration due to horizontal cracks. Moreover, current inspection cannot or underestimate the deterioration under wet case. Then, by comparing with the result of different distance wheel load and girder, it can be found that when the loading is far from girder, the vibration amplitude is larger, higher water pressure is generated and fatigue failure can be reached faster. Finally, by comparing with single loading, deflection decreasing of actual load are accelerated. Therefore, by considering the actual loading position, the simulation can be more closed to the actual situation.

Future research directions will be focus on improving the simulation accuracy by considering the stagnant water location and the complex deterioration include ASR, frost damage, chloride attack, etc. Additionally, in order to avoid horizontal crack and early stage punching shear failure, the waterproof should be functional in all time period. GPR system should be induced to check inside condition of slab. And the bottom surface crack condition should be combine with the top and inside condition of slab in order to increase the accuracy of survival analysis.

Acknowledgement

Firstly, I would like to start this dissertation with my deepest gratitude and indebtedness to my supervisor, Professor Tetsuya Ishida who accepted me to the Concrete Laboratory. For his stimulating ideas, numerous constructive suggestions and guidance, enduring patience and continuous encouragement throughout this study. Without his insightful comments and valuable suggestions, this research would never have been completed.

Words of thank must also to my supervisor committee: Professor Ichiro Iwaki, Associate Professor Kohei Nagai, Associate Professor Tomonori Nagayama and Lecturer Yuya Takahashi. For all their valuable and comments and critical ideas, through which the scope of the work could be enhanced.

Sincere appreciation is extended to Dr. Satoshi Tsuchiya for his invaluable advice, guidelines and comments helped in shaping the research. Also, I would like to thank my fellow students. Firstly, I would like to thank Dr. Eissa for providing me with basic knowledge of fatigue life simulation by using Com3. Help and constant support from Assistant Professor Yao Luan, Dr. Xiaoxu Zhu and Assistant Professor Tiao Wang during the course of this study is greatly appreciated.

My sincere appreciation goes to my friends, Danupon Subanapong and Kolneath Pen for sharing their knowledge and always helping me out. I am very grateful to Zhehui Yang, Xi Ji, Jing Zheng and other guys for being around me and spending time with me.

My profound gratitude to my family who gives me constant support, for helping me out with my life in Japan. Finally, I am thankful to everyone who has believed in me and supported me.

Contents

List of Figures

List of Tables

Chapter 1: Introduction

1.1) Bridge construction and maintenance status in Japan

A large number of bridges were constructed in Japan during periods of high economic growth (as shown in Figure 1-1). Fifty years later, performance degradations have been widely found in these bridges. Some bridges may fail without proper maintenance. Parts that have seriously deteriorated threaten the safety of users because of insufficient maintenance. Figure 1-2 shows some damage cases of RC slab of steel bridge. In the year of 2026, almost half of the bridge are over 50 years after construction [1, 2].

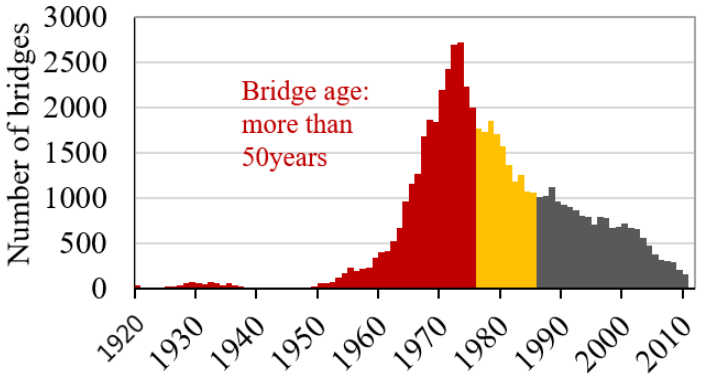

Figure 1-1 construction year of steel bridge with length of more than 15m(NILIM(2012))

Figure 1-2 damage cases of steel bridge RC deck

Nowadays, labor fees are continuously increasing, maintenance costs have become a heavy burden on the national budget, and there is a great demand for reduced maintenance costs. Therefore, a rational bridge deck slab maintenance system are need. Not only overall deterioration situation, but also detailed deterioration process, mechanism and fatigue life should be obtained. Against this background, as a first step, the Ministry of Land, Infrastructure, Transportation and Tourism (MLIT) announced on 1 July 2014 that close visual bridge inspection would now be required every five years for the approximately 700,000

bridges in Japan. Moreover, private highway companies began to conduct this kind of periodic inspection before the mandatory inspection policy was put in place. This policy has accelerated the data accumulation of inspection results, which now offers an opportunity for statistical analysis.

1.2) Current bridge inspection data processing method

In these circumstances, demands for asset management based on the statistical analysis of bridges are growing. As Mauch and Madanat (2001) and Mishalani and Madanat (2002) stated, there are two types of models that can be developed and applied to evaluate the deterioration process of infrastructure. The first is a state-based model, which forecasts the possibility that a structure will undergo a decline in condition-state at a given time [3, 4]. A typical example is the Markovian method, which is extensively used in United States (US) bridge management systems (Sharabah et al. (2006); Chikata et al. (2015), Tsuda et al. (2005)) [5–7]. However, as Agrawal et al. (2010) stated, the Markovian method has several limitations. A discrete transition interval is assumed; the future condition of structural elements depends not on their past history, but rather on their current condition, and different bridge component deterioration mechanisms cannot be efficiently considered [8]. Furthermore, the Markovian method cannot evaluate multiple variables, which means that it is difficult to compare the risks of each deterioration factor.

The other type of model is time-based, in which the time probability distribution of structural deterioration is computed. A typical example is survival analysis, which is more flexible and expandable than the Markovian method. Mishalani and Madanat (2002) focused on survival analysis and applied it to quantitatively evaluate the effect of several coefficients. However, they indicated that one limitation of their research was that the subsets of bridges were relatively small.

Yamazaki and Ishida (2015) conducted a survival analysis of concrete bridges in East Japan [9]. Similar to our research, the definition of East Japan only includes Aomori, Akita, Iwate, Yamagata; Miyagi Fukushima Prefecture and the Tokyo region are excluded. The Kaplan–Meier (KM) curve and Cox regression were used to evaluate the deterioration rate of bridge components under different structural features, traffic volume, etc. However, because the analysis was only conducted for one region, it cannot be considered to hold for the entirety of Japan. Goyal et al. (2017) also used a semi-parametric multivariate proportional hazards model to characterize the effect of external factors on the deterioration rates of bridge components [10]. As Ying et al. (2013) stated, semi-parametric survival analysis does not assume the distribution of hazard; therefore, it has more flexibility in capturing the features of the original data [11].

In addition, some analyses have tried to establish the relationship between bridge inspection data and environmental information. Iwaki et al. (2013) classified 2600 bridges according to the years in service, quantity of large vehicle traffic, amount of de-icing salt used, and average ambient temperature in winter in East Japan [12]. In another study, Lenisa (2013) examined 1662 bridges in Bolzano, which is a mountainous area of Northern Italy. These studies indicate that bridge deterioration is a complex phenomenon, and deterioration occurs when the environment matches a specific condition that accelerates deterioration [13]. Although these studies concluded that the ambient environment condition was a significant factor that could affect the degradation of bridge slabs, they only classified the samples and counted them, so the results remain ambiguous. Therefore, further analysis is needed.

Different deterioration phenomena are caused by different ambient conditions. The bridge situation in Japan can be roughly divided into two categories, represented by the East Japan and Tokyo regions. In East Japan, slabs undergo severe environmental conditions due to low temperatures, snowy weather, and a heavy use of de-icing salt. In the Tokyo region, slabs must carry heavy repeated dynamic traffic loads. Therefore, dominant deterioration factors in this two regions are different. Therefore, by analyzing data from these two typical but contrasting regions, it is possible to extrapolate the analysis of risk factors to almost all of the regions of Japan.

This study uses Cox multivariate proportional modeling to analyze bridges in the East Japan and Tokyo regions. The predominant risks of bridge slabs are quantitatively evaluated and the deterioration risk factors in most areas of Japan under different ambient conditions are identified. Introducing this methodology is expected to reduce maintenance and renewal costs and greatly improve work efficiency. Maintenance priority can be given to bridges with high risks to enhance safety management. Useful feedback and backup for future durable design and construction work can also be derived. In addition, large-scale data collected by close visual inspection and sound testing are used to enhance estimation accuracy. Structural features, environmental conditions, and other factors are selected as variables based on concrete engineering studies to evaluate their influence on bridges. Unlike previous studies, this study makes use of data cleaning and selection based on the basic concept of survival time.

1.3) Current study for deterioration process and mechanism for individual bridges

The study of deterioration process and simulation for individual bridge were carried out during the past decades. The bridge deck slab is a member in which the ratio of the stress generated by the live load is higher than the stress generated by the dead load. Therefore, from around 1965 (Showa 40), when the increase in vehicle traffic and size of vehicles were observed, cases of damage such as concrete peeling, sinking, or falling out became remarkable,

and thereafter the problem of damage to RC slabs has become a major issue in the maintenance of road bridges.

From the actual situation on site, usually in the initial deterioration process, one dimensional crack appeared on the bottom side of the RC slab surface. Then since affect by traffic loading, two dimensional cracks are developed. Under the shear moment and torsional moment, finally the punching shear failure happened [14]. Recently, some short-lived bridge deck slabs have been found was suddenly collapsed without obvious signs, and as Figure 1-4 shows, horizontal cracks usually can be observed in the cross section area. But the generation period and mechanism is still not clear [15].

Figure 1-3 punching shear failure of RC slab

And according to previous research, the fatigue loading test under wheel load are conducted by Matsui sensei (Maeda and Matsui, 1984) [16]. In the fatigue fracture process of RC floor slabs, it is assumed that the beam-like formation due to the wear of the through cracks in the cross section of the distribution rebar and the subsequent shear strength of the cross section of the main rebar dominate the floor slab behaviour. In this method, the current number of heavy vehicle traffic is used as the number of travels N, and the current roadway wheel load of 100KN is used as the acting load. The main purpose of this proposal is not to determine the fatigue life of each bridge exactly, but to confirm the difference in the fatigue life between different span lengths. They considered it as the difference in fatigue durability of slabs due to the difference span length, and used it as an index for determining the priority of maintenance [17].

And the fatigue design has been proved base on their result. But for new structures, still the full size experiment need to be conducted in laboratories. Under this circumstance, in order to quantify the mechanism of the fatigue failure, instead of the two dimensional beam model, the three-dimensional fatigue simulation of RC slabs under traveling wheel load are developed [18]. In this analysis, not only the difference between repeated fixed point loading and traveling wheel loading are shown, but also it has been proved that the model can successfully simulated the punching shear failure. Basic on the above result, the fatigue simulation has been used to calculate the fatigue life under different condition. Then, the correlation between survival

analysis and fatigue simulation are has also been studied, and by comparing the fatigue life under dry and wet cases, it shows that stagnant water plays decisive role in deterioration. On this basis, impact of location of the stagnant water on fatigue life of RC bridge decks have been investigated. However, the numeric fatigue life analysis only applied the load on the middle of a simple plate. In the actual situation, as the load position changes, the distance between the load and the girder also changes, and it will directly affect the fatigue life. Additionally, since the actual structure is more complicated, the size, shape and boundary condition is totally different comparing with simple plate, the strain and stress distribution, displacement and moment is also different. The detailed information will be given in chapter 5.

In this research, developed by the University of Tokyo, the existing and current models COM3, which is a non-linear finite element analysis can reproduce the high cycle fatigue of concrete structures. Firstly, the different between full scale model and simple plate model are compared. Then result of full scale model under different condition are explained. In order to check different deterioration process and mechanism of full scale numerical model, the displacement decreasing trend, the maximum principle strain distribution and horizontal crack generation time and condition are compared. The comparison will go through dry case - dry case, wet case - wet case comparison under different slab thickness and dry case - wet case comparison under same slab thickness. Then the available range of survival analysis and current inspection are discussed. Then the fatigue cycle and failure pattern are compared under different distance between wheel load and girder. Additionally, based on the lane position, the simulation by considering the actual loading position also conducted. Finally, impact of spatially non-uniform stagnant water on fatigue life of slab by using full scale model are evaluated in order to check the effect of stagnant water location and area. The detailed information will be shown in chapter 5.

1.4) Thesis summary

The thesis mainly consists of two parts, part one is survival analysis part two is full scale numerical simulation. Survival analysis is a statistical analysis method which comes from medical area and numerical simulation is a non-linear finite element analysis method.

In chapter 1, the general background of current bridge slab deterioration, maintenance and previous researches which relate to bridge inspection data processing and numerical RC bridge slab fatigue simulation are introduced.

In chapter 2, methodology of survival analysis is discussed. Through the introduction of non-parametric and semi-parametric, the characteristics, differences and application of each method are explained in detail.

In chapter 3, survival analysis result of East Japan region is shown. The deterioration feature, the effect of each variables and relative deterioration rate are quantified. Additionally, the risk score which represents the relative deterioration rate of each panel are calculated and plotted on the map.

In chapter 4, similarly survival analysis result of Tokyo region is shown. The deterioration feature, the effect of each variables and relative deterioration rate are quantified and the risk score are calculated and plotted on the map.

In chapter 5, the feature difference between survival analysis and full scale numerical simulation are discussed. And the necessary of conducting full scale numerical simulation are stated. The current proposed maintenance system should not only evaluate the relative deterioration rate, but also estimate the fatigue life of individual bridge slab. Therefore, the conducting of full scale numerical simulation is essential.

In chapter 6, the methodology of full scale numerical simulation is induced. Firstly, the basic concept and constitutive law of numerical scale simulation are given in order to show the entire calculation algorism more clearly. Then a common bridge superstructure is selected and FEM model with same size, reinforcement information, loading information are set. Additionally, to save massive computation time, the beam elements are used to replace part of the solid elements. Based on the second moment of area, the material properties of beam element are set.

In chapter 7, firstly, the results between full scale model and simple plate model are compared under dry and wet environmental condition. According to the different boundary condition, the maximum principle strain distribution and generated water pressure are totally different, therefore the central deflection results of full scale model and simple plate model are reversed. The result implies that the usage of full scale model is better since the setting of it is close to the actual situation. Then, the results of full scale model under different slab thickness and environmental condition are shown. Especially, the horizontal crack generation condition and time period is evaluated. The simulation results under dry and wet environmental condition are consistent with survival analysis which is showed in Chapter 3 and chapter 4, indirectly conforms the correctness of survival analysis. Then combining the on-site inspection and bottom side maximum principle strain of numerical simulation, the deficiency of current inspection and available range of survival analysis are evaluated. Additionally, the results of different loading position are shown to evaluate the different failure pattern.

In chapter 8, the actual loading case is simulated and compared with single wheel load case. Additionally, the partial water submerged case is also simulated and discussed. Since the current design didn’t consider this effect, the analysis can provide a reference for future design.

In chapter 9, the conclusions of each chapter of the core research of this thesis are presented in detailed.

1.5) Reference

1. Nagai, M., & Miyashita, T. (2009). Recent topics on steel bridge engineering in Japan-design and maintenance. In *Proceeding of the 10th Korea-China-Japan Symposium on Steel Structures* (pp. 65-76).
2. Tamakoshi, T., Yoshida, Y., Sakai, Y., & Fukunaga, S. (2006). Analysis of damage occurring in steel plate girder bridges on national roads in Japan. *Public Work Research Institute of Japan*.
3. Mauch, M.; Madanat, S. Semiparametric hazard rate models of reinforced concrete bridge deck deterioration. *J. Infrastruct. Syst.* **2001**, *7*, 49–57.
4. Mishalani, R.G.; Madanat, S.M. Computation of infrastructure transition probabilities using stochastic duration models. *J. Infrastruct. Syst.* **2002**, *8*, 139–148.
5. Sharabah, A.; Setunge, S.; Zeephongsekul, P. Use of Markov chain for deterioration modeling and risk management of infrastructure assets. In Proceedings of the International Conference on Information and Automation, Weihai, China, 15–17 December 2006; pp. 384–389.
6. Chikata, Y.; Suzuki, S.; Ogawa, F. A consideration on calculation process of Markov transition probability for deterioration prediction based on inspection results. *Jpn. Soc. Civ. Eng. J. Infrastruct. Syst.* **2015**, doi:10.11532/structcivil.61A.70. (In Japanese)
7. Tsuda, Y.; Kaito, K.; Aoki, K.; Kobayashi, K. Estimating Markovian transition probabilities for bridge deterioration forecasting. *Struct. Eng./Earthq. Eng.* **2006**, *23*, 241s–256s.
8. Agrawal, A.K.; Kawaguchi, A.; Chen, Z. Deterioration rates of typical bridge elements in New York. *J. Bridge Eng.* **2010**, *15*, 419–429.
9. Yamazaki, T.; Ishida, T. Application of survival analysis to deteriorated concrete bridges in East Japan. *J. Jpn. Soc. Civ. Eng.* **2015**, doi:10.2208/jscejcm.71.I_11.
10. Goyal, R.; Whelan, M.J.; Cavalline, T.L. Characterising the effect of external factors on deterioration rates of bridge components using multivariate proportional hazards regression. *Struct. Infrastruct. Eng.* **2017**, *13*, 894–905.
11. Yang, Y.N.; Kumaraswamy, M.M.; Pam, H.J.; Xie, H.M. Integrating semiparametric and parametric models in survival analysis of bridge element deterioration. *J. Infrastruct. Syst.* **2013**, *19*, 176–185.

12. Iwaki, I.; Koda, Y.; Ishikawa, M.; Oyamada, Y. Development of bridges management support tool for the Tohoku region. *Concr. Res. Technol.* **2013**, *24*, 75–87. (In Japanese)
13. Lenisa, A. The health state of infrastructure assets including 1758 bridges and 1087 km of road restraint systems along a mountain road network with an average age of 40 years. In Proceedings of the Brenner Congress 2013, Bolzano, Italy, 21–22 February 2013; pp. 153–164.
14. Rangan, B. V., & Hall, A. S. (1983, May). Moment and shear transfer between slab and edge column. In *Journal Proceedings* (Vol. 80, No. 3, pp. 183-191).
15. [Ryoma Komatsushiro et al (2016), Generation mechanism of horizontal crack inside RC floor slab. *The 8th Road Bridge Deck Slab Symposium*, November 2016]
16. MAEDA, Y., & MATSUI, S. (1984). Punching shear load equation of reinforced concrete slabs. *Doboku Gakkai Ronbunshu*, *1984*(348), 133-141.
17. Toru Furuichi, Shigeyuki Matsui, Hirotsugu Sami, & Toru Kodera. (2008). A Method for Determining Priority of Countermeasures for Floor Slabs Using Fatigue Life Estimation Theory. *Proceedings of the Japan Concrete Institute*, *30*(3), 1699-1704.
18. Maekawa, K., Gebreyouhannes, E., Mishima, T., & An, X. (2006). Three-dimensional fatigue simulation of RC slabs under traveling wheel-type loads. *Journal of Advanced Concrete Technology*, *4*(3), 445-457.

Chapter 2: Methodology of survival analysis

2.1) Introduction

Since part of the research is rooted in survival analysis, in this section, the basic concepts of the survival analysis are discussed. Through the introduction of non-parametric and semi-parametric, the characteristics, differences and application of each method are explained in detail.

Survival analysis "time to event analysis" is classified as a statistical method. It has been used for data involving time to a certain event (death, onset of a disease etc.). Initially applied to medicine filed, survival analysis now is one of the most widely used statistical methods which are developed and utilized to various disciplines such as pharmacy, biology and engineering.

In this chapter, the definition of non-parametric survival model and semi-parametric survival model are discussed. Then to calculate regression coefficient, partial likelihood function is induced. Finally, the way to dealing with censored and tied data are explained.

2.2) Non-parametric survival model

In general, non-parametric or "distribution-free" method refers to a type of statistic that does not require that the population being analyzed meet certain assumptions or parameters [1]. Kaplan Meier curves and estimates is the most frequently used method in survival analysis since Edward L. and Kaplan and Paul Meier collaborated to publish a seminal paper on how to deal with incomplete observation [2, 3]. Theoretically, survival function *S(t)* is estimated by the Kaplan Meier curve and estimate in equation which is shown below.

$$\hat{S}(t) = \prod_{t_{(i)}<t} \frac{n_i - d_i}{n_i} \tag{2-1}$$

where $\hat{S}(t)$ is Kaplan Meier curve and estimate, n_i is the population at time $t_{(i)}$ and d_i is the number of subjects have the event of interest at time $t_{(i)}$. Three things need to be prepared before conducting Kaplan Meier method. Serial time, status of objects and study group they are in. In actual situation, not all subjects need to reach the event of interest during observation time, they also can be censored. Censoring means the total survival time for that subject cannot be accurately determined. This can happen when something positive or negative for study occurs, such as lost to follow up, incomplete data or study end before the subject had the event of interest occurs. In fact, handling with censoring data is one the most important feature and advantage for survival analysis.

Kaplan Meier curve and estimate needs to follow three assumptions. First, at any time objects who are censored have the same survival prospects as those who continue to be followed. Second, the survival probabilities are the same for subjects recruited early and late in the study. Third, that the event happens at the time specified [4]. Failure to meet of any of the above conditions will bias the survival probability and cause imprecision result. For bridge inspection data, all the conditions are difficult to achieve perfectly. Sometimes, the observation stopped due to the components are relative safer than other parts. Along with the development of construction technique and accumulation of construction experience, the quality and design code are gradually improving. Therefore, the bridges which were constructed during the late years are more durable in terms of fatigue and chemical degradation resistance. Especially, because it is difficult to obtain data of construction quality, the effect of these factors are not fully considered in analysis. Additionally, since the inspection is conducted every five years, all we know is that the event happened between two inspections. It cannot be denied that these facts have a certain impact on the analysis result, but the availability of data on some factors that have a relatively large impact on bridge durability still allow the deterioration features can be successful analyzed.

2.3) Semi-parametric survival model

The KM estimator is used to show the survival probability between different study populations. Cox regression analysis is applied to synthesize all of the variables and calculate the hazard ratio of each group. Unlike the KM estimator, the Cox regression is a semi-parametric method proposed by Cox (1972); it assumes that the hazards of different groups are proportional in all periods. [5]. The biggest difference compare with Kaplan Meier curve is that Cox regression is used for investigating the effect of several variables quantitatively. All equations which are related to survival analysis are shown below. The probability density function $f(t)$ represents the exact time when the event occurs, as follows:

$$f(t) = \lim_{\Delta t \to 0} \frac{P(t \leq T < t + \Delta t)}{\Delta t} \tag{2-2}$$

The cumulative distribution function is defined as $F(t) = P(T < t)$. It is known that:

$$f(t) = \frac{d}{dt} F(t) \tag{2-3}$$

In survival analysis, a survival function is more frequently used. It is defined as $S(t) = P(T > t)$, which means the event is later than time T. In addition, $S(t) = 1 - F(t)$.

The hazard function $h(t)$ is defined as the probability of a subject experiencing an event at time $T + \Delta t$, under the condition of no event occurring from 0 to t (which means that the event occurs within a very short period). The following equation shows the mathematical expression for the hazard function:

$$h(t) = \lim_{\Delta t \to 0} \frac{P(t \leq T < t + \Delta t | T \geq t)}{\Delta t} = \lim_{\Delta t \to 0} \frac{F(t + \Delta t) - F(t)}{\Delta t} = \frac{f(t)}{S(t)} \qquad (2\text{-}4)$$

From this equation, it is known that $h(t)$, $f(t)$, and $S(t)$ are related. The Cox model with multiple variables is:

$$h(t) = h_0(t) e^{\sum_{i=1}^{n} x_i \beta_i} \qquad (2\text{-}5)$$

Equation (5) is a regression model that introduces logarithmic linearity for the hazard function, where x is a covariate, while β is a regression coefficient. $h_0(t)$ is called the baseline hazard function. As long as $h_0(t) > 0$, it can take any shape as a function of t. The hazard ratio (HR) is calculated as the failure ratio of two samples, whose covariates are x_i' and x_i'':

$$\mathrm{HR}(\mathrm{t}, x_1, x_0) = \frac{h_0(t) e^{x_1^o \beta_1 + \boldsymbol{x_2} \beta_2 + \cdots + \boldsymbol{x_n} \beta_n}}{h_0(t) e^{x_1^1 \beta_1 + \boldsymbol{x_2} \beta_2 + \cdots + \boldsymbol{x_n} \beta_n}} = \exp[\beta_i (x_i' - x_i'')] \qquad (2\text{-}6)$$

The hazard ratio can be interpreted as the ratio of the possibility of degradation for any time duration. If the hazard ratio is higher than 1, then the risk will increase as the variate increases, and vice versa. In this study, all variables are assumed to follow a standard distribution. For each numeric covariate, $N(\mu, \sigma^2)$ is calculated, where μ is the mean value and σ^2 is the variance. The covariates are then standardized to $N(0, 1)$ using the following equation:

$$z_i = \frac{x_i - \mu}{\sigma} \qquad (2\text{-}7)$$

where x_i is the original value of the covariate and z_i is the standardized value. Thus, for numeric variables, the hazard ratios represent the ratio of risk variety per standardized unit. More specifically, the hazard ratio minus 1 and multiplied by 100 expresses the hazard percent change for 1σ. For instance, if the hazard ratio is 1.3 and $\sigma = 200$, the risk will be 30% higher when the variate increases by 200.

Cox regression model is the most commonly used regression model for survival analysis. The advantages of this model can be summarized as 1) suitable for survival type data; 2) flexible choice of covariates; 3) fairly easy to fit; 4) standard software exists.

2.4) Partial likelihood estimation for Cox regression

Cox regression proposed a partial likelihood for regression coefficients of β [5, 6]. Suppose an individual i was observed (X_i, δ_i, Z_i), where X_i is a possible censored failure time random variable, δ_i is the failure or censoring indicator (1 is fail and 0 is censoring), Z_i represents a se of covariates. Assume there are K distinct failure (or death) times, and $\tau_1 < \cdots \tau_K$ represent the K ordered, distinct death times.

If there are no tied death times, Let $R(t) = \{i: X_i > t\}$ denote the individuals who are "at risk" for failure at time t, called the risk set. The partial likelihood is a product over the observed failure times of conditional probabilities, of seeing the observed failure, given the risk set at that time and that one failure is to happen. In other words, these are the conditional probabilities of the observed individual, being chosen from the risk set to fail.

At each failure time X_j the contribution to the likelihood is:

$$\begin{aligned}\mathcal{L}_j(\beta) &= P(individual\ j\ failure | one\ failure\ from\ R(X_j)) \\ &= \frac{P(individual\ j\ fail\ | at\ risk\ at\ X_j)}{\sum_{l \in R(X_j)} P(individual\ l\ fails\ |\ at\ risk\ at\ X_j)} \\ &= \frac{\lambda(X_j|Z_j)}{\sum_{l \in R(X_j)} \lambda(X_j|Z_l)}\end{aligned} \tag{2-8}$$

Under the PH assumption of $\lambda(t|Z)$, the partial likelihood function can be

$$\begin{aligned}\mathcal{L}(\beta) &= \prod_{j=1}^{K} \frac{\lambda_0(X_j) e^{\beta' Z_j}}{\sum_{l \in R(X_j)} \lambda_0(X_j) e^{\beta' Z_l}} \\ &= \prod_{j=1}^{K} \frac{e^{\beta' Z_j}}{\sum_{l \in R(X_j)} e^{\beta' Z_l}}\end{aligned} \tag{2-9}$$

The partial likelihood only uses the ranks of the failure times, which means that if the failure order were decided of a specified population, the coefficient of β does not change due to the change in survival time, but always being constant.

2.5) Censored data likelihood derivation

The likelihood contributions for right censored data fall into two categories: 1) individual is censored at X_i, the likelihood function can be written as

$$\mathcal{L}_i(\beta) = S_i(X_i) \tag{2-10}$$

and 2) individual fails at X_i and the likelihood function is

$$\mathcal{L}_i(\beta)\mathcal{L}_i(\beta) = f_i(X_i) = S_i(X_i)h_i(X_i) \tag{2-11}$$

The full likelihood function can be defined as

$$\begin{aligned}\mathcal{L}(\beta) &= f_i(X_i) = \lambda_i(X_i)^{\delta_i} S_i(X_i) \\ &= \prod_{i=1}^{n} \left[\frac{\lambda_i(X_i)}{\sum_{j\in R(X_i)} \lambda_j(X_i)}\right]^{\delta_i} \left[\sum\nolimits_{j\in R(X_j)} \lambda_j(X_i)\right]^{\delta_i} S_i(X_i)\end{aligned} \tag{2-12}$$

The first term contained almost all the information about β, while the last two term contain information about $\lambda_0(t)$ (Cox, 1972) [5].

By keep the first term, under the PH assumption:

$$\begin{aligned}\mathcal{L}(\beta) &= \prod_{i=1}^{n} \left[\frac{\lambda_i(X_i)}{\sum_{j\in R(X_i)} \lambda_j(X_i)}\right]^{\delta_i} \\ &= \prod_{i=1}^{n} \left[\frac{\lambda_0(X_i)\exp(\beta' Z_i)}{\sum_{j\in R(X_i)} \lambda_0(X_i)\exp(\beta' Z_j)}\right]^{\delta_i} \\ &= \prod_{i=1}^{n} \left[\frac{\exp(\beta' Z_i)}{\sum_{j\in R(X_i)} \exp(\beta' Z_j)}\right]^{\delta_i}\end{aligned} \tag{2-13}$$

The log-partial likelihood is:

$$\begin{aligned}\mathcal{L}(\beta) &= \log \prod_{i=1}^{n} \left[\frac{\lambda_i(X_i)}{\sum_{j\in R(X_i)} \lambda_j(X_j)}\right]^{\delta_i} \\ &= \sum_{i=1}^{n} \delta_i \left[\beta' Z_i - \log\left\{\sum\nolimits_{l\in R(X_i)} \exp(\beta' Z_l)\right\}\right] \\ &= \sum_{i=1}^{n} l_i(\beta)\end{aligned} \tag{2-14}$$

2.6) Tied data likelihood derivation

Theoretically, the all survival times are assumed to be continuous, indicates that all individuals have different failure or censoring time. But in actual data, time is discrete, therefore, two or more individuals can have same failure or censoring time. This situation is called tied data. The proportional hazards model assumes a continuous hazard - ties should not be heavy. However, when they do happen, there are a few proposed modifications to the partial likelihood to adjust for ties.

Cox (1975) issued a discrete method to handle this problem. It assumed that if there are tied failure times, they truly happened at the same time [7]. The partial likelihood is shown at follow:

$$\begin{aligned}\mathcal{L}(\beta) &= \prod_{j=1}^{K} \Pr\left(i_{j1}, \cdots i_{jd_j}\ fail \,\middle|\, d_j\ fail\ at\ \tau_j, from\ \mathcal{R}(\tau_j)\right) \\ &= \prod_{j=1}^{K} \frac{\Pr(i_{j1}, \cdots i_{jd_j}\ fail \mid in\ \mathcal{R}(\tau_j))}{\sum_{\ell \in s(j,d_j)} \Pr\left(\ell_1, \cdots \ell_{d_j} \,\middle|\, in\ \mathcal{R}(\tau_j)\right)} \\ &= \prod_{j=1}^{K} \frac{\exp\left(\beta z_{i_{j1}}\right) \cdots \exp\left(\beta z_{i_{jd_j}}\right)}{\sum_{\ell \in s(j,d_j)} \exp(\beta z_{\ell 1}) \cdots \exp\left(\beta z_{\ell_{d_j}}\right)} \\ &= \prod_{j=1}^{K} \frac{\exp(\beta S_j)}{\sum_{\ell \in s(j,d_j)} \exp(\beta S_{j\ell})} \end{aligned} \tag{2-15}$$

where $s(j, d_j)$ is the set of all possible sets of d_j individuals that can possibly be drawn from the risk set at time X_j. S_j is the sum of the Z's for all the d_j individuals who fail at X_j. $S_{j\ell}$ is the sum of the Z's for all the d_j individuals in the ℓ-th set drawn out $s(j, d_j)$. The disadvantage of this method is that with large numbers of ties, the denominator can have many terms and be difficult to calculate.

Kalbfleisch and Prentice proposed another extract method. The method based on the assumption that if there are tied events, that is due to the imprecise nature of our measurement, and that there must be some true ordering. All possible orderings of the tied events are calculated, and the probabilities of each are summed. [8].

Breslow and Pete suggested an approximation method with replacing the term $\sum_{\ell \in s(j,d_j)} \exp(\beta S_{j\ell})$ in the denominator by the term $(\sum_{\ell \in \mathcal{R}(\tau_j)} \exp(\beta z_\ell))^{d_j}$, so that the following modified partial likelihood would be used.

$$\mathcal{L}(\beta) = \prod_{j=1}^{K} \frac{\exp(\beta S_j)}{\sum_{\ell \in s(j,d_j)} \exp(\beta S_{j\ell})}$$

$$\approx \prod_{j=1}^{K} \frac{\exp(\beta S_j)}{(\sum_{\ell \in \mathcal{R}(\tau_j)} \exp(\beta z_\ell))^{d_j}} \qquad (2\text{-}16)$$

This approximation will be break down when the number of ties are large relative to the size of the risk sets, and then tends to yield estimates of β which are biased toward 0. The method used to be the default for most software programs, because it is computationally simple.

Efron suggested an even closer approximation to the discrete likelihood [9]. In general, if there are d_j tied survival times at the *j*th distinct survival time, then $\mathcal{L}_j(\beta)$ is approximated by

$$\mathcal{L}_j(\beta) = \frac{e^{\sum_{l \in D_j} z_l \beta}}{[\sum_{l \in R_j} e^{z_l \beta}]^{d_j}} \qquad (2\text{-}17)$$

Where, R_j is the risk set at the jth survival time and D_j is the event set at the jth distinct survival time.

$$\mathcal{L}(\beta) = \prod_{j=1}^{D} \mathcal{L}_j(\beta)$$

$$\approx \prod_{j=1}^{D} \frac{e^{\sum_{l \in D_j} z_l \beta}}{\prod_{k=1}^{d_j} (\sum_{l \in R_j} e^{z_l \beta} - \frac{k-1}{d_j} \sum_{l \in D_j} e^{z^l \beta})} \qquad (2\text{-}17)$$

Like the Breslow approximation, Efron's method also assumes that the failures occur one at a time, and will yield estimates of β which are biased toward 0 when there are many ties. However, the Efron approximation is much faster than the exact methods and tends to yield much closer estimates than the Breslow approach.

And there are some implications of ties. 1) When there are no ties, all options give exactly the same results; 2) When there are only a few ties, it won't make much difference which method is used. 3) When there are many ties (relative to the number at risk), the Breslow option performs poorly (Farewell & Prentice, 1980; Hsieh, 1995) [10, 11]. Both of the approximate methods, Breslow and Efron, yield coefficients that are attenuated (biased toward 0). 4) The Efron approximation nearly always works better than the Breslow method, with no increase in computing time. Therefore, in our analysis, the Efron method was selected to evaluate the regression coefficient β.

Cox regression assumes that the hazards of different groups are proportional in all periods. The advantage of the KM estimator and Cox regression model is that they fit the survival model without assuming the distribution, and can express the features of the original data (Bugnard et al. (1994)) [12]. Even if in many cases, a univariate analysis can only consider the effect of one variable, it provides the basic characteristics of each variable. Moreover, a greater understanding of our dataset can be obtained by carefully comparing the results of these two methods.

2.7) References

1. Siegel, S. (1957). Nonparametric statistics. *The American Statistician*, *11*(3), 13-19.
2. Kaplan, Edward L., and Paul Meier. "Nonparametric estimation from incomplete observations." *Journal of the American statistical association* 53.282 (1958): 457-481.
3. Rich, J. T., Neely, J. G., Paniello, R. C., Voelker, C. C., Nussenbaum, B., & Wang, E. W. (2010). A practical guide to understanding Kaplan-Meier curves. *Otolaryngology—Head and Neck Surgery*, *143*(3), 331-336.
4. Bland, J. M., & Altman, D. G. (1998). Survival probabilities (the Kaplan-Meier method). *Bmj*, *317*(7172), 1572-1580.
5. Cox, D. R. (1972). Regression models and life-tables. *Journal of the Royal Statistical Society: Series B (Methodological)*, *34*(2), 187-202.
6. Cox, D. R. (1975). Partial likelihood. *Biometrika*, *62*(2), 269-276.
7. Cox, W. M. (1975). A review of recent incentive contrast studies involving discrete-trial procedures. *The Psychological Record*, *25*(3), 373-393.
8. Anderson, J. A., & Senthilselvan, A. (1980). Smooth estimates for the hazard function. *Journal of the Royal Statistical Society: Series B (Methodological)*, *42*(3), 322-327.
9. Efron, B. (1977). The efficiency of Cox's likelihood function for censored data. *Journal of the American statistical Association*, *72*(359), 557-565.
10. Farewel, V. T., & Prentice, R. L. (1980). The approximation of partial likelihood with emphasis on case-control studies. *Biometrika*, *67*(2), 273-278.
11. Hsieh, Jen-Chuen, Måns Belfrage, Sharon Stone-Elander, Per Hansson, and Martin Ingvar. "Central representation of chronic ongoing neuropathic pain studied by positron emission tomography." *PAIN*® 63, no. 2 (1995): 225-236.
12. Bugnard, F.; Ducrot, C.; Calavas, D. Advantages and inconveniences of the Cox model compared with the logistic model: Application to a study of risk factors of nursing cow infertility. *Vet. Res.* **1994**, *25*, 134–139.

Chapter 3: Survival analysis result of East Japan region

.

3.1) Introduction

In this chapter, the deterioration feature and survival analysis result of East Japan region are discussed. According to the low traffic volume, the fatigue failure which is caused by heavy traffic loading is not the main reason of RC slab deterioration. However, large winter precipitation, snow fall and de-icing salt usage give a positive result for increasing risks. Therefore, the complex deterioration is the main reason to cause the bridge slab failure of this region. The survival probability and cox regression result are shown. Additionally, the risk score which represents the relative deterioration rate of each panel are calculated and plotted on the map. It can be clearly seen that in the mountain of Japan sea side, because of large de-icing salt usage and high winter precipitation, the risk scores are higher than other region.

3.2) Deterioration feature of East Japan

The most popular road bridge structure in Japan is the steel girder bridge with reinforced concrete slab. An reinforced concrete (RC) deck slab consists of four main layers: the concrete slab, the waterproof layer, the asphalt surface layer, and the asphalt base layer (Figure 3-1). Since a waterproof layer is not mandatory in Japan, waterproof layers are not installed in at least 20% of RC deck slabs in national roads. The total thickness of the two asphalt layers is around 70 mm to 80 mm.

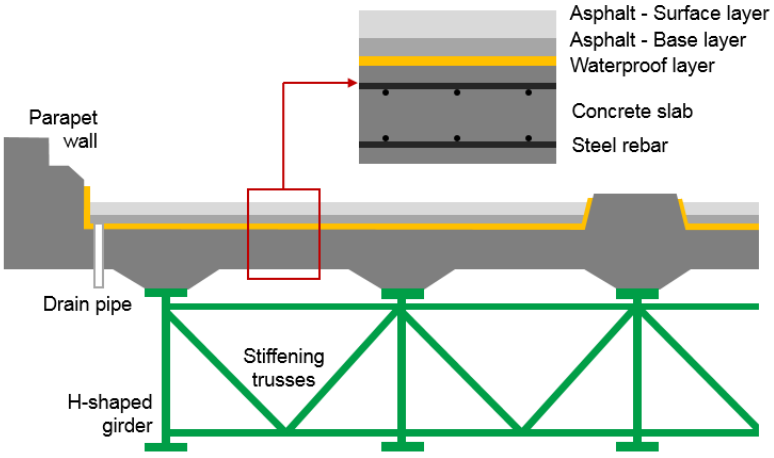

Figure 3-1 Typical cross-section of the bridge structure.

These structural features are standardized to resist the normal Japanese environment and a certain degree of climatic variation. Moreover, this design is durable enough to handle the mechanical damage caused by traffic loads. However, it does not have enough resistance to severe environments. One degradation phenomenon often observed is rust juice from cracks caused by de-icing salt. Normally, *NaCl* is used for de-icing. In Japan, the problem of de-icing

salt damage increased after the prohibition of studded tires on April 1991. Two years before this prohibition, the amount of de-icing salt used on national roads in East Japan was around 4500 t/year. From 2006 to 2008, this figure increased by a factor of 4.1, to around 19,500 t/year in average, or 12.11 t per km of road [1]. The Japanese design code for bridges does not account for such high salt concentrations, and thus they pose a threat to existing bridges.

To date, there have been many examples of complex deterioration in bridges in East Japan. Figure 3-2 gives a typical example, which was provided by the Ministry of Land Infrastructure and Transport East Japan Regional Development Bureau. The bridge was used for 36 years, and the average traffic volume was only 12,000 vehicles per day, but serious deterioration occurred [2]. The proposed mechanism is as follows. As Matsui (1987) found, when salt water enters the crack, freezing and thawing, alkali silica reaction (ASR) and rebar corrosion begin to occur. Therefore, cement paste parts are seriously damaged. As a consequence, bending and shear capacity are significantly reduced, and shear punching failure takes place [3] Additionally, soluble components such as $Ca(OH)_2$ and Na_2SO_4 dissolve in water and combine with carbon dioxide in the atmosphere, resulting in efflorescence. The appearance of efflorescence indicates a high probability of crack penetration and water invasion; thus, it is an important degradation indicator in concrete inspection.

Figure 3-2 deterioration example in East Japan

3.3) Data arrangement and description

The analysis object of this study was the bridge panel, which is defined as the slab area surrounded by the main girders and cross girders, as shown in Figure 3-3. Each deck slab featured multiple panels, which were considered independent objects. Studies have shown that panels in different positions show different deterioration rates. Consequently, the panels were separated into two groups, depending on whether they were in the centre of the slab.

The inspection standard for RC deck slab panels is shown in Table 1. The panel condition is classified into five categories, from sound to damaged. An RC deck slab is defined as 'failed' if the rating is C or worse in this analysis. This condition is defined as the occurrence of an event in the survival analysis. As previously explained, water leakage and efflorescence strongly accelerate the progress of deterioration. Thus, this threshold is reasonable for defining the event.

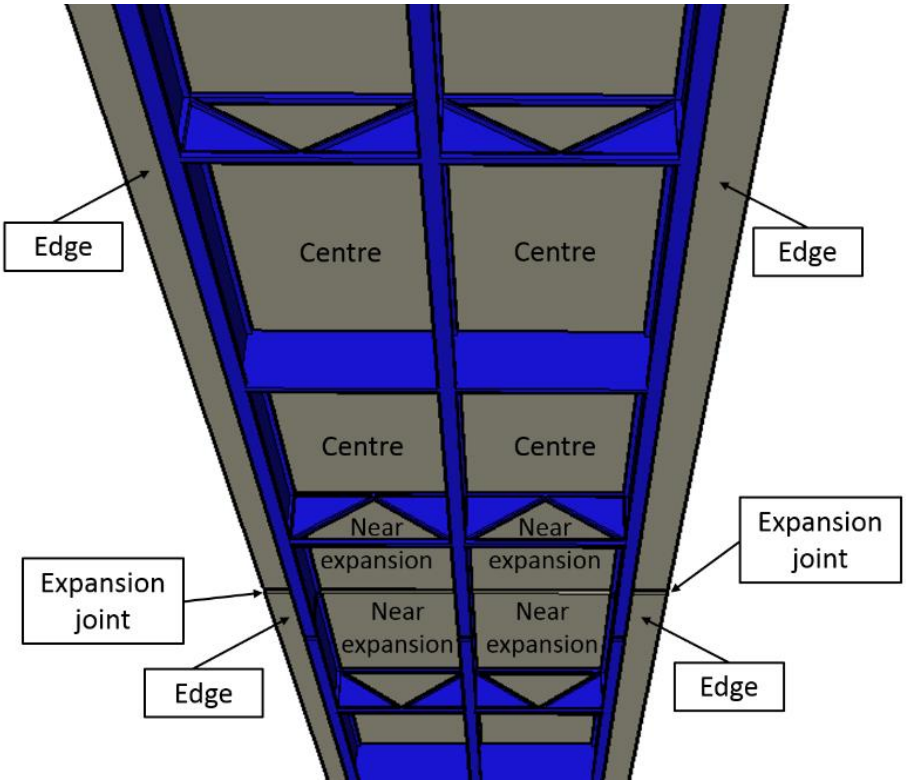

Figure 3-3 Definition of panel

Table 3-1 Inspection standard of reinforced concrete (RC) deck slab panel in East Japan.

Rating	Condition of RC Deck Slab
a	No failure
b	–
c	Water leakage from cracks is observed, but rust fluid is not observed
d	Efflorescence from cracks is observed, but rust fluid is not observed
e	Severe water leakage or efflorescence from cracks is observed Water leakage contains a considerable amount of rust fluid or mud

For the dataset, national road inspection data were used. Since the data were obtained from the current maintenance database, influential factors affecting slab deterioration such as poor material properties (shrinkage), inadequate pouring procedures, etc. is not available. So, as the first step, we only focus on structural features and environmental conditions. In Japan, national

roads are maintained by the local MLIT bureau. Inspections began only in 2003; thus, if a bridge was constructed in 1960, the first inspection was over 40 years after construction. Therefore, the earlier the construction year of the bridge, the longer the time before the first inspection, which means that the survival time cannot be obtained precisely. To mitigate the impact of this long blackout period while ensuring a reasonable amount of data, and also because repairs (which affect the precision of survival time calculations) were frequently conducted before 1980, only bridges constructed after 1980 were included in our dataset. In addition, environmental data such as precipitation, which are published by Ministry of Land, Infrastructure, Transport and Tourism, are available only from 1980.

In Yamazaki et al. (2015), if one bridge component was inspected multiple times, the continuous inspection record was treated as several independent data [4]. Therefore, each component could have several survival times (or censoring times). For example, as Figure 3-4 shows, if a panel was inspected three times, there are three survival times (or censoring times) in the dataset. This assumption is convenient for data sorting. However, theoretically, from the definition of the basic concept, one element can have only one survival time or censoring time. Thus, the previous data sorting method contradicted the basic concept of survival time.

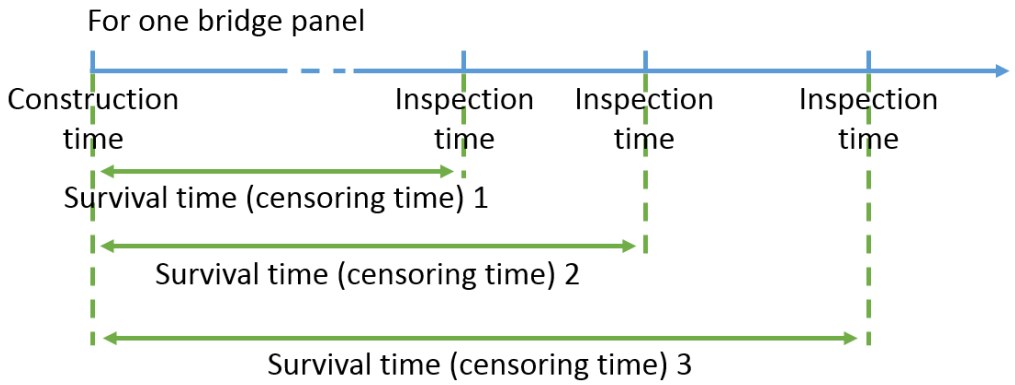

Figure 3-4 Previous survival time calculation (from Yamazaki and Ishida (2015)).

To obtain a more rational survival time (or censoring time), each continuous observation of each object was first treated as a separate datum, and pre-survival time was calculated as shown in Figure 3-5. One pre-survival time was then selected as the true survival time. As Case 1 shows, 0 represents the non-occurrence of the event, and 1 represents its occurrence. For each panel, if the event did not happen in the inspection period (all of the data are censored), the period between the construction time and latest inspection time was the survival time (properly speaking, the censoring time) of this object. For case two, if the event occurred, the period between the construction year and the time the event first occurred was the survival time.

Multiple survival times or censoring times for one object lead to redundant data, which could lead to imprecision in the KM curve and incorrect multivariate analysis results. Figure

3-6 shows the result of comparing KM curves; the red line presents the KM with redundant data, and the green line presents the KM curve after data cleaning. The dotted line shows the 95% confidence interval. It can be clearly seen that after data cleaning, the declination of the KM curve changed, indicating that the data cleaning process was necessary. Before data cleaning and sorting, the dataset included inspection data for 82,016 panels in 525 steel girder bridges. After selection and cleaning, our dataset included 17,557 panel inspection records for 183 bridges. The construction year distribution is shown in Figure 3-7.

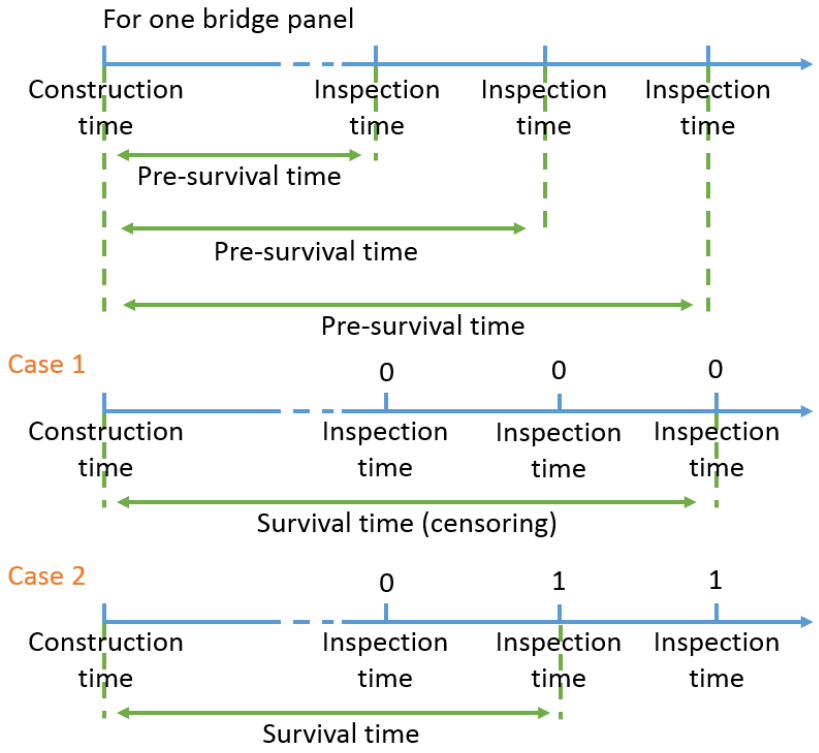

Figure 3-5 Calculation of survival time.

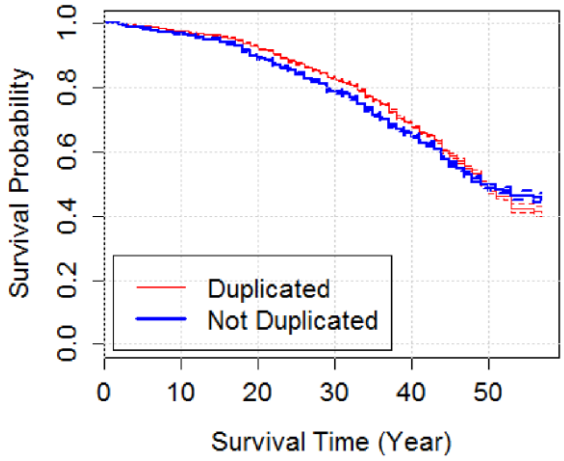

Figure 3-6 Comparison of the Kaplan–Meier (KM) curve with and without redundant data.

Multiple variables relating to bridge slab deterioration were used as explanatory variables. Structural features and environmental conditions including precipitation over four seasons,

winter temperature, etc. were considered and selected as variables. National Land Numerical Information published by the Ministry of Land, Infrastructure, Transport, and Tourism was used for weather data accumulation. These data were generated from observations by the Japan Meteorological Agency between 1981–2010. The resolution of these covariates is a 1 km mesh, and they were numerically analyzed to correct for the effects of topography and elevation. Using Rstudio Version 1.0.143, and referring to the bridge coordinates added by Iwaki et al. (2013), this National Land Numerical Information was combined with inspection records [5].

However, precise multivariate analysis results are difficult to obtain due to high correlation between some variables. In our dataset, environmental data such as precipitation over four seasons and winter temperature were highly correlated; therefore, without appropriately selected variables, univariate and multivariate analysis led to paradoxical results. For example, a univariate analysis of precipitation over four seasons showed an increase in the hazard ratio, while multivariate analysis showed that the risk of some variates tended to decrease. This unexpected result implies that the selection of an appropriate explanatory variable was a precondition for obtaining good results. In this analysis, the correlations of all of the variables below 0.5 were selected as explanatory variates.

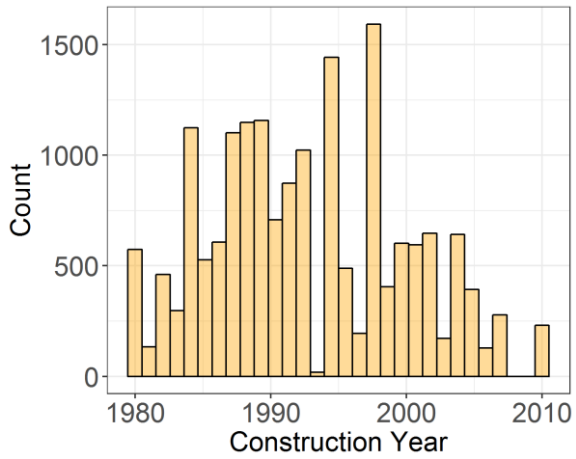

Figure 3-7 Construction year of panels in East Japan.

The covariates used in analysis are shown in Table 3-2. They were recorded as numerical and categorical covariates. All of the numerical covariates were standardized and are presented in the methodology section. Additionally, the unit, mean value, and standard deviation of all of the numeric variables are shown in the table. For categorical covariates, the crossing condition, panel position, slope, de-icing salt usage, and waterproof layer installation situation were separated into different groups. The definition for each group is also shown in the table. List-wise case deletion was executed for records with insufficient information.

In addition, as stated earlier, the inspection years of the data were 2003 to 2013, which is more than 20 years later than the construction years. Thus, some groups constructed earlier show longer survival time distribution. To solve this problem, the Cox stratified model was introduced to the analysis [6, 7]. This model allows a factor to be adjusted for without estimating its effect. The construction year was stratified in this analysis. For parameter estimation, if the data are stratified for g groups, the likelihood function can be written as follows:

$$\mathrm{L}(\beta) = \prod_{g=1}^{G} L_g(\beta) \tag{3-1}$$

$L_g(\beta)$ is the likelihood from stratum g.

Table 3-2 Variables used in analysis in East Japan.

	Name of Variable	**Unit/Code**
Objective variable	Bridge age	Year
	Event	0 = rating a and b 1 = rating c, d, and e
Numerical covariates	Number of vehicles	Unit: vehicles per day (whole cross section) Mean: 14,401.73 Standard deviation: 8260.05
	Span length	Unit: m Mean: 38.57 Standard deviation: 10.15
	Slab thickness	Unit: cm Mean: 22.39 Standard deviation: 1.66

	Winter precipitation	Unit: mm per season Average precipitation from December to February Mean: 287.34 Standard deviation: 178.83
Categorical covariates	Crossing condition	River: crossing over river and pond Overpass: crossing roads and railways Unknown
	Edge	Yes: the panel is at the edge of the slab No: the panel is at the centre of the slab
	Near expansion	Yes: the panel is near the expansion joint No: the panel is not near the expansion joint
	Slope	Below 1.0: slope less than 1.0% Over 1.0: slope more than 1.0% Unknown
	De-icing salt	Below 20: less than 20 t/km Over 20: more than 20 t/km
	Waterproof layer	Yes: installed waterproof layer No: not installed waterproof layer

3.4) Result for East Japan

In Figure 6, the red line represents the KM curve of all of the panels. Survival probability declined to 50% after approximately 25 years, implying that the deterioration rate is faster than in the Tokyo region, as will be shown in the next chapter. The representative KM of some category variables with very different survival probability declinations are shown in Figure 3-8. Figure 8a shows results based on whether panels are on the edge. Figure 8b shows results based on whether the panels are positioned near the expansion joint. Figure 8c presents the survival probability of two de-icing groups, below and above 20 t/km. The survival probability

declination of these variables was found to be very different, indicating that these factors could strongly affect the deterioration rate.

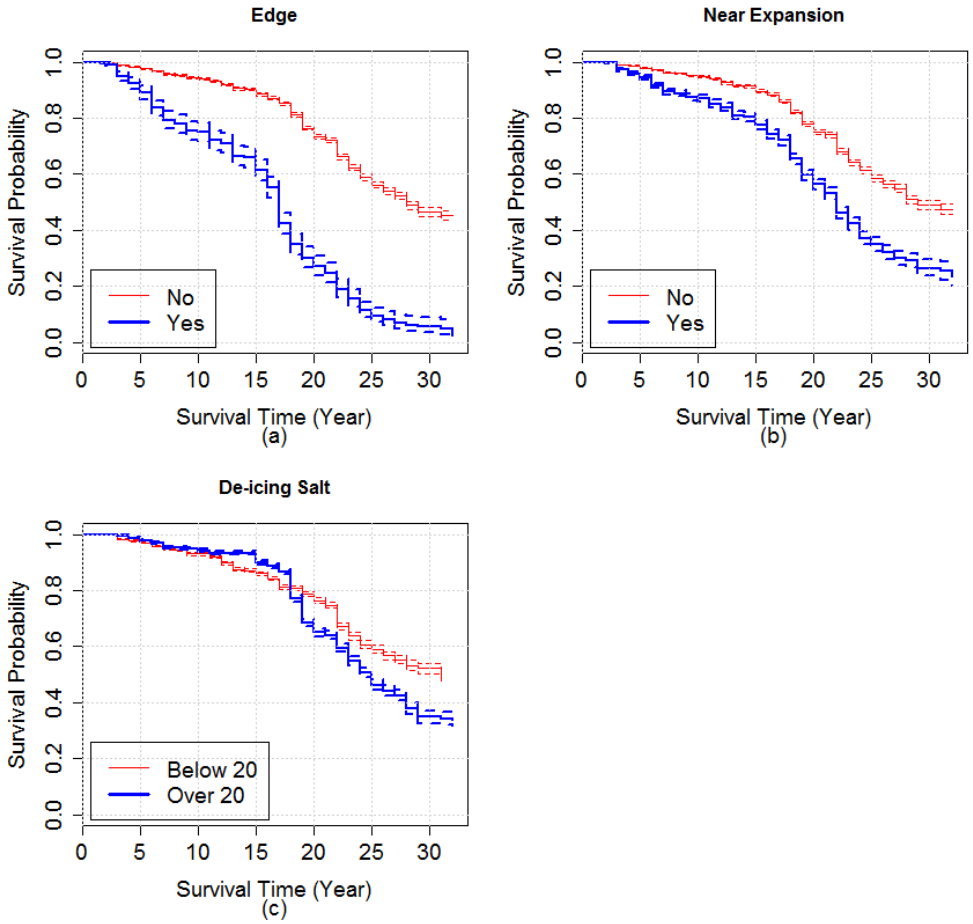

*Figure 3-8 Survival probability of some category variables in East Japan; (**a**) edges; (**b**) near expansion; (**c**) de-icing salt.*

The univariate analysis gave us a general understanding of the explanatory variables, separately and on one side. The KM curve confirmed the basic information of each category description variable and roughly plotted the deterioration rate. However, to evaluate the effect of all of the factors and determine the relationship between all of the explanatory variables, a multivariate analysis was performed; the result is shown in Table 3-3.

According to site condition and our data, the traffic in this region is 14402 per day for average, which is much more less than Tokyo region (44962 per day for average), but the deterioration is still happened. And many research mentioned about the harsh environment condition of this region [8, 9]. Therefore, we combined the climate data from national land science and institute, then the univariate analysis result is conducted.

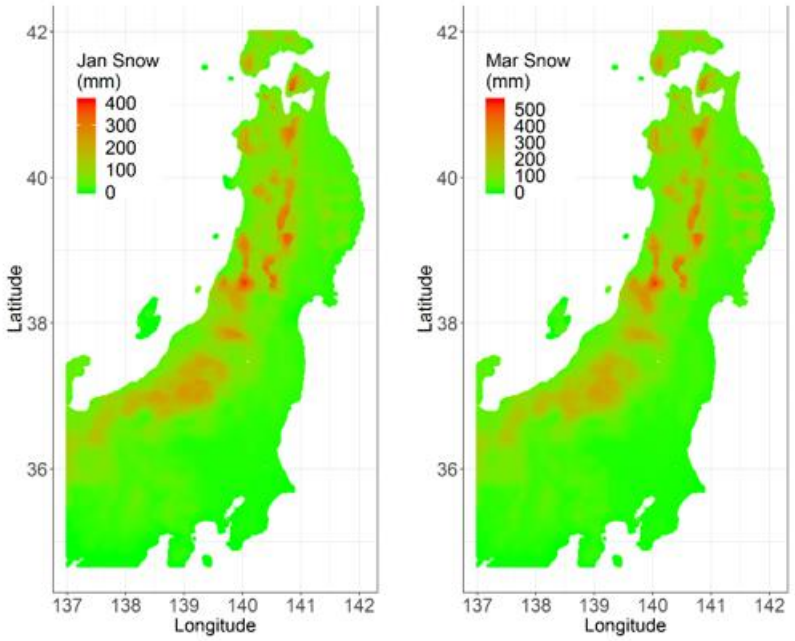

Figure 3-9 Snow depth distribution in East Japan

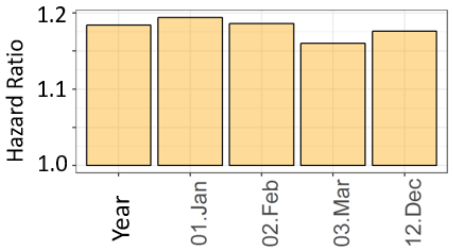

Figure 3-10 Hazard ratio of snow depth in East Japan

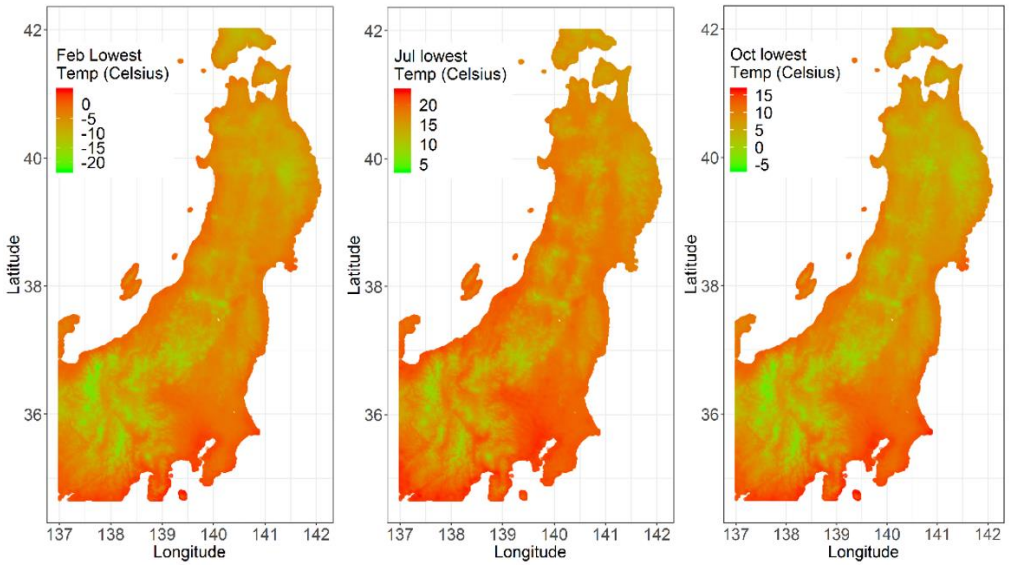

Figure 3-11 lowest temperature distribution in East Japan

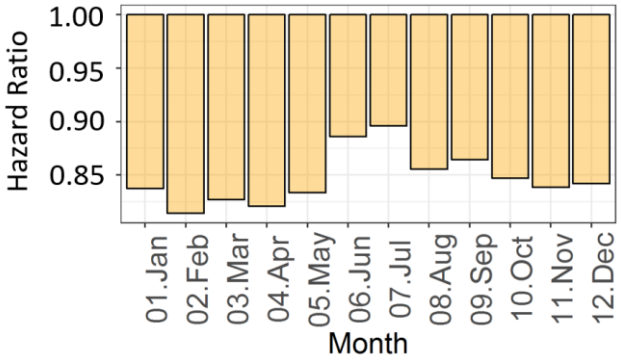

Figure 3-12 hazard ratio of lowest temperature in East Japan

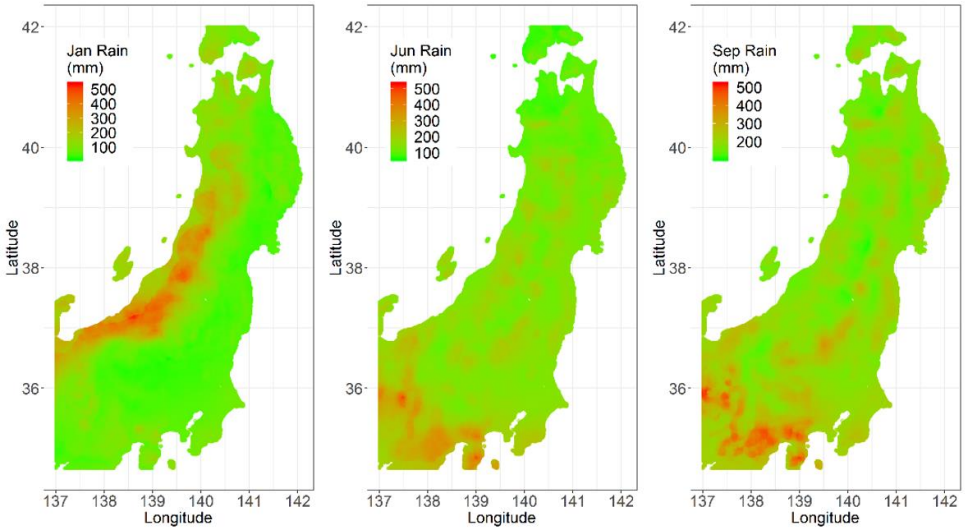

Figure 3-13 precipitation distribution in East Japan

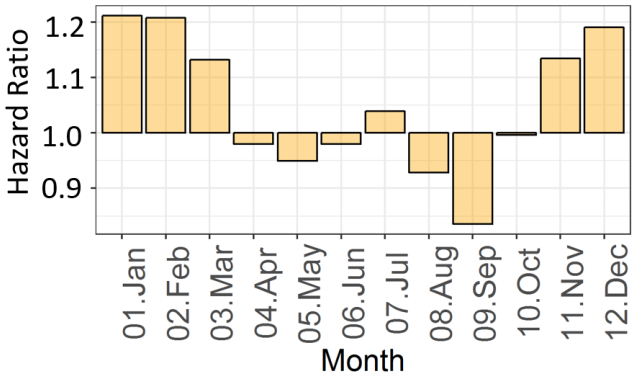

Figure 3-14 hazard ratio of precipitation in East Japan

Figure 3-9 shows the snow depth of East Japan, and Figure 3-10 shows the hazard ratio of univariate analysis result. It can be seen that in all time period, the hazard ratios increase along with the snow depth increases. Figure 3-11 shows the lowest temperature distribution of and Figure 3-12 shows the hazard ratio of every month. The hazard ratios decrease along with the lowest temperature increases. Correspondingly, the winter precipitation also increases the risk (Figure 3-13 Figure 3-14). But unfortunately, these variates are highly correlated. Therefore,

the precipitation which represent the overall impact of the environment on the bridge deck has been selected to conduct the multivariate analysis.

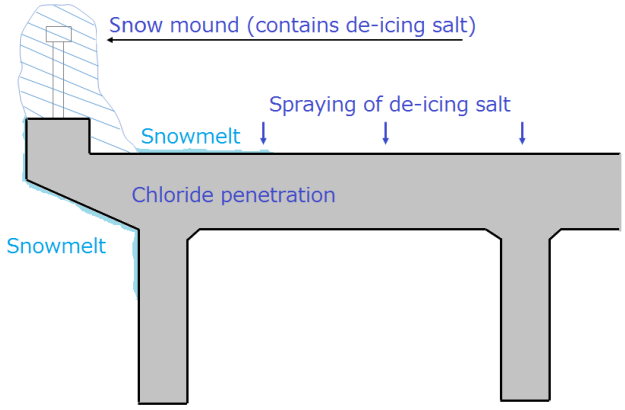

Figure 3-15 Mechanism of salt damage for slabs in East Japan.

The hazard ratio is interpreted as the ratio of the possibility of degradation over any time duration. The p value is from the Wald test, and determines the significance of the results. The equation is as follows:

$$p\ Value = \frac{(\hat{\beta} - \beta_0)}{\widehat{se}(\hat{\beta})} \sim \mathcal{N}(0,1) \tag{3-2}$$

Essentially, it tests whether $\hat{\beta}$ is statistically equal to β_0. In this analysis, β_0 always equals 0 because the hazard ratio is calculated using $exp(\hat{\beta})$. Therefore, the p value indicates whether $\hat{\beta}$ significantly contributes to the hazard ratio.

For numerical explanation variables, an increase in traffic volume slightly increased the hazard ratio. Moreover, the average slab thickness in East Japan was 22.4 cm, and the hazard ratio of the slab thickness was close to 1; the p value also showed that $\hat{\beta}$ did not make a significant contribution to the hazard ratio. This result implies that fatigue damage was not a major reason for the deterioration of the bridge slabs. However, winter precipitation and high de-icing salt usage greatly increased the risk of deterioration. The reason is shown in Figure 9. Due to heavy snowfall and snow removal, snow accumulated at the edge of the slab and became a snow mound. The snow mound melted little by little, and during this process, snowmelt with a large quantity of de-icing salt penetrated the crack, keeping the slab in a condition of consistently high humidity and salinity and resulting in further cracking and steel corrosion. Therefore, deterioration greatly accelerated.

Overpasses showed a smaller hazard ratio from the engineering point of view, while bridges constructed across rivers had relatively high humidity. Different panel positions had different hazard ratios. Panels near the expansion joint or edge showed high risk, as water could

easily contact the slab area through the expansion joint and penetrate the concrete near the edge of the slab, causing steel corrosion and concrete spalling. Slabs with waterproofing showed lower risk, meaning that a waterproof layer could improve slab durability. These results indicate that waterproofing should have been improved at the edge of the slab to increase durability. In addition, they show that a sloped slab had a lower risk, as water could not easily accumulate on it.

Table 3-3 Multivariate Cox regression analysis result for East Japan.

	Hazard Ratio	**Lower 0.95**	**Upper 0.95**	***p* Value**
Traffic	1.119	1.078	1.161	0.000
Span Length	0.907	0.877	0.938	0.000
Slab Thickness	0.966	0.931	1.002	0.067
Winter Rain	1.305	1.253	1.359	0.000
De-icing Salt				
Below 20	1.000			
Over 20	1.331	1.236	1.434	0.000
Crossing Condition				
River	1.000			
Overpass	0.951	0.880	1.028	0.209
Unknown	0.852	0.726	0.999	0.049
Edge				
No	1.000			
Yes	3.840	3.467	4.254	0.000
Near Expansion				
No	1.000			
Yes	1.645	1.532	1.766	0.000
Slope				
0.0–1.0	1.000			
Over 1.0	0.798	0.740	0.861	0.000
Unknown	3.730	3.076	4.521	0.000
Waterproof				
Yes	1.000			
No	1.377	1.259	1.505	0.000

The hazard function for survival analysis with multiple variates is defined as $h(t) = h_0(t)e^{\sum_{i=1}^{n} x_i\beta_i}$. $h_0(t)$ is called the baseline hazard. The baseline hazard does not depend on covariates; instead, it depends on time. $e^{\sum_{i=1}^{n} x_i\beta_i}$, which is called the risk score, is the total risk for each bridge. In other words, if the bridge has a large $e^{\sum_{i=1}^{n} x_i\beta_i}$, it statistically has a high

deterioration risk. Figure 3-16 gives the risk score distribution of all of the bridge slab panels. The risk scores were then divided into four approximately equal parts. The table within the figure shows the risk score range and data quantity of each level. Using the geographical coordinate information, risk scores were plotted in Google Maps (see Figure 3-17). The risk scores increase as the colors change from green to red. The Japan Sea side shows a higher deterioration risk than the Pacific side. Geographically speaking, East Japan is divided into the Japan Sea and Pacific sides along the Ou Mountain Range. As the dry seasonal wind from the north crosses the Japan Sea, it absorbs moist air, and clouds form. This moist air cloud is further enhanced by the ascending air current as it passes over the Ou Mountain Range, and more snow is precipitated during the process. After crossing the mountain range, it becomes dry air, and reaches the Pacific side. Therefore, snows are very heavy on the Japan Sea side, and a large amount of anti-freezing agent spray is required. On the Pacific side, because the air is relatively dry, there is less rain and snow. The results indicate that the bridge deterioration was highly influenced by weather conditions.

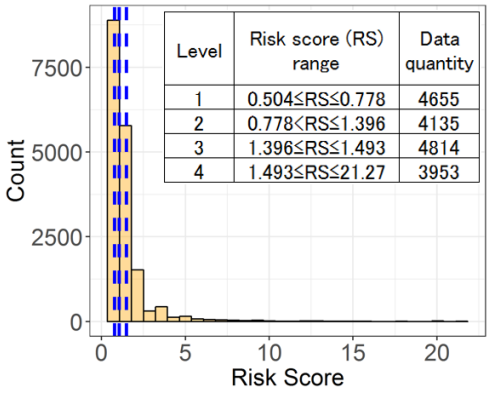

Figure 3-16 Risk score distribution in East Japan.

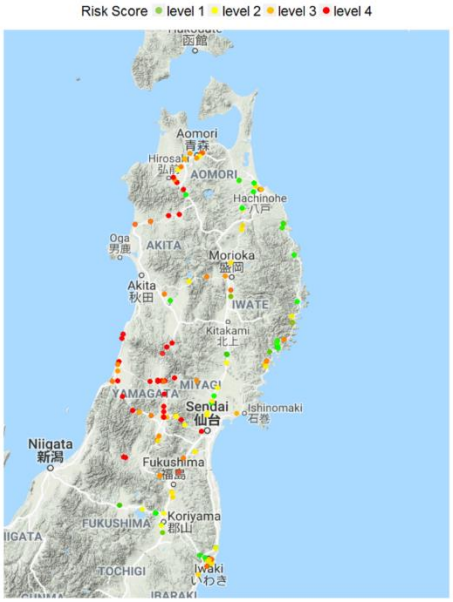

Figure 3-17 Risk score map for East Japan.

3.1) References

1 Shikanai, Y.; Matsuyama, K.; Yamane, S.; Kanemoto, Y.; Ishihara, K. Consideration about maintenance and repair in the concrete bridge where damage from chloride ions contained in the anti-freezing agent. Nippon Koei technical forum, *March 2015,* Nippon Koei Industrial Technology Committee, Tsukuba, Japan

2 Ministry of Land, Infrastructure and Transport East Japan Regional Development Bureau. *Guidance Secure Durability of RC Slabs under Anti-Freezing Agent Diffusing (Draft)*; Cross-ministerial Strategic Innovation Promotion Program; Infrastructure Maintenance, Renovation and Management; 2016 Available online: http://www.jst.go.jp/sip/dl/k07/k07_RC.pdf (accessed on 26 August 2018)

3 *Matsui Fatigue Strength and Effect of Water on Road Bridge RC Deck Slab Suffering Transfer Load*; Japan Concrete Institute: Tokyo, Japan, 1987; pp. 627–632.

4 Yamazaki, T.; Ishida, T. Application of survival analysis to deteriorated concrete bridges in East Japan. *J. Jpn. Soc. Civ. Eng.* **2015**, doi:10.2208/jscejcm.71.I_11.

5 Iwaki, I.; Koda, Y.; Ishikawa, M.; Oyamada, Y. Development of bridges management support tool for the Tohoku region. *Concr. Res. Technol.* **2013**, *24*, 75–87. (In Japanese)

6 Zhang, X., Loberiza, F. R., Klein, J. P., & Zhang, M. J. (2007). A SAS macro for estimation of direct adjusted survival curves based on a stratified Cox regression model. *Computer methods and programs in biomedicine*, *88*(2), 95-101.

7 Fibrinogen Studies Collaboration. (2009). Measures to assess the prognostic ability of the stratified Cox proportional hazards model. *Statistics in Medicine*, *28*(3), 389-411.

8 Tanaka, Y., Ishida, T., Iwaki, I., & SATO, K. (2017). Multiple protection design for durable concrete bridge deck in cold regions. *Journal of JSCE*, *5*(1), 68-77.

9 Matsumoto, J., Takewaka, K., Yamaguchi, T., & Umeki, M. A STADY ON DURABILITY OF CONCRETE STRUCTURES UNDER THE COMPLEX DETERIORATION CONDITION DUE TO CHLORIDE ATTACK AND ALKALI SILICA REACTION.

Chapter 4: Survival analysis result of Tokyo region

4.1) Introduction

The Tokyo expressway is over 330 km long and is under the control of Metropolitan Expressway Co., Ltd. Inspection data on parts of the Metropolitan Expressway's steel bridge deck slab, the Route 3 Shibuya Line and Route 5 Ikebukuro Line, were used for analysis. The construction years of both routes comprised around 1965 to 1975. By processing longitude/latitude coordinates and the management ledger, a detailed environmental/structural dataset was prepared.

As same before, the survival probability and cox regression result are shown. Heavy traffic load is the main reason to cause deterioration in this region. Correspondingly, increasing slab thickness can greatly decrease the deterioration risk. Additionally, by checking the hazard map, since the bridge in north area are newly constructed and the traffic volume are relative small, the risk scores are lower than the centre area of Tokyo.

4.2) Deterioration feature of the Tokyo region

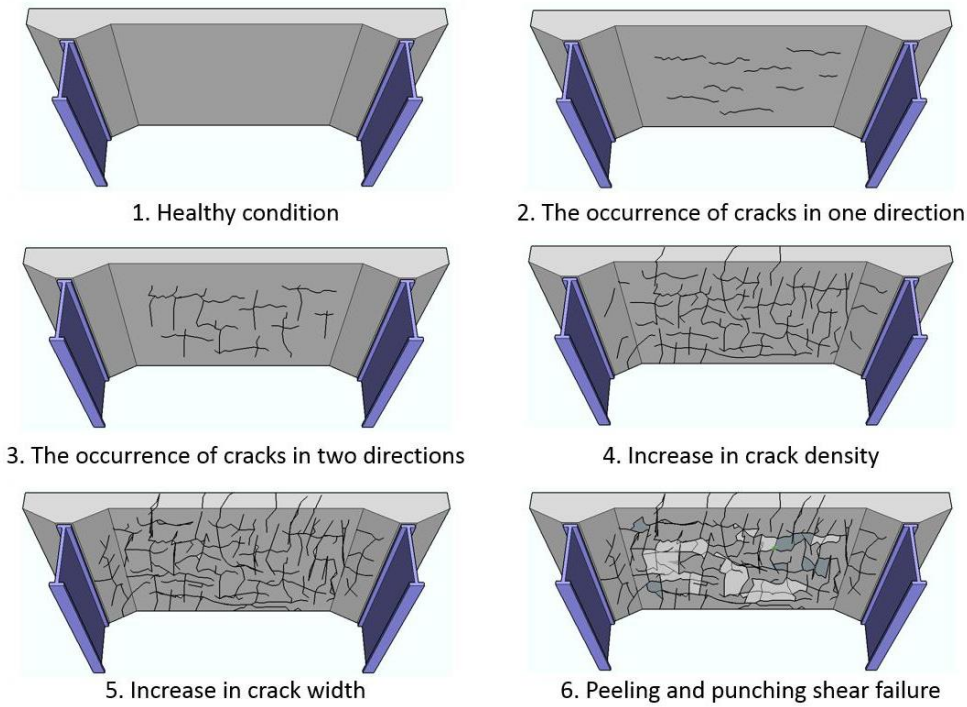

Figure 4-1 Crack progress and deterioration process of an RC slab.

Fatigue damage caused by repetitive vehicular traffic is the main reason for RC slab deterioration in the Tokyo region (Matsui et al. (1986)). [1] After decades of use, these slabs have deteriorated a great deal. Usually, during visual inspection, one and two-dimensional

cracks, water leakage, and efflorescence were observed on the bottom of the slab. As Matsui (1987) stated, in the initial state, deterioration of the slab starts with the appearance of transverse cracks, which is considered as related to shrinkage and construction joints [2]. Since they undergo a heavy traffic volume of around 45,000 vehicles per day on average, transverse cracks gradually increase, and longitudinal cracks also start to appear. As two-dimensional cracks develop further, mesh cracks can be observed. Then, as crack density and crack width increase, punching shear failure ultimately occurs. The process is shown in Figure 4-1. As stated earlier, during this process, water such as rainfall significantly accelerates the deterioration process. In addition to the development of two-dimensional cracks, the interlock effect becomes weak, and shear capacity is decreased. Eventually, punching shear failure occurs. According to this theory, a quantitative deterioration assessment has been done by Eissa et al. (2018) to predict the remaining fatigue life of bridge decks based on their site inspected cracks [3,4]. However, the research is based on mechanics aspects, which did not consider the environment effect. Therefore, this research can be considered a risk assessment by integrating both mechanics and ambient effect. As in East Japan, other factors such as structural features (slope, slab thickness, etc.) also affect the slab degradation rate.

4.3) Data arrangement and description

The inspection standard for highway RC deck slab panels is similar to East Japan. An RC deck slab is defined as 'failed' if two-dimensional cracks and the appearance of efflorescence at the bottom of the slab was observed. This is also the definition of an event in survival analysis, since these phenomena signify the appearance of penetration cracks and water invasion. Under this condition, further deterioration is highly accelerated. Thus, on the basis of the inspection standard, the event was defined as occurring when the slab condition reached this level or worse. This definition correlates with the event definition for the East Japan region. Event occurrence indicates that accelerated deterioration will occur due to a lack of (or inappropriate) repair and rehabilitation. The survival time calculation, data selection, and cleaning process were the same as for East Japan. However, the management level in the Tokyo region was relatively high; repairs were frequently conducted. According to our Tokyo dataset, 49.8% of the panels had been repaired and reinforced.

Table 4 shows repair work in the Tokyo region. If repair was conducted before inspection, the condition of bridge panels would already be improved, greatly changing the deterioration rate and introducing inaccuracies into the analysis. Therefore, it was necessary to consider the repair effect. If the repair work included crack injection, steel plate bonding, replacing and carbon fiber reinforcement, the occurrence of the event was assumed. According to this assumption, if these slab repairs were conducted, a complementary survival time was

calculated. These complementary survival times were then compared with the survival times previously obtained. As Figure 4-2 shows, if it was shorter than the previous survival time, the complementary survival time was chosen as the object's new survival time (Case 1). If not, the previous survival time was reserved as analysis time (Case 2). Moreover, if the data had only a censoring time (indicating the event had not occurred by inspection time) but repair work, which is shown in Table 5, was conducted, the complementary survival time replaced the censoring time (Case 3). The original dataset contained 71,888 data points; after cleaning and selection, 27,041 data points were left. Figure 4-3 shows the construction year distribution of all of the panels.

Table 4-1 Repair types in Tokyo region.

Repairing Types	
Crack injection	Steel plate bonding
Replacement	Carbon fiber reinforcement
Girder repair and construction extension	No repair

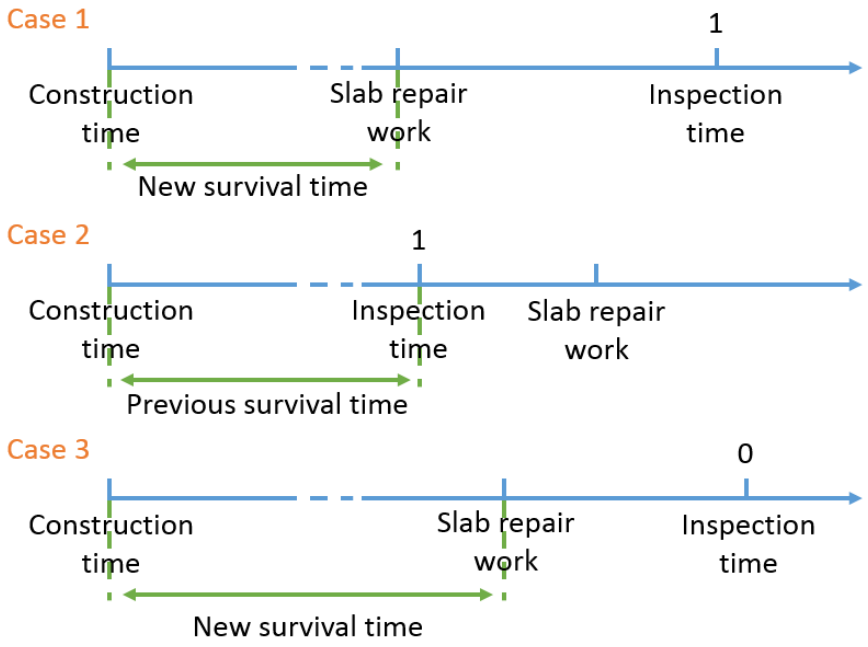

Figure 4-2 Survival time calculation (considering slab repair work).

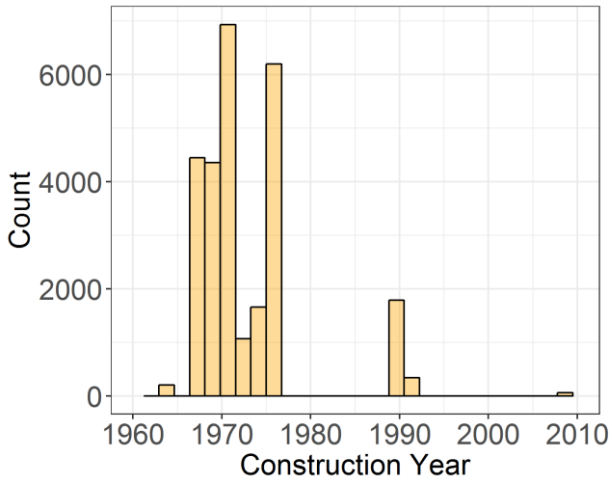

Figure 4-3 Construction year of panels in the Tokyo region.

Variables used in the analysis are shown in Table 5. As for East Japan, the mean value and standard deviation of numeric covariates and detailed definitions of category covariates are also shown. The selection process was the same as for East Japan. The National Land Numerical Information published by MLIT was used for weather data accumulation. As already stated, the bridges of these two regions are governed by different organizations; therefore, the inspection systems are different. East Japan bridge inspection mainly focuses on water leakage and efflorescence. However, Tokyo region bridge inspection not only focuses on efflorescence, it also pays attention to crack density. Therefore, some variables in the dataset were different than for the East Japan dataset. Traffic volume, structural features, panel position, design code, and precipitation were used as variables.

Table 4-2 Variables used in analysis in Tokyo region.

	Name of Variable	**Unit/Code**
Objective variable	Bridge age	Year
	Event	1 = two-dimensional cracks and the appearance of efflorescence at the bottom of the slab
Numerical covariates	Number of vehicles	Unit: Vehicles per day (whole cross-section) Mean: 44,961.71 Standard deviation: 11,528.41
	Span length	Unit: m Mean: 35.00 Standard deviation: 9.69
	Slab thickness	Unit: cm Mean: 19.79 Standard deviation: 2.04

	Winter precipitation	Unit: mm per season Average precipitation from December to February Mean: 158.04 Standard deviation: 5.70
	Slope	Mean: 1.51% Standard deviation: 1.38%
Categorical covariates	Crossing condition	River: crossing over river and pond Overpass: crossing roads and railways
	Edge	Yes: the panel is near the expansion joint No: the panel is not near the expansion joint
	Girder type	Simple: simple girder Continuous: continuous girder
	Design code	Before S39: S31 and S39 After S39: S48, S55, etc.

Design codes were divided into two groups: the first for design codes from 1964 and 1956, and the second for those after 1964 (1973, 1980, etc.). The reason for this division is that major reforms in mechanical resistance specifications occurred after 1964. Table 6 compares the minimum ratio for the distributing bar and slab thickness between different design standards. It can be clearly seen that the amount of the distributing bar specified increased after 1964. Additionally, the minimum slab thickness increased after 1973.

Table 4-3 Comparison of minimum design distributing bar and slab thickness between different design standards.

Standard	Minimum Distributing Bar	Minimum Slab Thickness
1956 1964	25% greater than main rebar	14 cm
1967 1973 1980	70% greater than main rebar	16 cm

Currently, judgment of the cause of deterioration depends on bridge engineers' experience and skills. However, visual inspection and sound testing are inefficient and rely too much on inspectors' personal judgment. In many cases, it was difficult to identify a single factor responsible for deterioration. In such cases, deterioration was simply recorded in the inspection ledger as 'complex deterioration with multiple deterioration factors'. This method would not contribute to efficient maintenance based on the structural and environmental conditions of individual bridges. Thus, identifying predominant risk factors is urgently necessary.

4.4) Results for the Tokyo region

Figure 15a shows the survival probability of all of the bridge panels. The survival probability fell to 50% in 45 years. Figure 4-4 b–d show the survival probability of three category explanation variables: edge, design code, and girder type. For each variable, each group shows a different declination trend, indicating that these groups affect the deterioration rate. In particular, a large gap between design codes is shown in Figure 4-4 c, which reveals that safety was greatly improved by the design code overhaul after 1964. Kawai et al. (2016) also stated that according to their analysis, slabs designed before 1964 showed shorter fatigue life [5].

The multivariate Cox regression analysis result is shown in Table 4-4. Unlike the East Japan results, risk increased more than 30% when traffic volume increased by one standard unit. From the engineering point of view, a slab undergoing frequent wheel load from traffic reaches its fatigue limit faster. However, increasing the slab thickness decreased the risk, because a thick slab has enhanced loading capacity. According to our data, the average slab thickness in the Tokyo region was only 19.8 cm. Thus, unlike in East Japan, repeat traffic loading was a major factor in deterioration. These results reveal that slab thickness should be increased to resist traffic load.

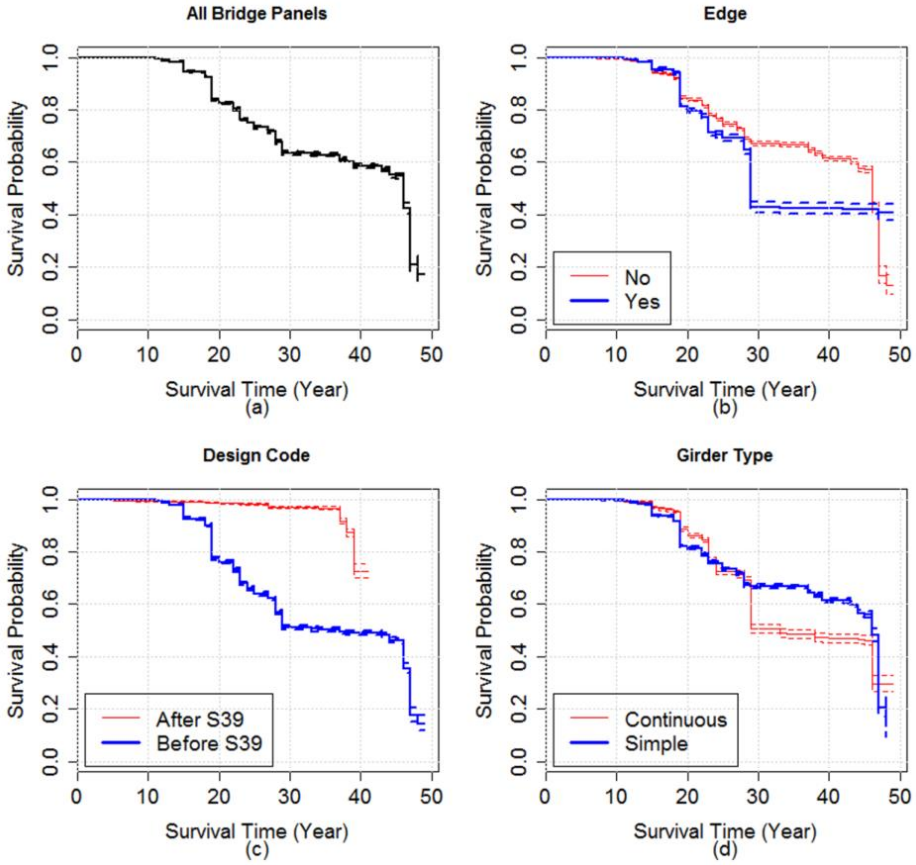

Figure 4-4 Survival probability of some category variables in Tokyo region; (a) all panels; (b) edges; (c) design code; (d) girder type.

As in East Japan, the risk decreased as the slope increased because of faster water runoff. Moreover, winter precipitation showed high risks. Since winter precipitation was highly correlated with precipitation in other seasons, this result indicates that precipitation increased the deterioration rate. As in East Japan, slabs usually have a longer lifespan under relatively low ambient humidity. Okada et al. (1982) pointed out that the degradation rate of reinforced concrete slabs was faster if water was present. If water has sufficiently penetrated the cracks of a concrete slab, there is a possibility of fatigue fracture even under the design load, which is about one fifth of the static stress [6]. Water penetration through cracks probably promotes scratch polishing and high water pumping pressure on the cracked surface, and rapidly increases crack width. Thus, in both East Japan and the Tokyo region, slab deterioration is significantly influenced by water.

Table 4-4 Multivariate Cox regression analysis result of Tokyo region.

Variables	Hazard Ratio	Lower 0.95	Upper 0.95	*p* Value
Traffic	1.357	1.317	1.399	0.000
Slab Thickness	0.621	0.597	0.646	0.000
Winter Precipitation	1.180	1.128	1.233	0.000
Slope	0.808	0.789	0.828	0.000
Span Length	0.965	0.936	0.996	0.025
Edge				
No	1.000			
Yes	1.156	1.099	1.217	0.000
Girder Type				
Simple	1.000			
Continuous	0.756	0.710	0.806	0.000
Design Code				
After S39	1.000			
Before S39	3.923	3.461	4.447	0.000
Crossing Condition				
Overpass	1.000			
River	0.979	0.910	1.053	0.562

Panels at the edge of the deck tended to have a higher likelihood of deterioration, because these panels were more frequently in contact with water such as rainfall. The report from the Chugoku Regional Development Bureau (2016) also revealed that deterioration of the edge of the slab was more serious than in the centre [7].

The results also show that continuous girders had a lower deterioration rate. From the engineering perspective, continuous girders are safer because they have fewer expansion joints. Thus, water has less opportunity to penetrate and contact the unprotected part of the slab. However, as Figure 15d shows, the survival probability declination of continuous girders was

faster. In the specifications for highway bridges [8], the minimum slab thickness designation for continuous girders is smaller than for simple girders, as Table 4-5 shows.

Table 4-5 Design specification of slab thickness for simple girder and continuous girder.

Classification	Span Direction of Slab	
	Orthogonal to Vehicle Traveling Direction	**Parallel to Vehicle Traveling Direction**
Simple Girder	4L + 11	6.5L + 13
Continuous Girder	3L + 11	5L + 13
L: span of the slab against T load (m)		

In terms of the design code, the slab panels constructed according to the Specifications for Steel Highway Bridges issued in 1956 and 1964 showed high risk, indicating that a small amount of distributing bar and thin slab thickness greatly decreases the safety of slabs.

Figure 4-5 shows the risk score distribution of all of the bridge slab panels. Risk scores were again divided into four approximately equal parts. The table within the figure shows the risk score range and data quantity of each level. Using the geographical coordinate information, risk scores were plotted in Google Maps, as shown in Figure 4-6. In the north area, risks were relatively low, but in the central and south parts of Tokyo, risks were high, as the traffic volume in those areas is relatively high. Additionally, most slabs in this area were constructed according to design codes prior to 1964. By referring to the risk score map, a manager can easily determine which part is at high risk. Therefore, the efficiency of inspection and rehabilitation can be improved, and optimal construction decisions can be made.

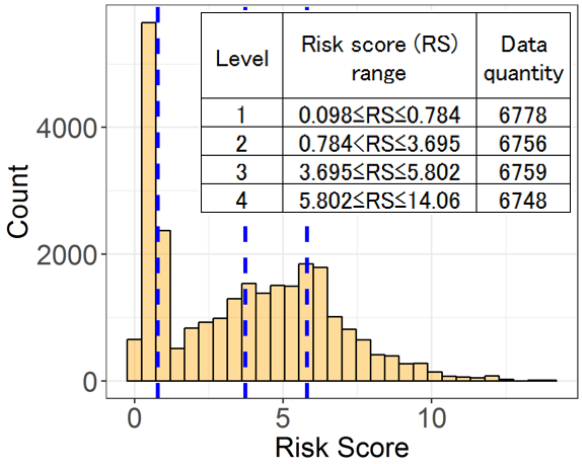

Figure 4-5 Risk score distribution in the Tokyo region.

Figure 4-6 Risk score map of the Tokyo region.

4.5) Comparison and discussion between East Japan and Tokyo region

First, the different deterioration characteristics of different regions were clarified. Reduplicative dynamic traffic load was a major reason for the deterioration of bridge deck slabs in the Tokyo region. However, it was not a high risk in East Japan, because the traffic volume there was not as high as in the Tokyo region. Correspondingly, thicker slabs had much greater loading capacity; therefore, a decreased hazard ratio was evident in the Tokyo region. In East Japan, because of lower traffic volume and thicker slabs, slab thickness was not a major deterioration factor.

Second, water including winter precipitation increased the deterioration rate in both regions. Especially in East Japan, during the extended snow melting process, salt water penetrates into cracks and accelerates the deterioration process. Under this condition, rebar is corroded and slab is seriously damaged unless there is appropriate protection and repair work. Correspondingly, water flow is faster for slabs with greater slopes; thus, the hazard ratio tends to be smaller. Moreover, waterproofing in East Japan reduced risk, indicating the importance of preventing water from penetrating the slab.

Third, panels in different positions had different deterioration rates. Usually, the panel on the edge of the slab or near the expansion joint had high risks because of the high possibility of contact with water. In Tokyo, even panels in the centre of the slab that directly carried heavy traffic loads had a smaller hazard ratio than the edge area. In addition, for both areas, because the water flow was more rapid with a greater slope, the hazard ratio was small. These results

statistically prove that water plays an important role in deterioration. Therefore, waterproofing on the edge should be enhanced against severe environments.

Fourth, using geographical coordinate information, risk scores were mapped; distinctions between high-risk and low-risk areas were shown. In East Japan, due to its special geographical environment, the Japanese seaside is snowy in winter, resulting in the use of large amount of de-icing salt. Therefore, the deterioration condition and rate in this area is relative high. In the south of the Tokyo region, since traffic volume in those areas is relatively high and most slabs in this area were relatively thin according to design codes prior to 1964, the total risk score is high. As a result, through this quantitative multiple deterioration factors assessment, the priority of maintenance in the case of an insufficient budget will be determined by more accurate statistical analysis rather than personal subjective judgment. Briefly speaking, it can be applied to optimize decision-making. Therefore, under the premise of ensuring more efficient and accurate countermeasures, financial burdens can be lessened.

In this study, the risk factors for bridge deck slab components were quantitative evaluated. The results for these two typical regions can be extrapolated to the entirety of Japan and used for optimal decision making. By considering the content and quantity of risk factors, deterioration patterns can be clarified. Therefore, design, maintenance and rehabilitation can be rationalized.

In future research, the amount and quality of covariates should be enhanced in order to improve the analysis precision. For example, some initial variables that significantly affected the speed of deterioration, such as the material properties (shrinkage), inadequate pouring procedures, concrete mixture, and depth of concrete cover were not recorded, so we did not consider these factors. By cooperating with authorities, we can retain and digitize this information for future data-driven bridge maintenance. In addition, for existing covariates, we must improve the data quality to accurately evaluate risk factors; for example, it would be a significant step forward if we could simulate the freeze–thaw cycle by calculating factors such as the concrete surface temperature.

4.6) References

1. MATSUI, Shigeyuki, and Yukio MAEDA. "A rational evaluation method for deterioration of highway bridge decks." *Doboku Gakkai Ronbunshu* 1986.374 (1986): 419-426.
2. Ministry of Land, Infrastructure and Transport East Japan Regional Development Bureau. *Guidance Secure Durability of RC Slabs under Anti-Freezing Agent Diffusing (Draft)*; Cross-ministerial Strategic Innovation Promotion Program; Infrastructure Maintenance, Renovation and Management; 2016 Available online:

http://www.jst.go.jp/sip/dl/k07/k07_RC.pdf (accessed on 26 August 2018)

3. Fathalla, E.; Tanaka, Y.; Maekawa, K.; Sakurai, A. Quantitative deterioration assessment of road decks based on site inspected cracks. *Appl. Sci.* **2018**, *8*, 1197, doi:10.3390/app8071198.
4. Fathalla, E.; Tanaka, Y.; Maekawa, K. Remaining fatigue life assessment of in-service road bridge decks based upon artificial neural networks. *Eng. Struct.* **2018**, *171*, 602–616.
5. Kawai, Y.; Nakamura, S.; Abe, T. A study on the fatigue performance design of RC highway deck slabs based on the required confidence level. *J. Struct. Eng.* **2016**, *62A*, 1160–1167.
6. Okada, K.; Okamura, H.; Sonoda, K.; Shimada, I. Cracking and fatigue behavior of bridge deck RC slabs. In *Proceedings of the Japan Society of Civil Engineers*; Japan Society of Civil Engineers: Tokyo, Japan, 1982; No. 321, pp. 49–61.
7. Road Maintenance Plan Group; Chugoku Regional Development Bureau; Ministry of Land, Infrastructure, Transport and Tourism. *Bridge Repair Plan for Long Span Life*, version 2015; 2016, Road Maintenance Plan Group G; Chugoku Regional Development Bureau; Ministry of Land, Infrastructure, Transport and Tourism, 6-30 Hacchihachihori, Naka-ku, Hiroshima-shi, 730-8530 Hiroshima Joint Government Building 2
8. Japan Road Association. *Specification for Highway Bridges, Part Two: Steel Bridges*; 2012, japan road association, 3-3-1, Kasumigaseki, Chiyoda-ku, Tokyo 100-8955, Japan.

Chapter 5: Feature of survival analysis and necessity of full scale numerical simulation

5.1) Introduction

In this chapter, the advantage and limitation of survival analysis are discussed. Then, in order to supplement the deficiencies of survival analysis, the numerical simulation is induced. Basically, one of the biggest advantages of survival analysis is grasping of the overall situation of the data. However, it cannot give any further prediction [1]. In order to obtain the service life of each individual bridge, numerical simulation is used. Then, the correlation between two methods has also been studied (Furukawa and Ishida, 2019), not only the reliability of the two methods are indirectly confirmed, but also by comparing the fatigue life under dry and wet cases, it shows that stagnant water plays decisive role in deterioration. On this basis, impact of spatially non-uniform stagnant water on fatigue life of RC bridge decks have been investigated (Eissa et al., 2019) [2]. However, the numeric fatigue life simulation only applied the load on the middle of a simple plate. In the actual situation, as the load position changes, the distance between the load and the girder also changes, and it will directly affect the fatigue life. Additionally, since the actual structure is more complicated, the size, shape and boundary condition is totally different comparing with simple plate, the strain and stress distribution, displacement and moment is also different. Therefore, full scale numeric simulation by considering the relation between the position of wheel load, stagnant water and girder is essential.

5.2) The characteristic of survival analysis

In this research, Cox regression are used to evaluate the bridge inspection data of Tokyo and East Japan region. Through the analysis, the result shows that different deterioration characteristics of different regions can be clarified. And by using the equation of hazard function, risk score can be calculated. Then the risk score can be plotted in the map and the high risk zone and low risk zone can be distinguished.

The Cox model has 3 main advantages [3]. First, it allows us to take into account all the objects even if they were not observed for the same period of time and even if the studied event (next calving) did not take place before the end of the survey. Second, it does not require the division of the studied variable into discrete classes. This is an advantage as it allows us to keep the information as precise as possible and eliminates the always difficult problem, of which group end points to choose. Finally, it allows us to formulate the results according to the increase in the studied time interval in d when the factor is present [4].

Despite all these advantages the use of the Cox model is very limited by its very restrictive application conditions (the hazards should be proportional). If the studied variable consisted of a large number of classes, the hazards were rarely proportional all along the curve. Even if the hazard ratio can give an overall assessment, but still the individual differences cannot be accurately revealed. Additionally, for bridge assessment, the fatigue life of individual bridge or slab need to be calculated in order to make reasonable repairing and rehabilitation plan.

Cox regression, which can only give the relative deterioration rate of each selected variables. For example, if the hazard ratio of no expansion group is 1 and the group with expansion is 1.287, it means that the deterioration rate of the group with expansion is 28.7% higher than the no expansion group, but the service life of the both group cannot be obtained.

5.3) Current numerical simulation

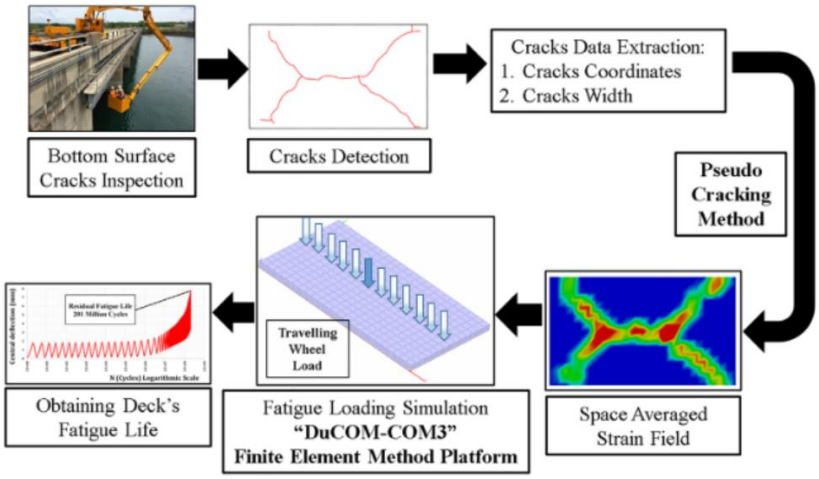

Figure 5-1 Overview of remaining fatigue life prediction methodology

In order to obtain the service life of individual bridge, the numerical simulation is induced. In the past decade, some long term performance simulation has been upgraded, and its practical application is being discussed in more detail on the scheme of asset management. The inspection data assimilation of current damages like cracks, material properties and magnitude of traffic loads with life simulation technology has been developed such as the pseudo-cracking method. The data assimilation technology with the use of multi-scale simulation grogram and pseudo-cracking method was verified, and it can be used to predict the remaining fatigue life of deck slab of bridges in previous research under some limited conditions. And Figure 5-1 shows the overview of remaining fatigue life prediction methodology.

5.4) Current management system

As mentioned before, survival analysis cannot give any further prediction. In order to obtain the service life of each individual bridge, numerical simulation is used. Because both of the methods are the used to assess the deterioration of the bridge, in previous research, in order to develop an efficient inspection system, the prediction accuracy of the two method are examined. Here, a comparison of the two methods is conducted by analyzing RC decks in Tokyo region. Based on previous research (Fathalla et al. 2019) [5], it has been demonstrated that the deterioration of RC decks can be greatly accelerated under stagnant water. To confirm the effect of stagnant water, the comparison is executed for both dry and water-submerged states.

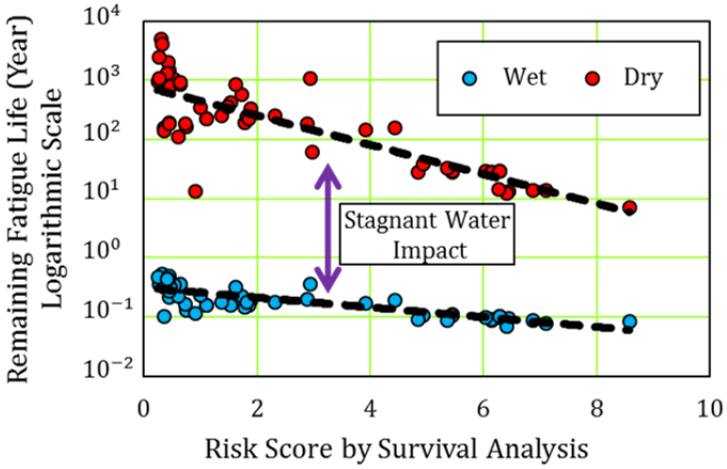

Figure 5-2 Comparison of dry and wet environmental condition for the analysed RC decks

Because fatigue failure is main reason to cause the deterioration of RC bridge in Tokyo region (Fang et al. 2018) and up to now our ANN models can only deal with specific environmental condition. Therefore, in this research, data of RC slab from Metropolitan Expressway is random selected. The analysis object is panel, which is defined as an area surrounded by longitudinal-main girders and transverse-cross girders. For survival analysis, all data include Line 3 and Line 5 are simulated in the same process which have been done before to calculate the risk score (Fang et al. 2018) [6]. Then, 55 panels under different situations are selected. On the other hand, for ANN model, not only structure information but also the crack information which can be extracted from slab bottom side photos are used to conduct ANN models. However, since the crack width cannot be collected from the photo, all crack width is assumed as 0.1mm for simplification base on the previous site investigation. This value is reasonable in terms of engineer's judgement. The comparison result of dry case and wet case is shown in Figure 5-2. The vertical axis expresses the remaining fatigue life estimated by ANN model in dry case in logarithmic scale and the horizontal axis expresses the risk score calculated by survival analysis. High risk score means serious deterioration possibility. So theoretically

speaking, high risk score means a short remaining life. Although the two methods are completely different, it can be seen that as the risk score increases, which indicates that the reliability of both terminologies are demonstrated. Additionally, fatigue life in dry case is 100 times higher than fatigue life in wet case, indicates that RC deck slab is extremely dangerous under wet case. It can be concluded that waterproof has a very large inhibitory effect on bridge deck slab deterioration since it can stop the stagnant water from concrete.

Based on the above result, survival analysis and numerical analysis are used to build a more complete management system. Figure 5-3 shows the current proposed management system. Firstly, the site inspection of bridges is periodically conducted and data are accumulated. The data describes the overall structure of the bridge, traffic volume and material properties information. By combining the information of the climate data from national land science and institute, survival analysis is conducted to evaluate the hazard ratio of groups and risk score of each bridges. For some bridge which have high risks, non-destructive investigation like 3D radar are used to get more information about the bridges. Then by using the fatigue life evaluation and AI model, the fatigue life of each high risk bridge can be calculated. Based on these information, repairing and rehabilitation are planned.

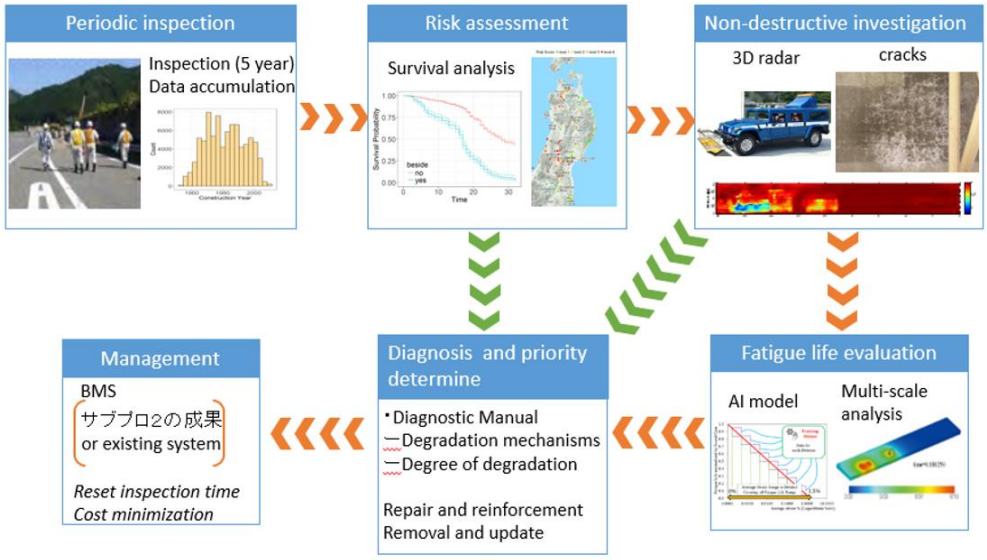

Figure 5-3 Current proposed bridge management system

5.5) Objective of full scale numerical simulation

Up to now, the numeric fatigue life simulation only applied the load on the middle of a simple plate [7, 8]. In the actual situation, as the load position changes as Figure 5-4 shows, the distance between the load and the girder also changes, and it will directly affect the fatigue life. Additionally, since the actual structure is more complicated, the size, shape and boundary condition is totally different comparing with simple plate, the strain and stress distribution, displacement and moment is also different.

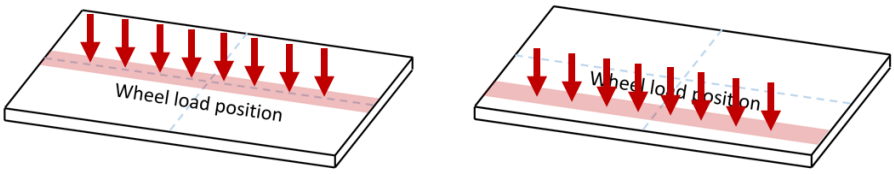

Figure 5-4 Fatigue analysis under different wheel load position

Therefore, full scale numeric simulation by considering the relation between the position of wheel load, stagnant water and girder is essential. The purpose of the study is to conduct a more accurate analysis of the life of the bridge under the premise of dry and wet case by considering the boundary conditions of the actual bridge and the distance between the vehicle load position and the girder.

Additionally, the credibility and precision of survival analysis are highly depended on the on-site inspection and inspection data. Currently, the top surface of the slab cannot be observed because of the pavement. Current inspection mainly only can check the condition of bottom side of the slab. If the on-site inspection cannot accurately reflect the degree of deterioration of the bridge deck, the accuracy of the survival analysis will be correspondingly reduced. In particular, if data such as vehicle weight and crack patterns cannot be recorded, the impact of such factors cannot be considered in the survival analysis. Therefore, the inspection deficiency and available range of survival analysis need to be investigated.

5.6) References

1. Kattan, M. W. (2003). Comparison of Cox regression with other methods for determining prediction models and nomograms. *The Journal of urology*, *170*(6), S6-S10.
2. Fathalla, E., Tanaka, Y., & Maekawa, K. (2019). Fatigue life of RC bridge decks affected by non-uniformly dispersed stagnant water. *Applied Sciences*, *9*(3), 607.
3. Bugnard, F.; Ducrot, C.; Calavas, D. Advantages and inconveniences of the Cox model compared with the logistic model: Application to a study of risk factors of nursing cow infertility. *Vet. Res.* **1994**, *25*, 134–139.
4. Lee et al, 1989 Lee LA, Ferguson JD, Galligan DT (1989) Effect of disease on days open assessed by survival analysis. J Dairy Sci 72, 1020-1026
5. Fathalla, E., Tanaka, Y., Maekawa, K., Sakurai, A. (2019). "Quantitative deterioration assessment of road bridge decks based on site inspected cracks under stagnant water." J. Adv. Concr. Technol., 17(1), 16–33.

6. Fang, J., Ishida, T., & Yamazaki, T. (2018). “Quantitative Evaluation of Risk Factors Affecting the Deterioration of RC Deck Slab Components in East Japan and Tokyo Regions Using Survival Analysis.” Applied Sciences, 8(9), 1470.
7. Fathalla, E., Tanaka, Y., Maekawa, K. (2018). “Remaining fatigue life assessment of in-service road bridge decks based upon artificial neural networks.” Engineering Structures, 171, 602-616.
8. Fathalla, E., Tanaka, Y., Maekawa, K. (2018). “Quantitative deterioration assessment of road bridge decks based on site inspected cracks.” Applied Sciences, 8, 1197.

Chapter 6: Methodology of full scale numerical simulation

6.1) Introduction

In this chapter, the outlines the method of reproducing the fatigue phenomenon of concrete, which is slab fatigue durability evaluation system by numerical analysis is induced. Firstly, the basic concept and law of numerical scale simulation are presented in order to allow readers to understand the entire calculation algorism more clearly. Then the bridge model which include size, reinforcement information, loading information for numerical simulation are introduced. Additionally, to save massive computation time, the beam elements are used to replace part of the solid elements.

6.2) Methodology for numerical simulation

High cycle fatigue damage of concrete means that not only plastic deformation due to repeated one-dimensional tensile or compressive load progresses but also the elastic rigidity decreasing during unloading and reloading gradually develops due to the development of micro cracks inside the concrete. In the numerical analysis, fatigue is incorporated as a fracture parameter for each of the basic constitutive laws of compression and tension, and the decrease in rigidity due to bond fatigue between reinforcing bars and concrete is reflected in the analysis as damage on the tensile side.

On the other hand, the shear stress transmission mechanism in the direction along the crack surface of concrete is generated by the meshing of the crack surfaces in ordinary concrete containing aggregate. The high cycle fatigue of the shear transmission mechanism is a phenomenon in which the meshing action is reduced due to abrasion and smoothing. In the numerical analysis, along with the physical mechanism, the relationship between the shearing stress transmitted with the crack width normalized and the deviation of the crack surface is formulated. Also, under fatigue loading, a micro-damage term that reduces the shear stress transmitted according to the number of repetitions is introduced.

Three-dimensional nonlinear finite element analysis COM3 can handle the behaviour of concrete elements from before cracking to after cracking consistently from these three basic constitutive laws.

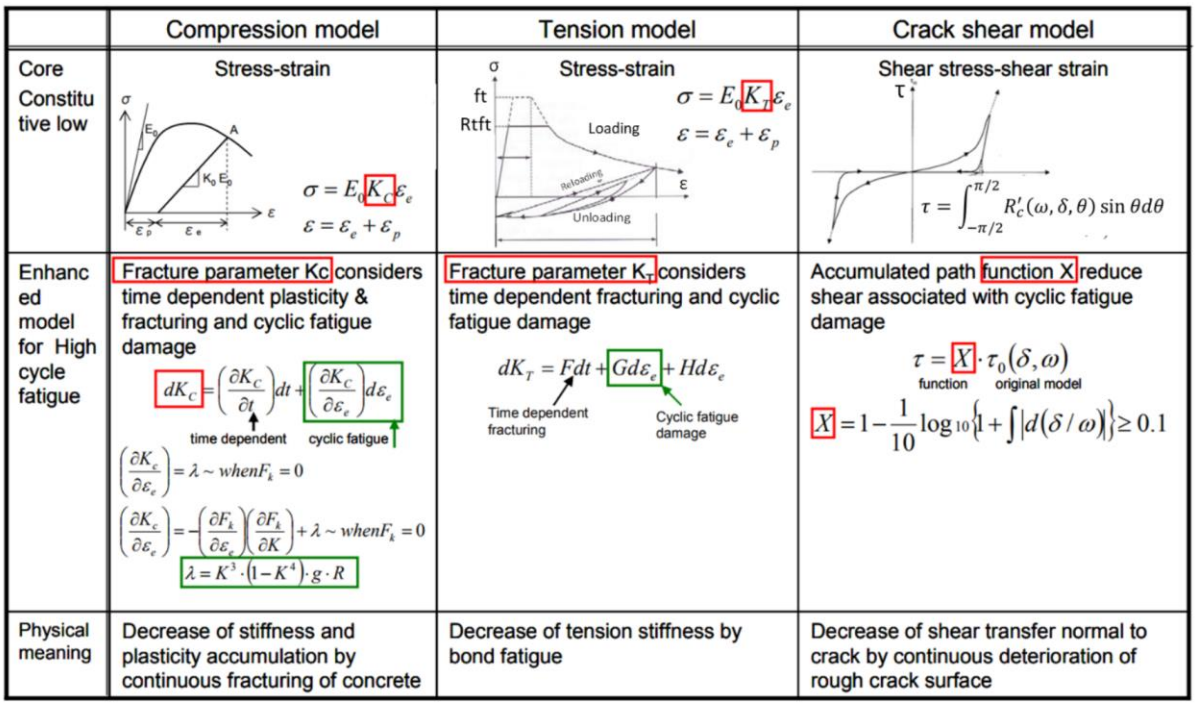

Figure 6-1Constitutive laws of cracked concrete for high cycle fatigue

For fatigue load simulation, the full scale simulation program is used. The method is widely validated by previous research [1-5]. Figure 6-1 shows the set of constitutive laws of cracked concrete for high cycle model used in our simulation program. These constitutive laws explained the damage caused by fatigue loading according to decreasing in stiffness and strength, and increasing in time-dependent deformation. Since the constitutive model was designed to deal with any loading path of complexity, the multi-scale analysis can estimate the fatigue strength in the case of convoluted stress paths like moving wheel load, the fatigue lifetime is based upon the direct-path integral scheme. Three main constitutive laws which contain compression strength, tension and shear transfer among crack's planes are integrated together.

The concrete is damaged due to fatigue is considered in compression and tension where the elastic stiffness of concrete rooted in the micro-cracks reduces gradually during the fatigue loading process. This fatigue damage mechanism is expressed by the evolution law of the damage parameter that indicates strain rate's effect, as shown below.

$$\varepsilon = \varepsilon_e + \varepsilon_p \tag{6-1}$$

$$\sigma = E_o \varepsilon_e K_c \tag{6-2}$$

$$dK_c = \left(\frac{\partial K_c}{\partial t}\right) dt + \left(\frac{\partial K_c}{\partial \varepsilon_e}\right) d\varepsilon_e \tag{6-3}$$

$$d\varepsilon_p = \left(\frac{\partial \varepsilon_p}{\partial t}\right) dt + (\frac{\partial \varepsilon_p}{\partial \varepsilon_e}) d\varepsilon_e \quad (6\text{-}4)$$

Where, ε is the total strain, ε_e is the elastic strain, ε_p is the plastic strain, σ is the total stress, E_o is the initial stiffness, and K_c is the damaging parameter (damage evolution due to internal stresses' repetitions is implemented in the rate type evolution of K_c).

The reduction in stiffness due the bond fatigue between concrete and reinforcement is expressed by K_T in tension, as shown below,

$$\sigma = E_o \varepsilon K_T \quad (6\text{-}5)$$

$$dK_T = Fdt + Gd\varepsilon + Hd\varepsilon \quad (6\text{-}6)$$

Where, F indicates time dependent fracturing due to tension creep. H indicates instantaneous facture due to tension softness, and G indicates the fracture damage due to load repetitions, considering the loss of bond between reinforcement and concrete, in addition the increase of crack width due to loss of bond.

Moreover, the time-dependent drying shrinkage of concrete between the cracks are considered. The crack planes show roughness rooted in the size of suspended aggregates. This roughness is gradually smoothened under cyclic effect if shear slip until the aggregates interlock is gradually lost. This damage is considered by adding the term X to the formulation in order to decrease the shear transfer according to the number of cycles, as shown below.

$$\tau = (\mathrm{X}).\tau_{or}.(\delta, w) \quad (6\text{-}7)$$

$$\mathrm{X} = 1 - \frac{1}{10} log10(1 + \int |d(\frac{\delta}{w})|) \quad (6\text{-}8)$$

Where, τ is transferred shear under high cycle load, τ_{or} is the transferred shear stress calculated by ordinary contact density function, w is the crack width, δ is the crack slip, and X is the modification factor considering accumulation of shear deformation during the loading cycles.

The constitutive law is upgraded to deal with concrete-water interaction [6, 7], which is shown in Figure 6-2. Based on the theory of Biot's theory, two-phase composites which are the solid skeletons and pores media can be dealt with. The mechanical model of the pore water for compression from the atmospheric pressure was assumed to be averaged substantial linear stiffness. Since the fatigue loading causes opening or closure of the cracks. The pore water pressure can encounter positive and negative pressure. According to the cracks condition, positive pressure is expressed as the one over atmospheric pressure, while the negative is

expressed as the one below atmospheric pressure. After cracking, the interaction between the condensed water and cracked concrete becomes anisotropic. Therefore, the anisotropic mechanism is assumed after the formation of connected crack planes through the fracture regions in the simulation scheme.

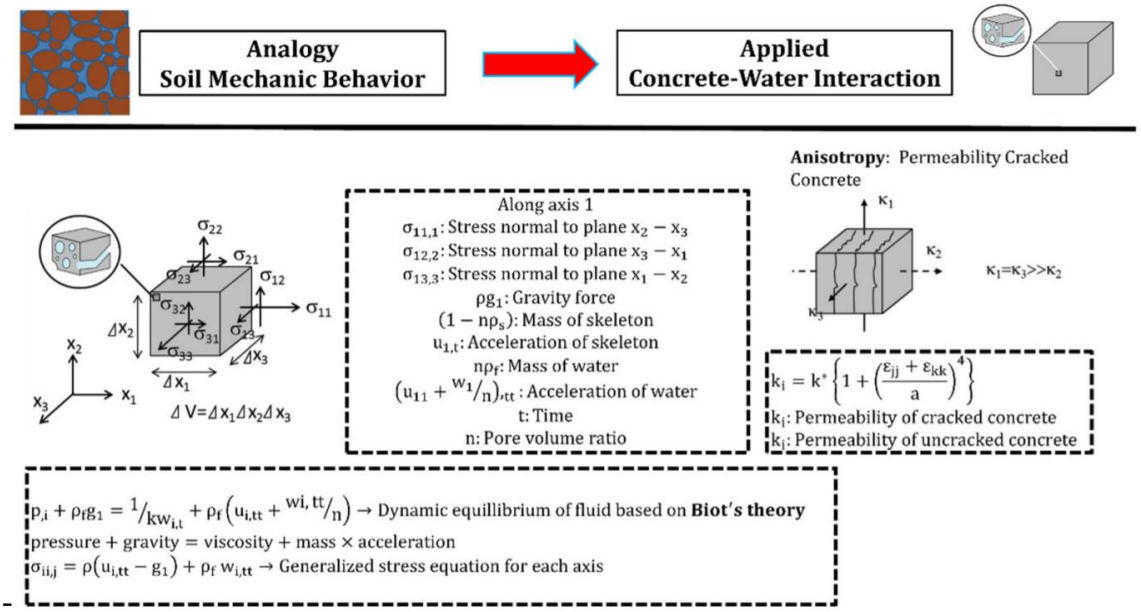

Figure 6-2 Concrete-water interaction constitutive laws

The damaged RC structure also can be taken into consideration. The pseudo-cracking method is a numerical technique to estimate the remaining fatigue life of bridge deck. By using the predictor-corrector approach which is based on energy equilibrium principle, inner unknown cracks are generated in the finite element model [8, 9]. By using this technology, the fatigue life simulation can be successful conducted.

6.3) Description of full scale numerical bridge model

In this research, the Yagikawa Bridge has been selected as our full numerical simulation model. The reason is that the design of Yagikawa Bridge is commonly used in East Japan region. One span of this bridge which is 30 meters long, has been selected to create finite element model. The design properties of this bridge is shown in Table 6-1. The slab thickness is 240mm and the bridge contains 4 I girders.

Table 6-1 Material properties of RC deck of the bridge

Material property	Concrete	Steel reinforcement
Young's modulus (N/mm2)	24744	205,000
Compressive strength (N/mm2)	30	295
Tensile strength (N/mm2)	2.2	295

The material properties of RC deck of the bridge are shown in Table 6-2, the compression strength of the concrete are setted to 30N/mm^2 and strength of the steel is 295N/mm^2.

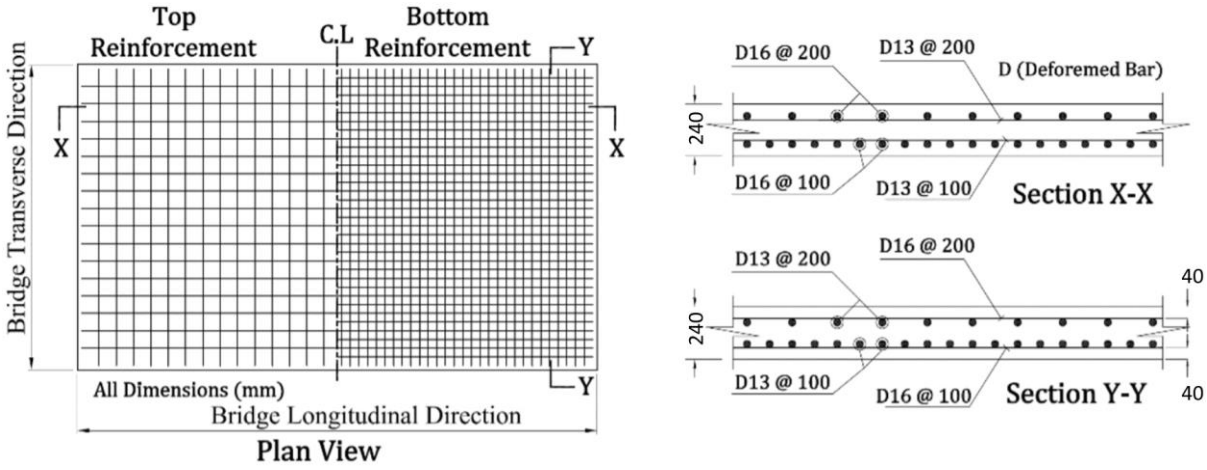

Figure 6-3 Dimensions and reinforcement of the RC deck of the bridge

The dimensions and reinforcement of the RC deck of the bridge is shown in Figure 6-3. The rebar spacing is 200mm in the top layer and 100mm in the bottom layer. D16 is used for main reinforcement and D13 is used for distributing bar.

The finite element model which is created by Hypermesh 14.0 is shown in Figure 6-4. The biggest size of the element in x-y direction is 25cm×25cm. To simplify the model, the cross beam is omitted. There are 76351 nodes and 60480 elements in the model. The x direction contains 120 layers; the number of element is all same in the y-z cross section. And for each section, it has 631 nodes and 504 elements.

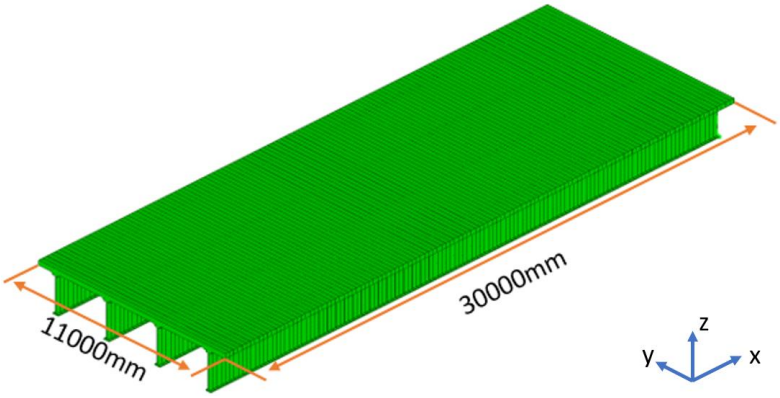

Figure 6-4 Full scale finite element model

6.4) Beam-solid hybrid model

Because the model contains too many nodes and elements, the simulation will consume a lot of computation time. Shorten the long calculation time, not only can provide timely feedback to the bridge more efficiently, better help engineers to carry out planned maintenance of the bridge, but also save a lot of money on the budget. Therefore, a method that can quickly calculate the fatigue life of the bridge and also can ensure the accuracy at the same time needs to be developed.

In this research, the beam element is induced to replace part of the solid element in order to accelerate the calculation process. Firstly, the whole finite element model is divided into 5 parts in x direction and each part has 6 meters long, as shown is Figure 6-5. The middle part is selected as our analysis target because it is the centre part of the bridge; the moment and displacement is bigger than the other parts.

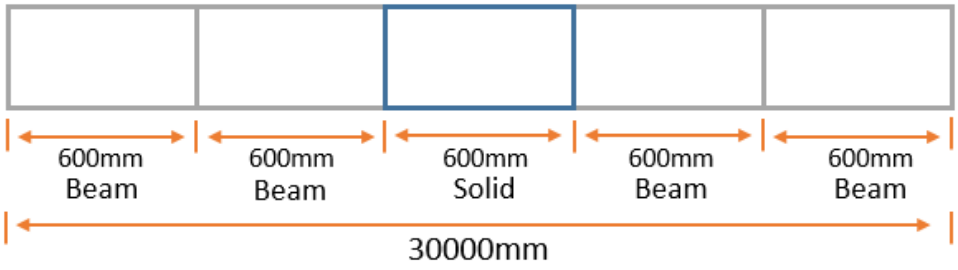

Figure 6-5 Solid-beam hybrid model replacing information

In order to make the full model and beam-solid hybrid model give the same displacement under same loading condition, the properties of the beam element need to be set properly. Here, the total number of beam element on each y-z cross section, the position of each beam element, and the size of each beam element need to be decided.

To make the structure stable enough and by considering the force can be transmitted evenly from the beam element to solid element, for each girder, there is one steel beam element

embedded in the solid element, at the centre position of the I girder. Additionally, there are three concrete beam element embedded in the centre position RC element on z direction. Each concrete beam element is in the middle of two steel beam element. The length of each beam element is 6 meters. Hence, for each y-z cross section, there are 7 beam elements.

To ensure that the solid model and beam-solid hybrid element produce same deformation under same force, the beam-solid hybrid model and solid model should have same second moment of area in y-z cross section. Here, the side length of all beam elements are assumed to be same.

$$n \cdot I_b = I_s \tag{6-9}$$

Where, n is the number of total beam element, I_b is the second moment of area of every beam element in y-z cross section, and I_s is the second moment of area of solid element in y-z cross section.

And as mentioned before, there are two type of beam element, which are concrete beam element and steel beam element, therefore

$$n_1 I_{b_c} + n_2 I_{b_s} = I_s \ , \ (n_1 + n_2 = n) \tag{6-10}$$

Where, n1 is the number of concrete beam element, n2 is the number of steel beam element, I_{b_c} is the second moment of area of concrete beam element, and I_{b_s} is the second moment of area of steel beam element.

By using the ratio of the Yung's modules of concrete and steel, the concrete beam can be switched into steel beam element.

$$n_1 \left(\frac{b_c h_c^3}{12} \cdot \frac{1}{R_E} \right) + n_2 \left(\frac{b_s h_s^3}{12} \right) = I_s \ , \ (R_E = \frac{E_s}{E_C}) \tag{6-11}$$

Where, b_c, b_s are the width of concrete and steel beam element, h_c and h_s are the height of concrete and steel beam element. R_E is the ratio of Young's modules of steel and concrete, E_s and E_c is the Young's modules of steel and concrete.

Here, shape of cross section is assumed to be square. And we have

$$\left(n_1 \frac{1}{12} \cdot \frac{1}{R_E} + n_2 \frac{1}{12} \right) \cdot b^4 = I_s \tag{6-12}$$

For the calculation of second moment of area of y-z cross section of solid model, the equation which is shown below.

$$I_z = I'_z - y_G^2 \cdot A \tag{6-13}$$

$$I'_z = \int_A z^2 dA = b \int z^2 dy \tag{6-14}$$

$$y_G = \frac{\int_A zdA}{A} = \frac{b \int zdy}{A} \tag{6-15}$$

Additionally, the thickness of each section is used to calculate the second moment of area of the section by weighted averaging.

$$I = \frac{I_1 w_1 + I_2 w_2 + \cdots + I_n w_n}{(w_1 + w_2 + \cdots + w_n)} \tag{6-16}$$

Where, I_1, I_2, I_n is the second moment of area for each layer and w_1, w_2, w_n is the thickness of each layer in x direction.

However, beam elements are separated from each other, and solid elements are connected to each other, therefore, if they receive a force that is off-centre in the x-axis direction, the degree of distortion which is produced by two model are different. Since the torsional rigidity of the beam element is smaller than the solid element, larger torsion will be occurred when same force is applied. In order to increase the torsional rigidity, at certain distance in x direction, some steel beam elements are used to connect the beam element to form triangles. After modification, the beam-solid hybrid model is shown in Figure 6-6.

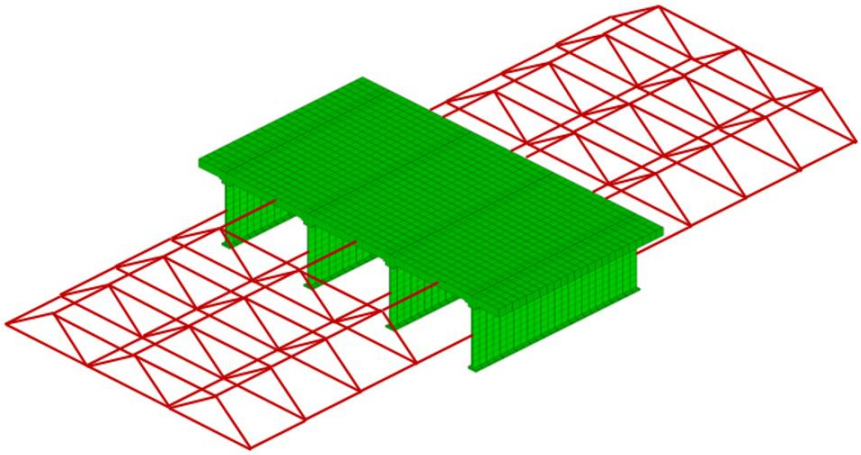

Figure 6-6 Beam-solid hybrid finite element model

6.5) Loading information

The loading information are shown in Table 6-2. Referring to the Japanese specification for highway bridges-part III [10], the deck is subjected to traveling wheel design load of 98kN.

The running speed of wheel is selected as 60km/h, i.e., the legal speed limit for the national routes in Japan.

Table 6-2 Wheel load information

Wheel load information	
Wheel load	98kN
Wheel load speed	60km/h
Wheel load size	250mm(x direction)×500mm(y direction)

6.6) Numerical simulation failure criterion

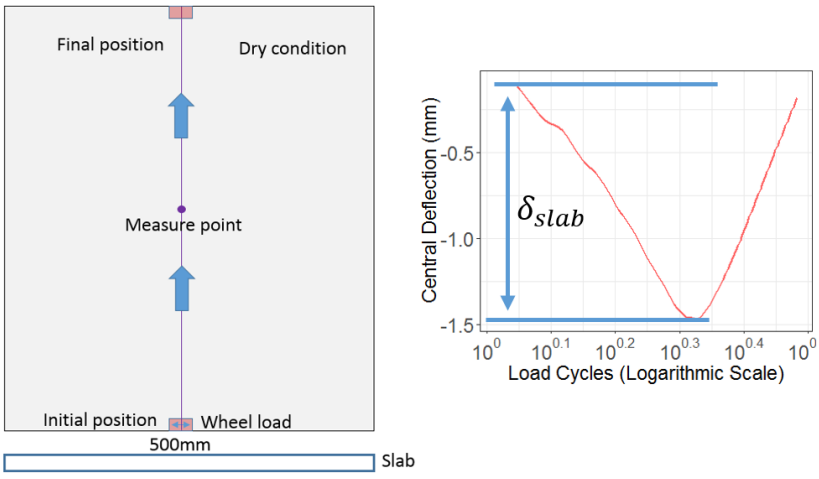

Figure 6-7 Definition of fatigue limit state

According to the past experiment results [11], the fatigue limit state was specified by the central live load deflection computed by assuming that the bond between concrete and reinforcement is lost in flexure. Thus, when the live load deflection defined by the equation which is shown below would reach the limit state deflection of no bond, it is judged as the fatigue failure. Then, we also accept this criterion so that the past research works can be referred. As this limit state deflection experimentally around 3 times of its initial value.

$$\delta_{N\,slab}/\delta_{1\,slab} \geq 3 \tag{7-1}$$

$$\delta_{1\,slab} = \delta_{1\,all} - \delta_{steel\,girder\,1} \tag{7-2}$$

$$\delta_{1\,slab} = \delta_{1\,all} - \delta_{N\,slab} = \delta_{N\,all} - \delta_{steel\ girder\ N} \quad (7\text{-}3)$$

Where $\delta_{1\,slab}$ the initial deflection of slab at measurement is point, and $\delta_{1\,slab}$ is the final deflection of slab at measurement point. $\delta_{1\,all}$ is the deflection of the measurement point and $\delta_{steel\ girder\ 1}$ is the initial deflection of girder. Correspondingly, $\delta_{N\,all}$ and $\delta_{steel\ girder\ N}$ are the final deflection of measurement point and final deflection of girder.

This criterion only gives a roughly judgement about fatigue failure. In Chapter 7 and 8, depending on the different situation, the criterion will also change.

6.7) References

1. Maekawa, K., Okamura, H., & Pimanmas, A. (2003). *Non-linear mechanics of reinforced concrete*. CRC Press.
2. Maekawa, K., Ishida, T., & Kishi, T. (2003). Multi-scale modeling of concrete performance. *Journal of Advanced Concrete Technology*, *1*(2), 91-126.
3. Fujiyama, C., Gebreyouhannes, E., & Maekawa, K. (2008). Present achievement and future possibility of fatigue life simulation technology for rc bridge deck slabs. *Soc. Soc. Manag. Syst. Internet J*, *4*.
4. Maekawa, K., Ishida, T., Chijiwa, N., & Fujiyama, C. (2015). Multiscale coupled-hygromechanistic approach to the life-cycle performance assessment of structural concrete. Journal of Materials in Civil Engineering, 27(2), A4014003.
5. Maekawa, K., Toongoenthong, K., Gebreyouhannes, E., & Kishi, T. (2006). Direct path-integral scheme for fatigue simulation of reinforced concrete in shear. Journal of Advanced Concrete Technology, 4(1), 159-177.
6. Maekawa, K., & Fujiyama, C. (2013). Crack water interaction and fatigue life assessment of RC bridge decks. In Poromechanics V: Proceedings of the Fifth Biot Conference on Poromechanics (pp. 2280-2289).
7. Barros, H., Faria, R., Ferreira, C., Maekawa, K., & Fujiyama, C. (2013). Rate-dependent model of structural concrete incorporating kinematics of ambient water subjected to high-cycle loads. Engineering computations.
8. Fujiyama, C., Tang, X. J., Maekawa, K., & An, X. H. (2013). Pseudo-cracking approach to fatigue life assessment of RC bridge decks in service. Journal of Advanced Concrete Technology, 11(1), 7-21.
9. Tang, X. J., Fujiyama, C., An, X. H., & Maekawa, K. (2013, September). PSEUDO-CRACKING APPROACH TO FATIGUE LIFE ASSESSMENT OF EXISTING RC BRIDGE DECKS BASED ON CRACK INSPECTION DATA. In Proceedings of the Thirteenth East Asia-Pacific Conference on Structural Engineering and Construction

(EASEC-13) (pp. F-2)

10. Japan Road Association, Specification for Highway Bridges-Part III Concrete Bridges, 2012.
11. Tanaka Y., Maekawa K., Maeshima T., Iwaki I., Nishida T., and Shiotani T., 'Data assimilation for fatigue life assessment of RC bridge decks coupled with hygro-mechanistic model and nondestructive inspection', Journal of Disaster Research, 2017.

Chapter 7: Fatigue life and deterioration process of full scale model under different slab thickness and environmental condition

7.1) Introduction

In chapter 7, firstly, the results between full scale model and simple plate model are compared under dry and wet environmental condition. Inconsistent results are obtained according to the different size, shape and boundary condition, the maximum principle strain distribution and generated water pressure are totally different.

Secondly, the results of full scale model under different condition slab thickness and environmental condition are shown. Especially, the horizontal crack generation condition and time period is evaluated. The simulation results under dry and wet case are consistent with survival analysis which are showed in Chapter 3 and chapter 4, indirectly conforms the correctness of survival analysis. Then combining the on-site inspection and bottom side maximum principle strain of numerical simulation, the deficiency of current inspection and available range of survival analysis are evaluated.

Finally, the fatigue simulation under different distance between wheel load and girder are analyzed. Not only the fatigue cycle, but also in order to investigate the failure pattern and mechanism, the failure mode, the top surface, bottom surface and cross sectional maximum principle strain are shown.

7.2) Result comparison between full scale model and simple plate model

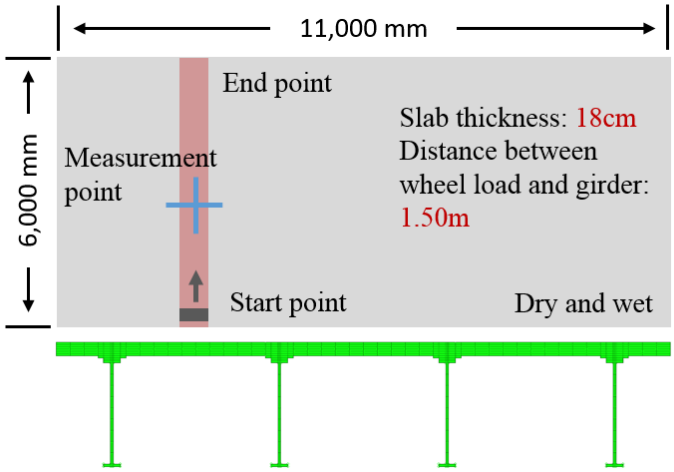

Figure 7-1 Basic information of full scale model

Basic information of full scale model simulation is shown in Figure 7-1. The slab thickness is 18 cm and the loading position is in the center of the two girders. The distance from each girder is 1.50m. Simulation conducted under both dry and wet environmental condition.

Figure 7-2 shows a typical template of previous fatigue life analysis. The length and width of the bridge deck are fixed values which have been set to 6 meters and 3.5 meters. The wheel load position is set in the middle of the slab. The simulation model of the studied RC decks is discretised in the x-y plane to mesh size of 250 multiply by 250 mm, while it is discretised into four layers in the z-direction. The reinforcement ratio, the slab thickness and wheel load speed are the same as full scale model. The slab is fixed on a hollow steel plate. The boundary conditions are chosen to be hinged supports, which allow rotational motion and restraint the translational motion. The edge of the steel plate is fixed in vertical direction. More detailed information can be referred to previous research [1-3]. In order to reduce the interference of external factors, the mesh size of RC slab for both models are used as 25cm multiply by 25cm.

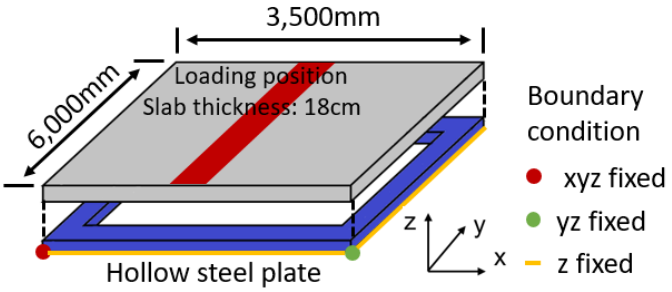

Figure 7-2 basic information of simple plate

The fatigue results are compared under dry and wet case. The fatigue cycle under dry case are shown in Figure 7-3. It can be seen that the fluctuation of each cycle of full scale model is smaller than simple plate model, but to reach 3 times initial displacement, the full scale model need less loading cycles.

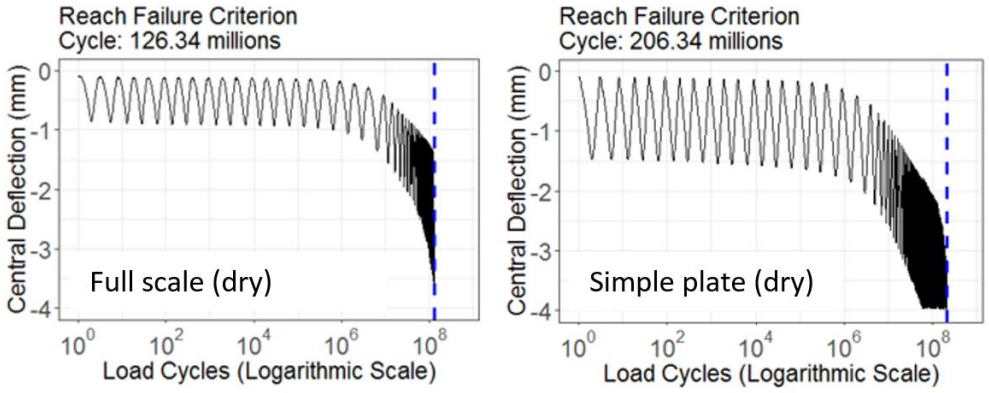

Figure 7-3 Central deflection results of full scale and simple plate model under dry environmental condition

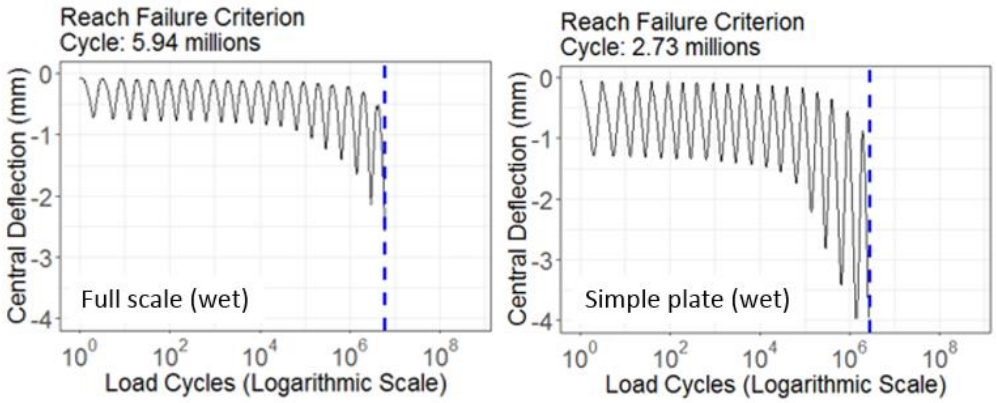

Figure 7-4 Central deflection results of full scale and simple plate model under wet environmental condition

For the wet case, the results are shown in Figure 7-4. For the full scale model, it gives 5.94 million cycle and for simple plate model, it only gives 2.73 million cycle. Here it can be seen that the result of full scale model and simple plate model under dry and wet environmental condition are reversed.

In order to check the reason of the reversed result, the maximum principle strain of the top and bottom side of full scale model and simple plate model under dry case when the wheel load is in the centre of the slab are shown. Only the panel which has been applied loading on it has been selected and showed in Figure 7-5 for full scale model. It can be seen that even if the fluctuation of each cycle of simple plate model is larger, but the maximum principle distribution is more dispersed than full scale model. For the simple plate, as mentioned before, the edge of the slab is fixed on a hollow steel plate. Therefore, slab cannot be moved freely in longitudinal direction and the only the centre part of the slab can be deformed under wheel loading. On the other hand, for the full scale model, since only the end position of longitudinal direction is fixed in vertical direction, not only the slab but also the main girder also shows displacement increasing when the wheel load is applied. Additionally, the maximum principle strain of full scale model is more concentrated. Therefore, the damage will be happened earlier. Based on this, the full scale model shows fast displacement decreasing.

For wet case, it gives the same displacement result that the fluctuation of simple plate model is larger than full scale model and the maximum principle strain of top and bottom side are also the same as dry case as Figure 7-6 shown. However, under wet environmental condition, the deterioration is mainly caused by inside water pressure of slab. If the deflection of each cycle is larger, the generated water pressure will be higher. The initial average water pressure of 6 cm thickness from the surface down of full scale model and simple plate model when the wheel load is in the centre of the slab are compared, and the result is shown in Figure 7-7. Since the displacement decreasing of simple plate RC slab caused by live load is larger, generated water pressure of simple plate model is almost twice than the full scale model.

Therefore, the displacement decreasing of simple plate model is faster than full scale model under wet case.

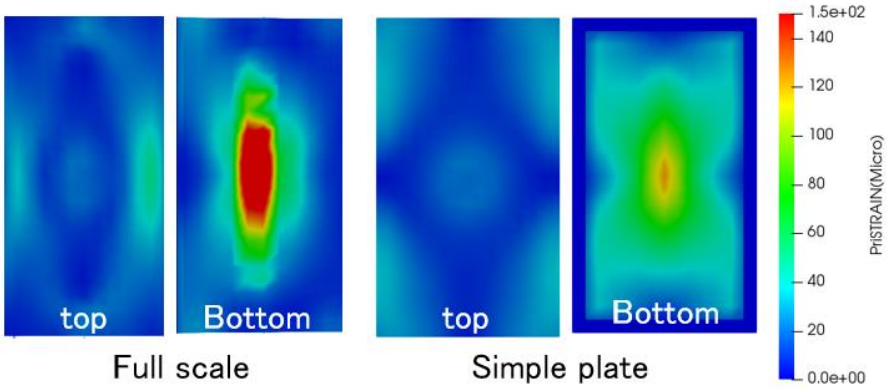

Figure 7-5 Maximum principle strain of top and bottom surface of full scale and simple plate model under dry environmental condition

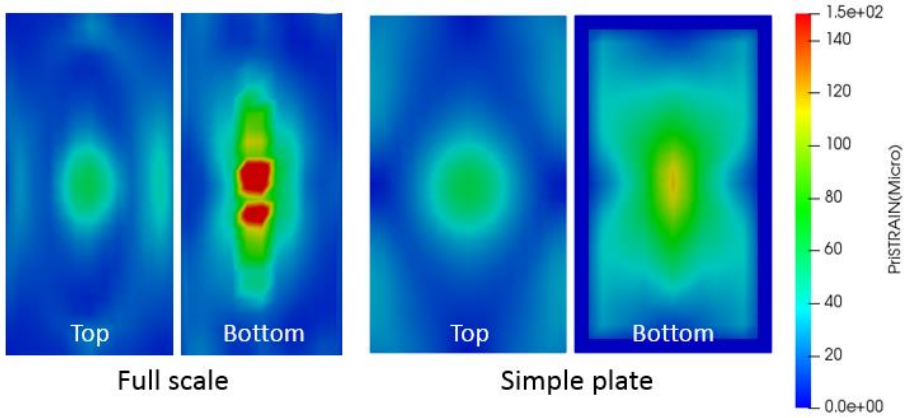

Figure 7-6 Maximum principle strain of top and bottom surface of full scale and simple plate model under wet environmental condition

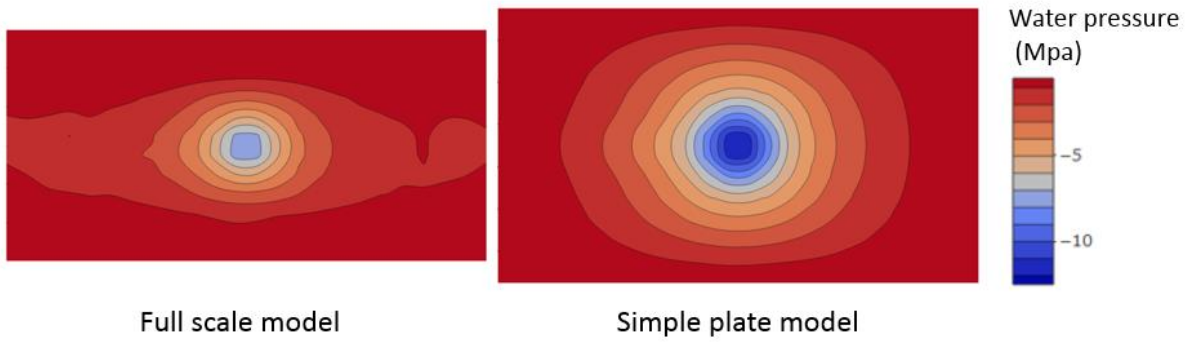

Figure 7-7 Initial water pressure of full scale model and simple plate model

As a consequence, since different models give total different size and boundary condition, the simulation result is different, therefore, in order to gives precise result, the full scale model which is close to the actual situation would be better.

7.3) Result of panel centre loading case under dry and wet environmental condition

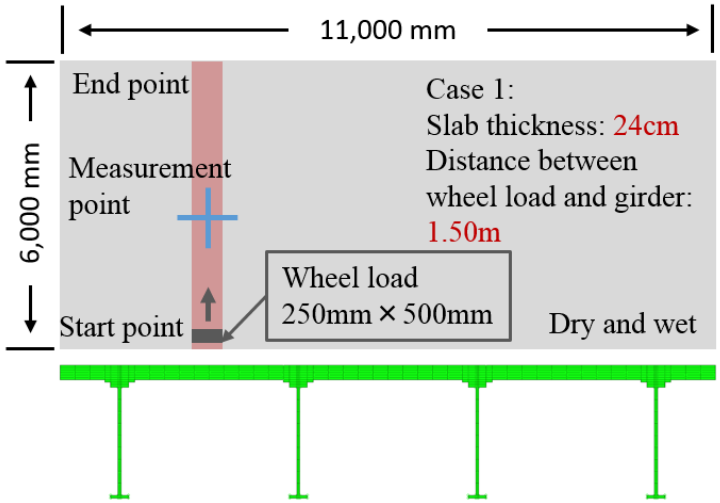

Figure 7-8 Central wheel loading position with slab thickness of 24cm under dry and wet environmental condition (case 1)

The results of full scale model under different condition slab thickness and environmental condition are shown. Firstly, as Figure 7-8 shows, the simulation under dry and wet condition are conducted. Since our target is the centre solid element part, therefore the load is only applied on the solid elements. The distance between two girders are 3 meters, and the wheel load between both two girders are 1.5 meters.

Figure 7-9 shows the dry and wet environmental condition results of case 1. For dry case, even if around 347. 64 million of wheel load cycles applied on the top surface of the slab, but the structure didn't lose in flexure. The final displacement of the slab is only 1.1mm. For wet case, fatigue limit state was reached only after 16.44 million load cycle applied, which indicated that the slab is much more vulnerable under wet environmental condition. According to previous study, when water penetrates into the cracks, the water pressure inside the crack will increases if there is loading applied. Due to the polishing effect on the cracked surface, deterioration of RC concrete can be significantly accelerated.

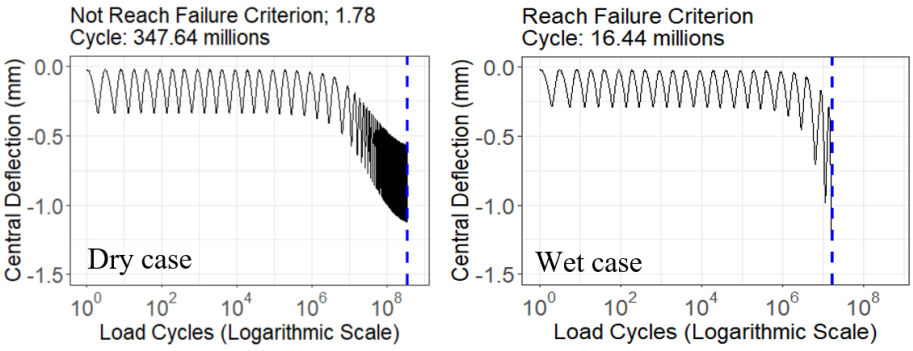

Figure 7-9 Central deflection results of case 1 under dry and wet environmental condition

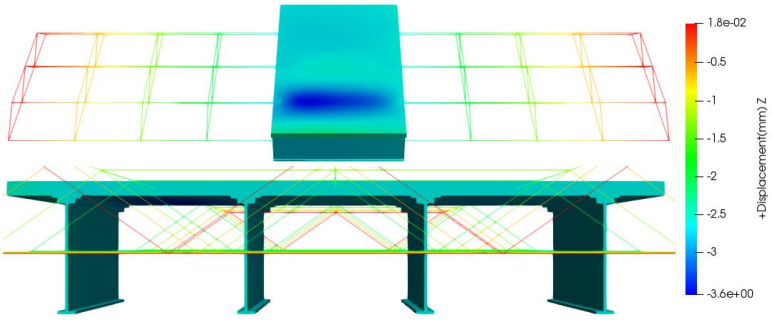

Figure 7-10 Overall displacement of case 1 under dry condition

The displacement of case 1 under dry condition is shown in Figure 7-10. According to the fatigue cycle result, the overall displacement of the wheel load position is relatively small and didn't reach the fatigue criterion. Therefore, the re-analysis by setting more loading cycle loading is needed. On the other hand, the displacement of case 1 under wet environmental condition shows large deflection on the wheel load passing position at final simulation stage (as shown in Figure 7-11), which can be considered that the punch shear failure happened.

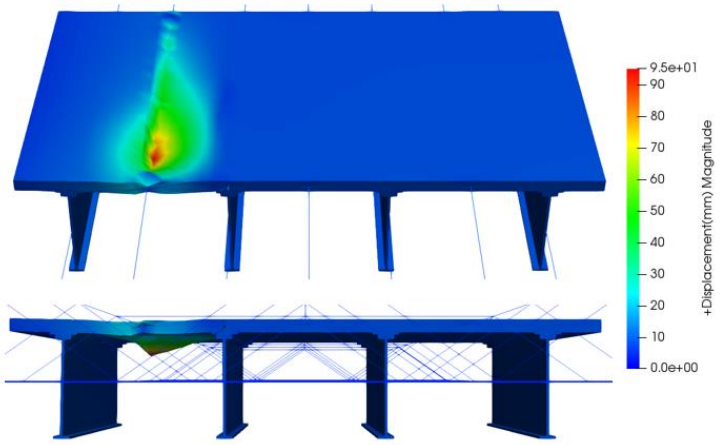

Figure 7-11 Overall displacement of case 1 under wet environmental condition

Additionally, the maximum and minimum principle strain transformation trend of wet environmental condition are shown. Figure 7-12 and Figure 7-13 shows the top and bottom surface maximum principle strain distribution. It can be seen that on the top surface, the maximum principle strain where the wheel load passing position increases along with the loading cycle increase. However, on the bottom side, even if the strain shows increases trend, but comparing with the top side, it shows a delayed trend. Therefore, under the wet environmental condition, the deterioration process is more severe on the top surface. The reason is that since the top surface is directly receiving the loading force, the water pressure is higher on top surface.

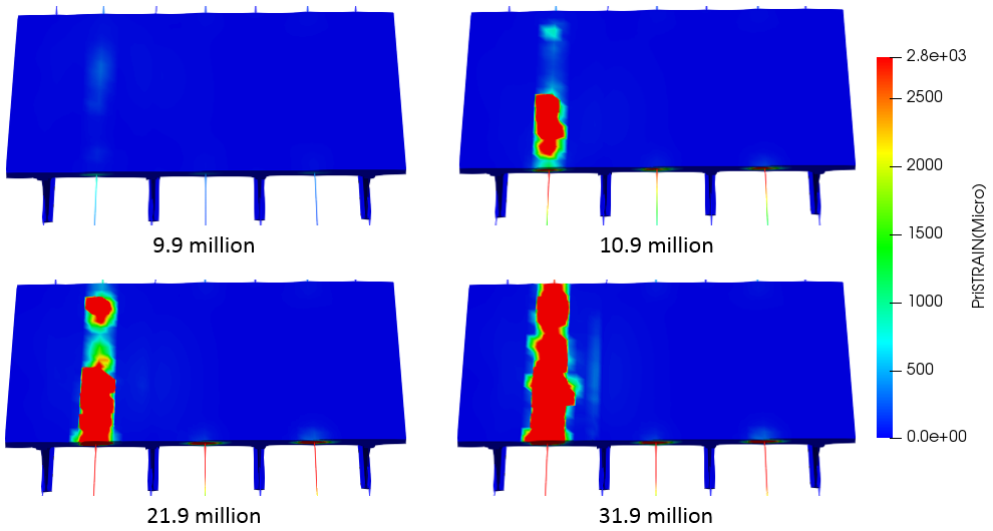

Figure 7-12 Top surface maximum strain distribution transformation under wet environmental condition as loading cycle increasing (case 1)

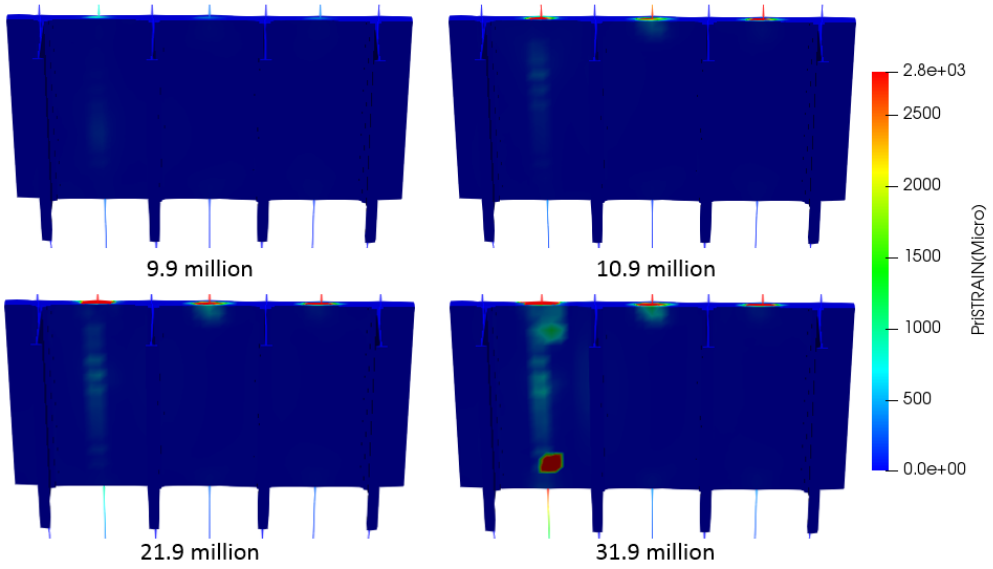

Figure 7-13 Bottom surface maximum strain distribution transformation under wet environmental condition as loading cycle increasing (case 1)

Figure 7-14 and Figure 7-15 show the transformation of top and bottom layer minimum strain distribution under water submerged stage as loading cycle increasing of case 1. It is consistent with the maximum principle strain. Basically, there is always surface where the shear strength becomes zero depending on the direction when a strength applied on an object. The strain at that time is called principle strain. And the largest one is called maximum principle strain and the smallest one is called minimum principle strain. The maximum value in the maximum principle strain and strain distribution is the place where the tensile stress and strain are the highest, from the maximum principle the equivalent crack width of the concrete can be calculated. And the minimum value in the minimum principle strain and strain distribution is the place where the compressive stress and strain are the highest. And if the object is under

tension at one side, without being compressed in all direction, the object will be stretched on another surface which is perpendicular to this direction. Therefore, the maximum and minimum strain distribution usually has the same trend. Additionally, since as mentioned before the maximum principle strain decided the crack of the RC slab, which is more important, therefore in the later section, only the maximum principle strain is showed.

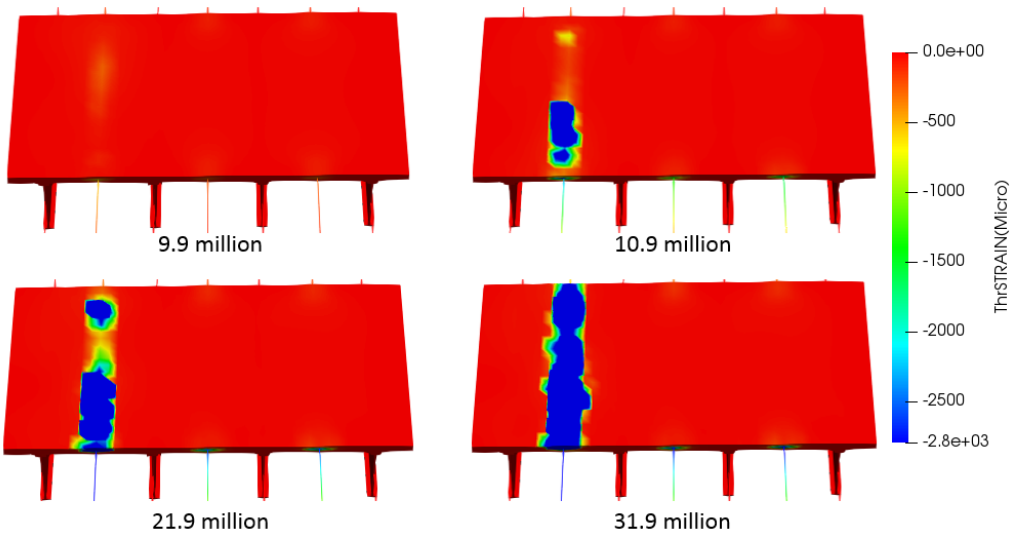

Figure 7-14 Top surface minimum strain distribution transformation under wet environmental condition as loading cycle increasing (case 1)

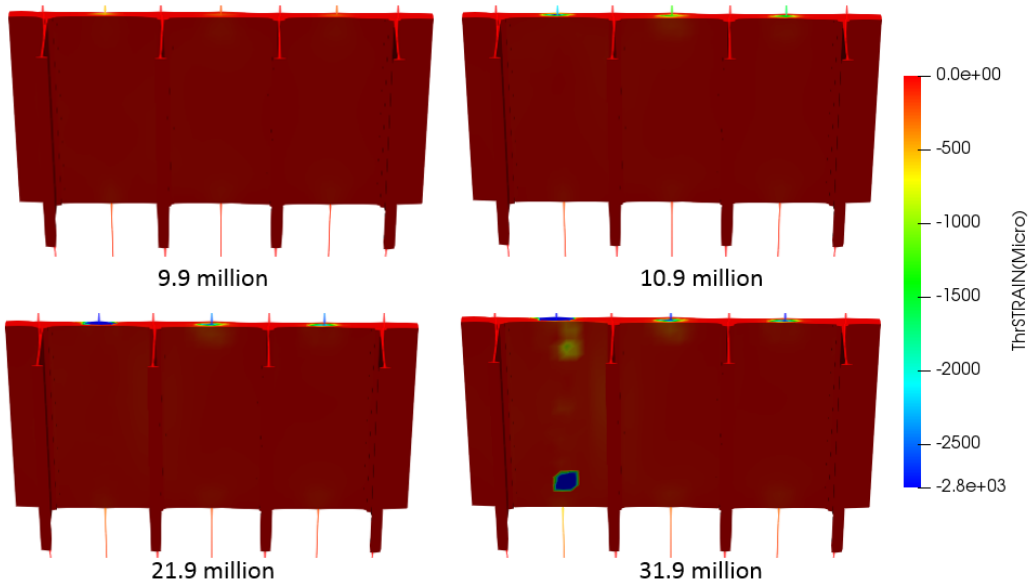

Figure 7-15 Bottom surface minimum strain distribution transformation under wet environmental condition as loading cycle increasing (case 1)

Result with different slab thickness is shown to compare. The fatigue simulation of slab with a relative thin thickness are analysed. During the early period, the slab with a relative thin thickness were constructed since the traffic volume is relatively small and wheel load is light.

However, after the economic grows, the traffic volume and traffic load are significantly increased, it has been widely found that the thin slab didn't durable enough to resist the fatigue loading. Therefore, after 1964, the design code has been widely modified as previous chapter shown. Especially in Tokyo region, to resist the heavy traffic loading, the steel plate was actively implemented. Figure 7-16 shows the outline of centre wheel loading position with slab thickness of 18cm under dry and wet environmental condition, which only the slab thickness is different in order to give a reasonable comparison. It gives the same result that under wet environmental condition, the fatigue cycle is greatly reduced (Figure 7-17).

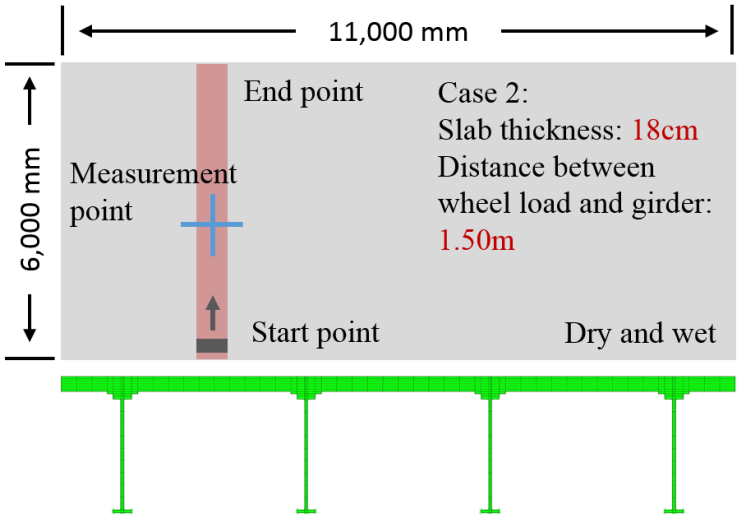

Figure 7-16 Central wheel loading position with slab thickness of 18cm under dry and wet environmental condition (case 2)

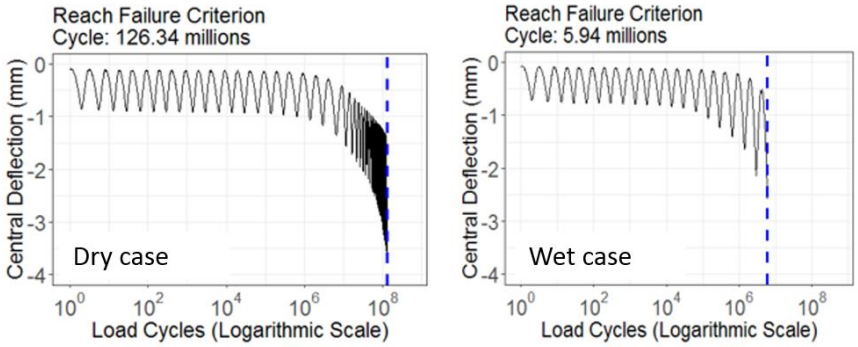

Figure 7-17 Central deflection results of case 2 under dry and wet environmental condition

Additionally, the final overall displacement distribution under both dry and wet environmental condition are shown in Figure 7-18 and Figure 7-19. Under both environmental condition, central deflection is decreased more than 45cm, indicates the punching shear failure happened at final stage. Even if the final failure mode is the same, for dry case, it needs relative more loading cycle.

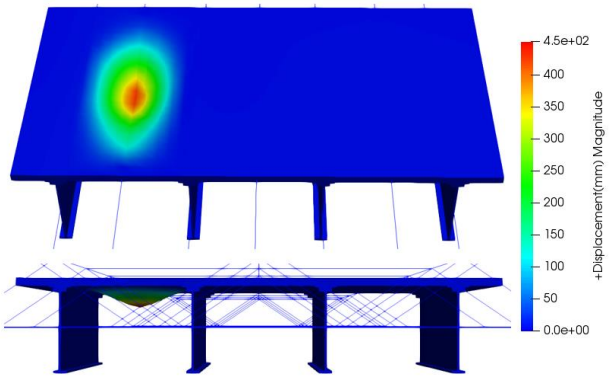

Figure 7-18 Overall displacement of case2 under wet environmental condition at final stage on simulation

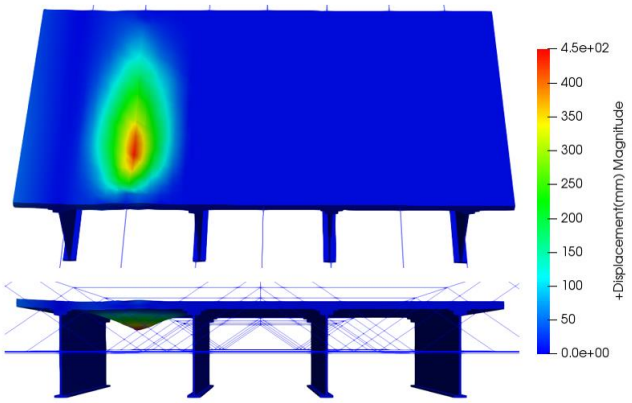

Figure 7-19 Overall displacement of case2 under dry environmental condition at final stage on simulation

7.4) Consistency confirmation between numerical simulation and survival analysis result

Up to now, since full scale model is considered which can give more precise result, therefore, the limitation of current inspection and the available range of survival analysis can be investigated by comparing the result with full scale numerical simulation.

Firstly, the full scale numerical model is compared between different slab thickness and environmental condition. As Figure 7-20 shown, for the slab thickness of 24cm, the simulation stops after 347 million cycle without obvious displacement decreasing, therefore re-analysis by setting longer loading cycle is needed. But still result shows that under dry case, the fatigue cycle will be greatly increased as slab thickness increases. Then, the result between different slab thicknesses under wet environmental condition are compared. Even if the slab thickness increased 6cm, but the fatigue cycle only increased around 4 times. Therefore, the fatigue cycle has a big difference under different environmental condition. Finally, the case between dry and wet case are compared. Under same slab thickness, the fatigue loading cycle has a 20 times difference, indicate that the slab is relative durable under dry case as previous section shown.

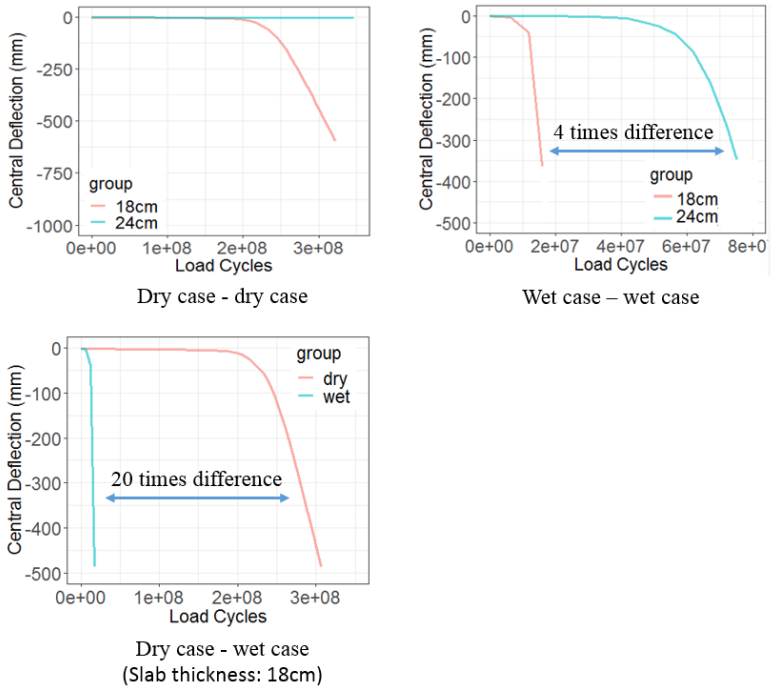

Figure 7-20 Central deflection results comparison under different slab thickness and environmental condition

In order to investigate the result credibility of survival analysis, the consistency between numerical model and survival analysis are checked. Additionally, through the maximum principle strain distribution, the inspection limitation and survival analysis available range are also checked. Firstly, for Tokyo region, since the winter precipitation is relative slow and the waterproof layer functional in all time period, therefore the slab in Tokyo region can be considered as under dry case. On the other hand, in East Japan, erosion happened by snow mound and de-icing salt. Additionally, in our inspection data, 40% of the panel recorded as bad waterproof. The fact of large of the slab has bad waterproof can also be referred to investigation by Civil Engineering Research Institute for Cold Region. The result revealed that 85% of the waterproof do not meet the standard (Toshihisa el at., 2012) [4]. Therefore, the situation can be considered as close to wet environmental condition.

The result which comes from a part of survival analysis shows in Table 7-1 and Table 7-2. For dry case, the survival analysis result of Toyo region shows that if the slab thickness increases 2.04cm, the risk (deterioration rate) will be decreased 37.9%. Therefore, it can be calculated that if the slab increased from 18cm to 24cm, totally the risk (deterioration rate) will be deceased around 111.4%, indicates that increase the slab thickness can greatly decrease the risks under dry case. However, for wet case, the survival analysis gives the result that if the slab thickness increases 1.66cm, the total risk only decreased around 15.9%, which is smaller than in dry case.

Table 7-1 Survival analysis result of slab thickness in Tokyo region

Tokyo region	Hazard ratio	Standard unit	18cm to 24cm
Slab Thickness	0.621	2.04cm	111.4%

Table 7-2 Survival analysis result of slab thickness in East Japan

East Japan	Hazard ratio	Standard unit	18cm to 24cm
Slab Thickness	0.956	1.66cm	15.9%

The survival probability of two regions are compared as Figure 7-21 shown. In Tokyo region, the traffic volume is more than 44000 per day and the average slab thickness is only 19.8cm. On the other hand, for East Japan region, the traffic volume is only about 14000 per day and the slab thickness is 22.3cm. If only considering the traffic load and ignoring environmental condition, the slab in East japan region should have more fatigue cycle and the survival probability decreasing should be slower than Tokyo region. But it can be seen that the survival probability decreasing of East Japan is faster than Tokyo region. For example, when the survival probability is decreased to 60%, the Tokyo region need almost 40 years, but the East Japan region only gives the result of 25 years, indicate the great impact of environmental condition. The comparison show that the result of survival analysis is consistent with the numerical fatigue simulation.

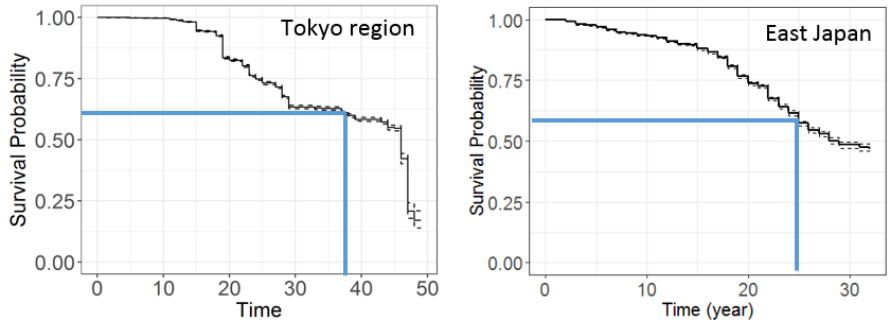

Average traffic volume: 44962 per day
Average slab thickness: 19.8cm

Average traffic volume: 14401 per day
Average slab thickness: 22.3cm

Figure 7-21 Survival probability comparison between Tokyo region and East Japan

7.5) Current inspection deficiency and available range of survival analysis

Currently, since the bottom surface inspection and survival analysis are the first step for our proposed maintenance system. It is not only necessary to provide the use conditions and scope of application for the existing inspection and maintenance system, and on this basis, in order to make the system more complete and accurate in the future, but also opinions on the feasibility of the scope which can be used to improve the accuracy and expand the application should be investigated.

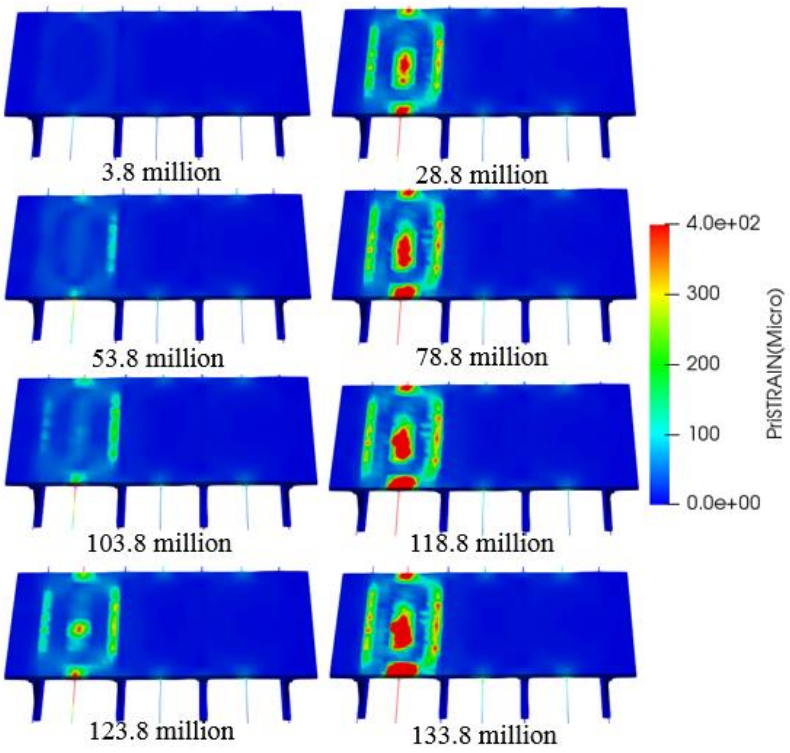

Figure 7-22 Top surface maximum principle stain distribution transformation under wet environmental condition with thickness of 18cm

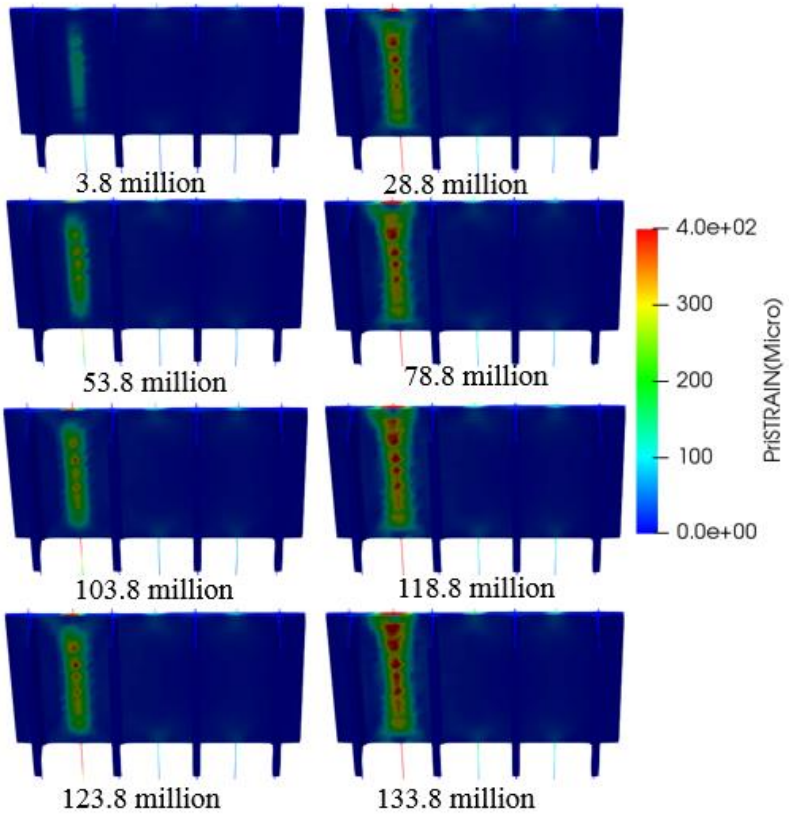

Figure 7-23 Bottom surface maximum principle stain distribution transformation under wet environmental condition with thickness of 18cm

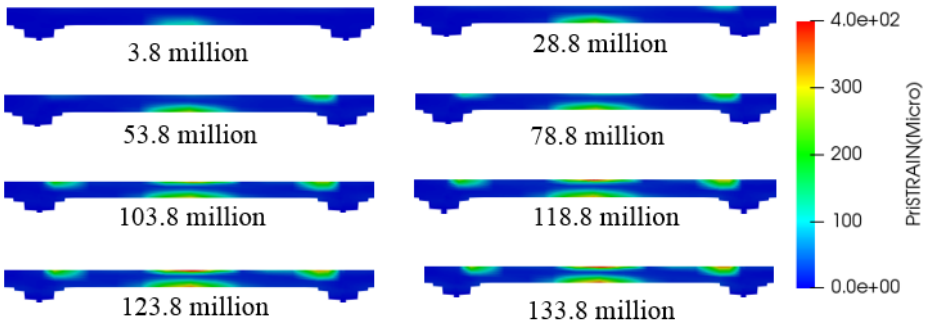

Figure 7-24 Loading applied panel cross sectional maximum principle stain distribution transformation under dry environmental condition with thickness of 18cm

Since for the slab with a thickness of 24cm, the fatigue resistance is relative high, at final stage of our simulation, it didn't show any serious damage, therefore, the discussion only focus on the slab with the thickness of 18cm. In order to check the current inspection limitation, firstly the maximum principle strain distribution of the top and bottom surface of dry case are shown. You can see that as Figure 7-22 and Figure 7-23 shown, through all time period, the maximum principle strain in the bottom side are consistent with the top side. Additionally, the centre cross sectional principle strain shows in Figure 7-24 in order to check the internal condition of slab. And from the cross section area of the slab, the maximum principle strain is relative small than the top and bottom side, indicates that compare with inside, the outside of the slab shows more damages. Therefore, the deterioration of slab under dry case thought a relative long time period and since the damage are shows in the surface area, the current inspection can easily check the condition of it and the survival analysis can consider this type of deterioration.

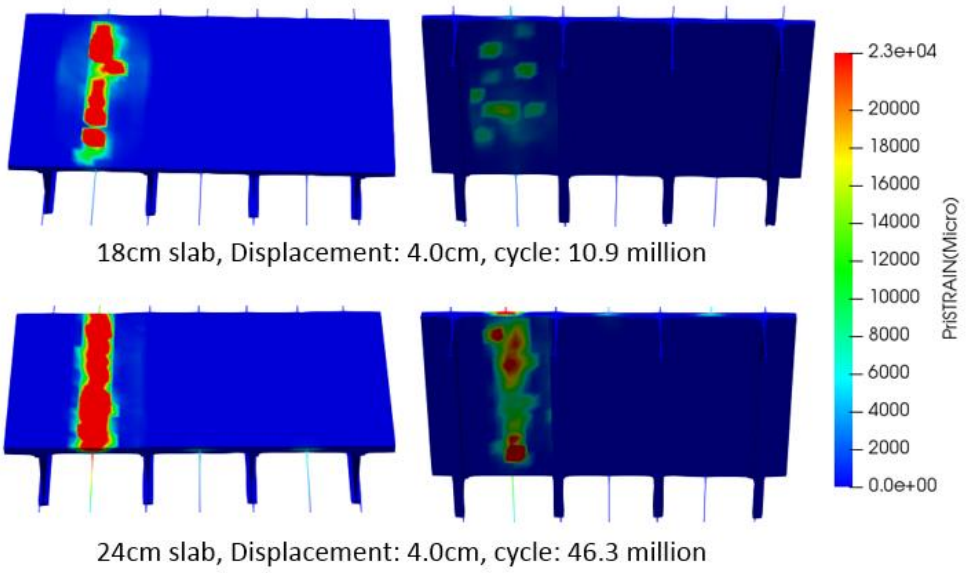

Figure 7-25 Top and bottom surface maximum principle strain distribution under wet environmental condition

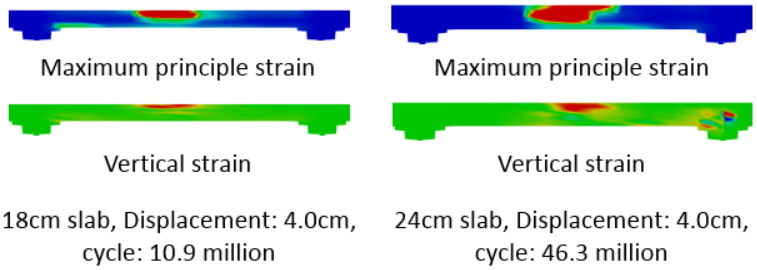

Figure 7-26 Loading applied panel cross sectional maximum principle strain and vertical strain distribution under wet environmental condition

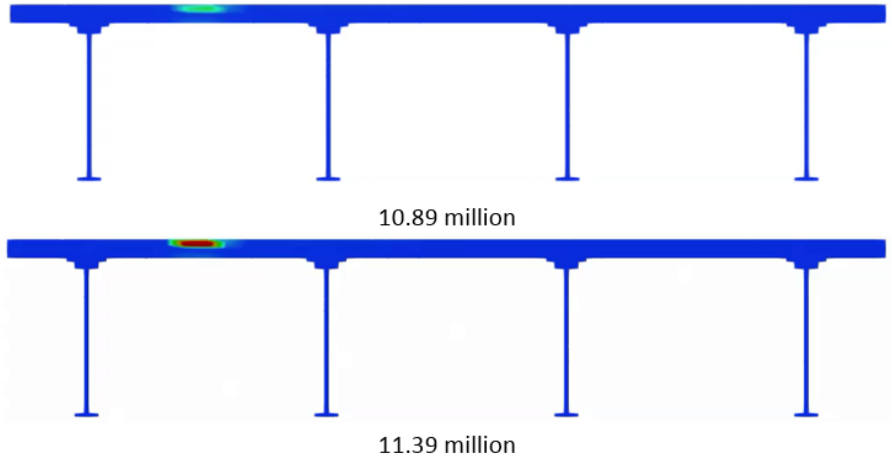

Figure 7-27 Horizontal crack occurring time for 24cm slab thickness case

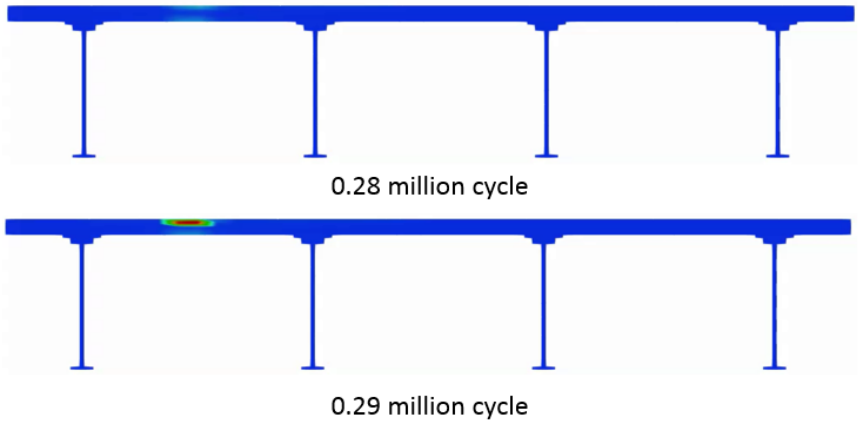

Figure 7-28 Horizontal crack occurring time for 18cm slab thickness case

For wet case, similarly, the maximum principle strain of top and bottom surface under same displacement are shown in Figure 7-25 both the 18cm and 24cm slab. Comparing with top surface, the maximum principle strain in the bottom surface shows a delayed trend. Additionally, the maximum principle and vertical strain in the cross sectional area are also compared as shown in Figure 7-26 It can be clear see that for both 18 cm and 24 cm slab, the horizontal crack are generated. To be more clearly, the time period when the horizontal crack generated are also investigated.

In order to get a more accurate picture of when horizontal cracks occurred, the results were sorted out more carefully. From the result, the horizontal crack for the 18cm slab thickness case is generated at 0.29 million cycle and for the 24 cm slab case, the horizontal crack is generated at 11.39 load cycle, which is the initial period of the whole deterioration process (Figure 8-20 and Figure 8-21).

Figure 7-29 and Figure 7-30 shows the maximum principle strain of bottom side when the horizontal crack generated. According to the maximum principle strain value and the distribution area, the equivalent crack width in this area can be calculated. It can be seen that the maximum principle strain is around 100, and the length of the small square is 25cm, the maximum crack width is the maximum principle strain multiply by the length of 3 squares, which is 75cm, therefore the maximum crack width is less than 0.1mm. As a consequence, the occurring of the horizontal crack is earlier than the two dimensional crack, which cannot be considered in survival analysis.

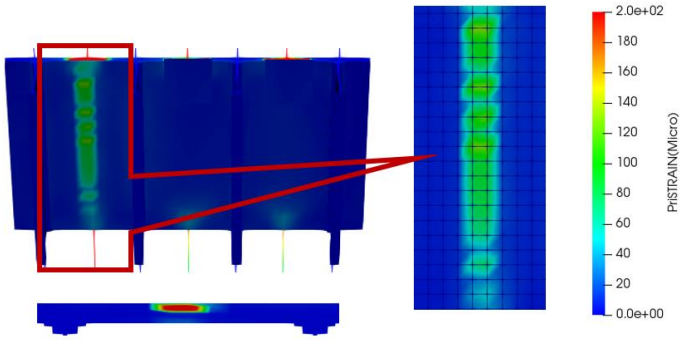

$$crack\ width = 1 \times 10^{-4} \times 75cm = 0.08mm$$

Figure 7-29 Bottom surface maximum principle strain distribution when the horizontal crack generated for 24cm slab

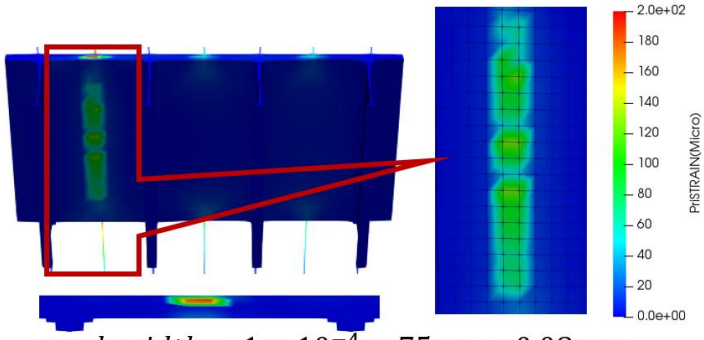

$$crack\ width = 1 \times 10^{-4} \times 75cm = 0.08mm$$

Figure 7-30 Bottom surface maximum principle strain distribution when the horizontal crack generated for 18cm slab

The bridge slab deterioration can be divided into 4 periods, which are latent period, progress period, acceleration period and deterioration period (as shown in Figure 7-31). In latent period, one dimensional crack happened, and through the progress period, two

dimensional crack are formed. Then at acceleration period, water leakage and efflorescence happened, and this is our survival analysis event. Currently, according to the road bridge deck maintenance management manual, it is said that the horizontal crack is generated after the acceleration period [5]. Therefore, under this condition, two dimensional crack should be observed from the bottom side of the slab. But according to our result, the horizontal crack is generated at incubation period, which is the initial stage of deterioration.

Additionally, Figure 7-32 shows the maximum principle strain just before and after the horizontal crack generation, which are almost same. This indicates that the horizontal crack cannot be capture by visualizing the bottom side of the crack. This phenomenon can also be observed from the site. The Figure 7-33 shows that the slab can be suddenly collapse within a really short period. The left side figure shows the condition 5 years before the failure happened and the right side shows the punching shear failure of the slab. From the efflorescence, it can be considered that the deterioration is highly correlated to the wet environmental condition and slab inside deterioration [6].

The current inspection is mainly to visually check the condition of the slab. The two dimensional crack and effloresce are the main checking object which can be observed at the bottom side of the RC slab. However, from our current result, especially, for the wet case, the horizontal cracks inside the slab occurred at beginning, and the observation of deterioration of the bottom side of the slab is delayed. It can be considered that if visible deterioration like cracking occurs on the bottom of the slab are appeared, the overall degree of deterioration is already serious. Therefore, the waterproof layer should be functional all the time to prevent the water invading.

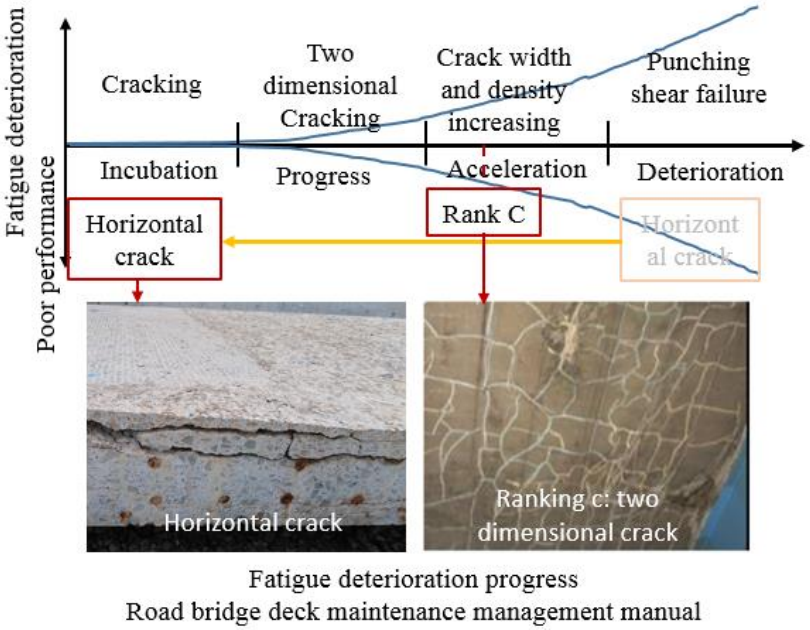

Figure 7-31 Bridge slab deterioration process

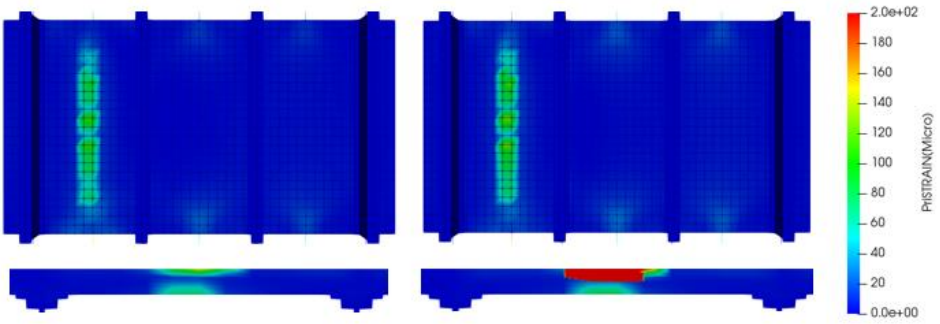

Figure 7-32 Maximum principle strain distribution before and after the horizontal crack generated

Figure 7-33 Punching shear failure happened within 5 years

7.6) Result of different distance between wheel load and girder with different slab thickness under different environmental condition

In order to check the distance between wheel load and girder affect the fatigue life more clearly, several cases which different distance between wheel load and girder are set as figure 8-27 shown. The structure is the same as case 1 and case 2 and the distance between wheel load and girder is from 1.25m to 0.50m.

Simulation results are shown in Figure 7-34. The fluctuation of each case became small as the distance between wheel load and girder become close. All dry cases didn't reach failure criterion before all simulation steps completed (Figure 7-35). Therefore, it can be concluded that under dry case, the slab is durable under dry condition no matter where the wheel load is applied. Result of distance between wheel load and girder under wet environmental condition with slab thickness of 24cm are shown in Figure 7-36. It gives the same result that as the distance keeps getting close, the fatigue life is also increasing. Usually, if the distance between wheel load and girder is close, the fluctuation of each cycle is small, therefore, the maximum strain is also small. According to this, the damage accumulation is slow.

For comparison, the result of slab with a slab thickness of 18cm also shown. The cases are shown in Figure 7-37.

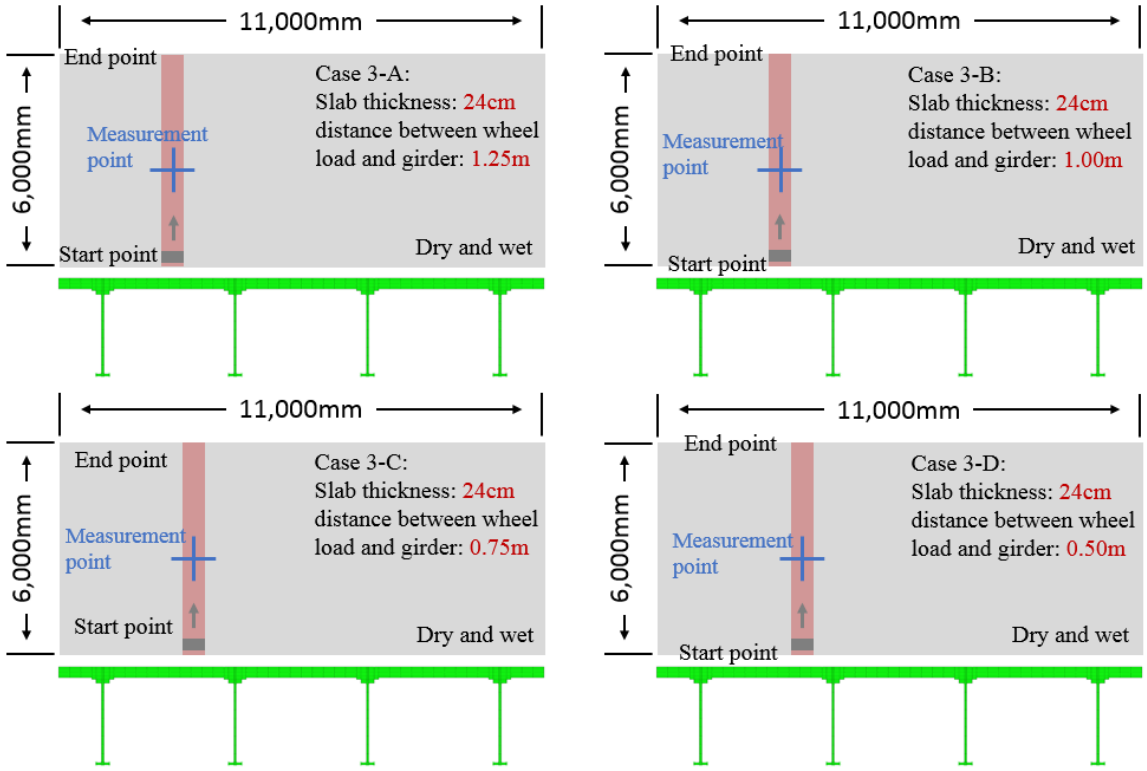

Figure 7-34 Different distances between wheel load and girder with 24cm slab thickness

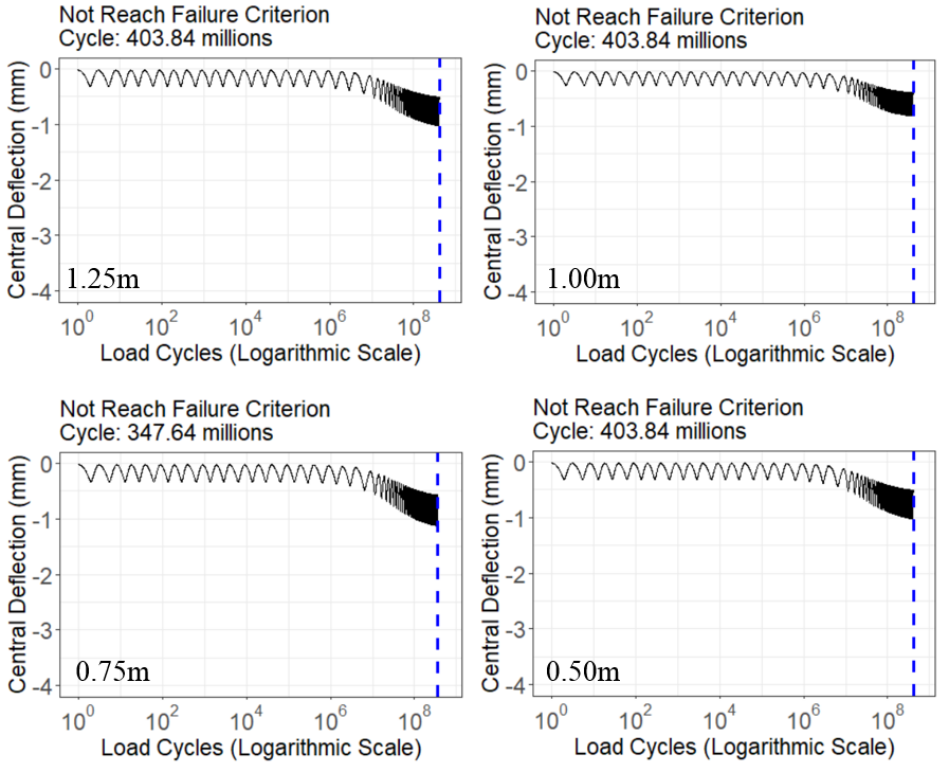

Figure 7-35 Central deflection results of different distance between wheel load and girder under dry environmental condition with slab thickness of 24cm

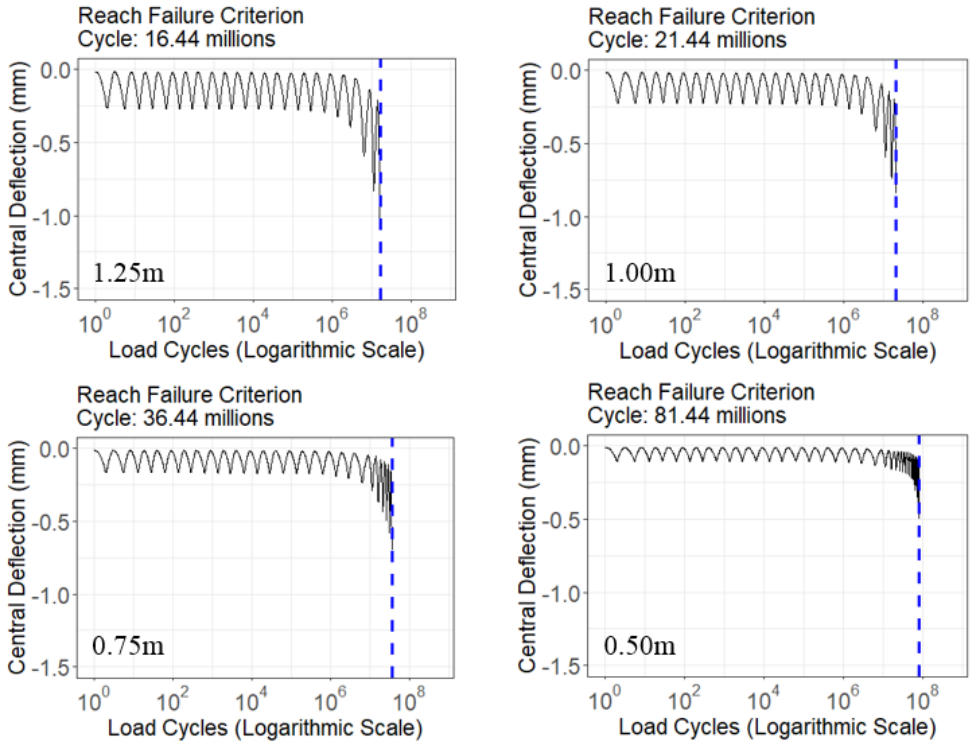

Figure 7-36 Central deflection results of different distance between wheel load and girder under wet environmental condition with slab thickness of 24cm

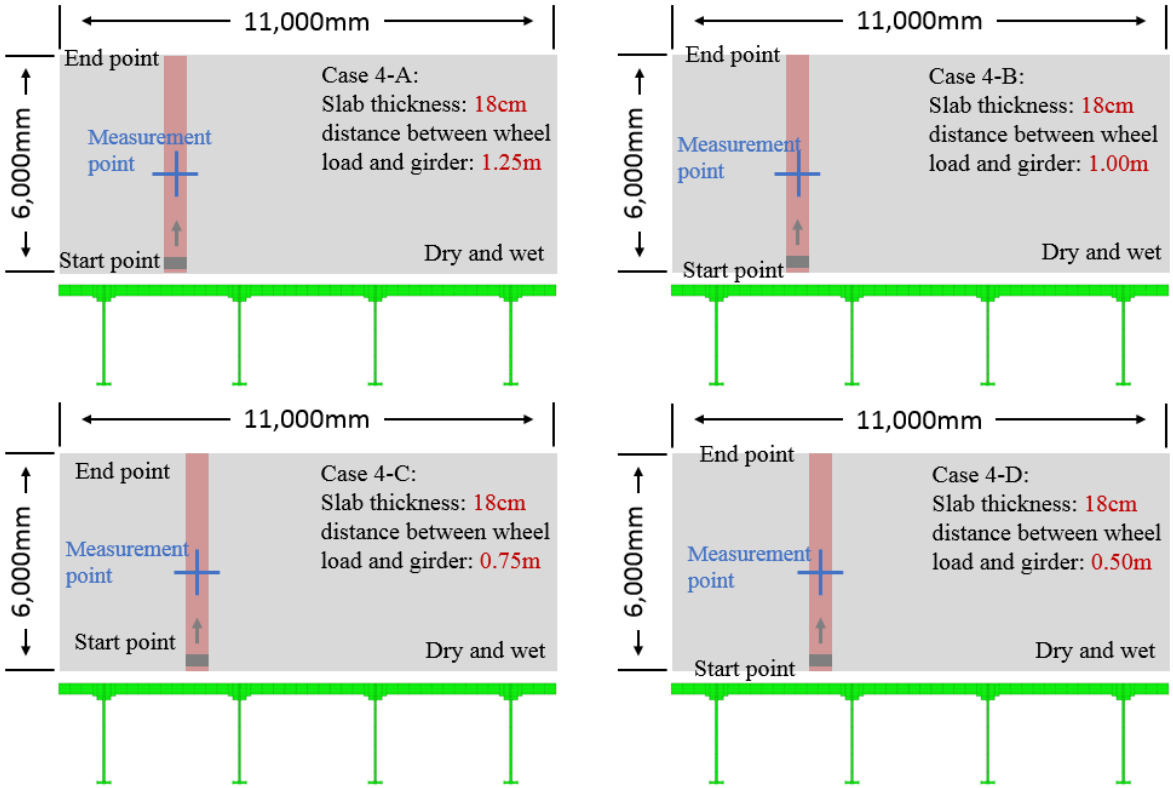

Figure 7-37 Different distances between wheel load and girder with 18cm slab thickness

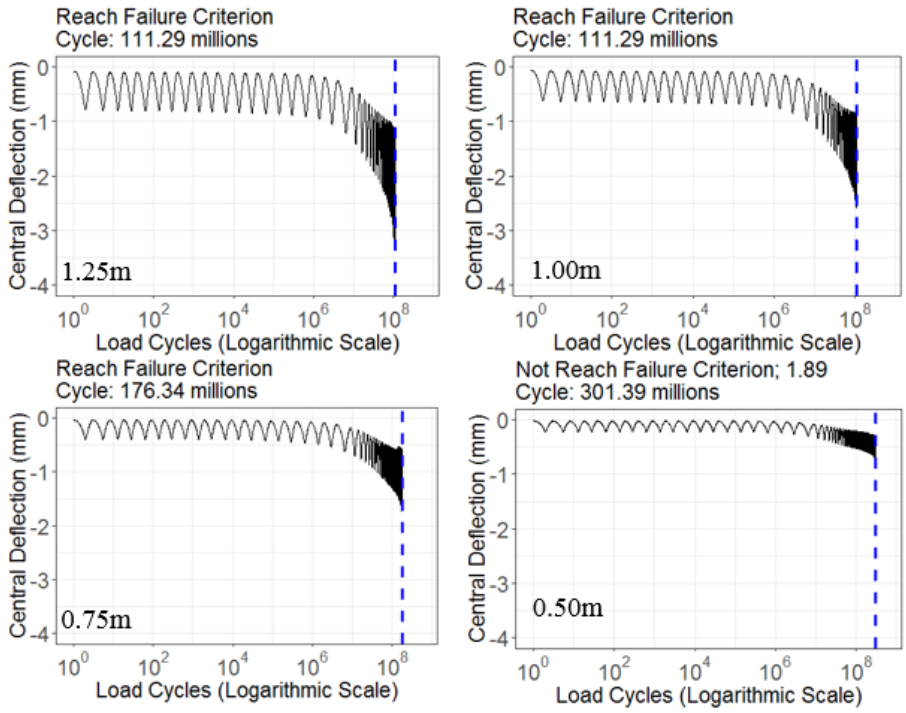

Figure 7-38 Central deflection results of different distance between wheel load and girder under dry environmental condition with slab thickness of 18cm

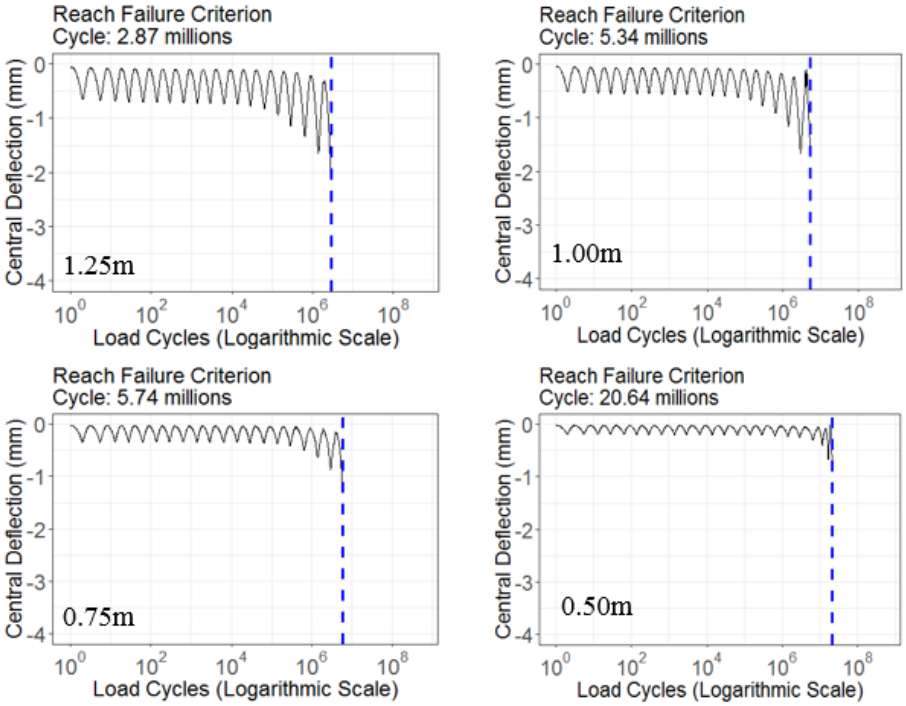

Figure 7-39 Central deflection results of different distance between wheel load and girder under wet environmental condition with slab thickness of 18cm

Figure 7-38 shows the dry environmental condition results of slab thickness with 18cm under different distance between wheel load and girder. The results show similar pattern compare with the results of 24cm. Along with the distance between the wheel load and girder

increase, the fluctuation of each cycle become large. Additionally, the result of case 4-A only gives 126.34 million cycles, which means that the slab thickness is one of a domain factor to affect the fatigue cycle. For case 4-E, the design simulation fatigue cycle is over 300 million. Therefore, it can be considered that the when the loading is close to girder, the structure is durable to resistance the fatigue load.

Figure 7-39 shows the wet environmental condition result of slab thickness of 18cm under different distance between wheel load and girder from 1.25m to 0.50m. Comparing with dry condition, the slab under wet condition reaches fatigue criterion much faster. It can be roughly see that under the slab thickness with 18cm and wet condition, the fatigue cycle are increasing as the distance between wheel load and girder get close, which gives the same result of 24cm slab.

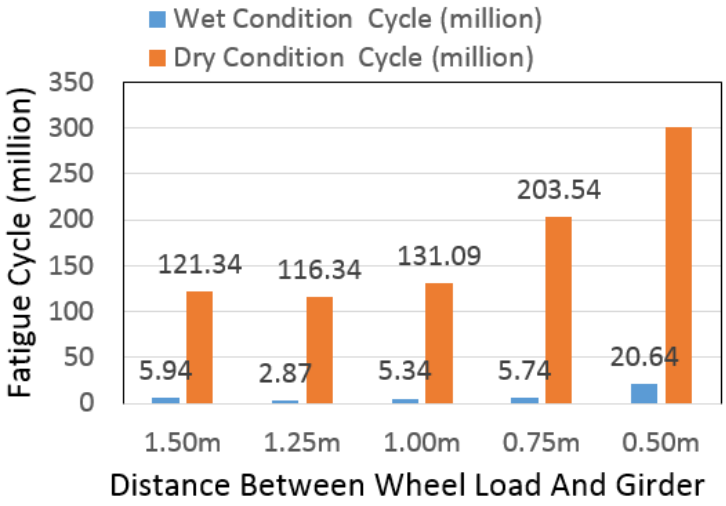

Figure 7-40 Comparison results of different distance between wheel load and girder with slab thickness of 18cm under different environmental condition

Since with the slab thickness of 24cm under dry environmental condition, the slab did not reach the fatigue criterion, therefore, in this section, the discussion is mainly focus on the slab with thickness of 18cm. Dry and wet environmental condition results comparison of different distance between wheel load and girder under slab thickness of 24 and 18 cm are shown in Figure 7-40. The fatigue cycle under dry cases are 20 to 50 time higher than water submerged case. And as mentioned before, the result confirmed the importance of waterproof. Usually the bridge slab can be under service through long time period with appropriate waterproof and maintenance.

The slab with thickness of 18cm and 24cm with different distance between wheel load and girder under water submerged case are compared. As Figure 7-41 shown, generally, as mentioned before, if the distance between girder and wheel load is far, the fatigue cycle is short. However, there are some exceptions. The case with a slab thickness of 18cm and distance of 1.25m between the wheel load and girder gives short fatigue cycle than the distance of 1.50m.

The result is considered to be related to the couple effect of fluctuation and shear strength. If the distance between wheel load and girder is far, the fluctuation is large and the fatigue can be reached fast. On the other hand, if the wheel load is closer to girder, the shear strength will be increased. And from the previous research, under repeated wheel load, the punching shear failure eventually happened. Obviously, if the shear strength is larger, the fatigue failure can also be reached faster. Therefore, the fatigue cycle is affected by not only the fluctuation of the slab, but also shear strength between girder and wheel load. The two effect restrict each other and their fatigue life will be reduced to minimum under a certain distance between wheel load and girder.

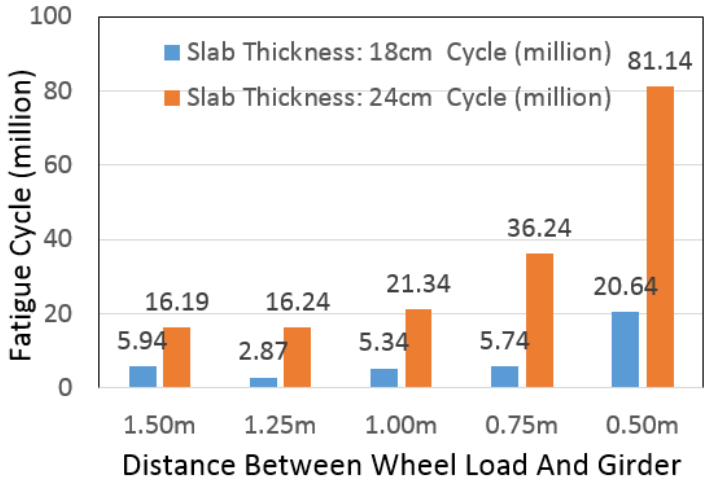

Figure 7-41 Slab with thickness of 18cm and 24cm case comparison results of different distance between wheel load and girder under water submerged case

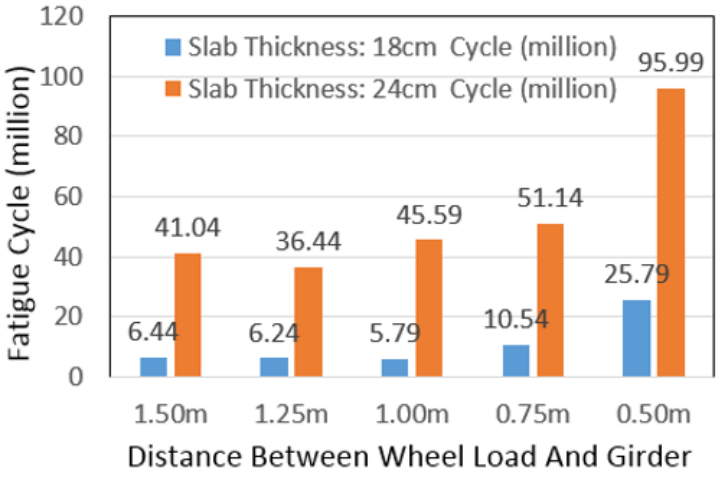

Figure 7-42 Comparison result under different definition of fatigue failure criterion

However, based on our fatigue criterion, if the initial displacement of RC is larger, the final displacement which need to reach the fatigue criterion also need to be 3 times larger than the initial. And if the distance between girder and wheel load is closer, the initial displacement is smaller, therefore it may easier for some cases to reach the current fatigue criterion we used.

In order to confirm the fatigue life is affect by not only fluctuation but also by shear strength, the fatigue failure criterion are reset. For case 1-A, based on the current fatigue criterion, the fatigue cycle is 5.94 million. At this point the displacement of RC at the loading position is 3.5mm. Here, the new fatigue failure criterion are made by using 3.5mm displacement of RC slab at the centre of wheel load position. Then the fatigue cycle are recalculated. The result is shown in Figure 7-42. It can be seen that for the case which the distance between wheel load and girder is 1.25m, it also can reach the new fatigue failure criterion faster than the case with 1.50m. Therefore, the failure mode also need to be checked to confirm the assumption. Detailed strain distribution and strain progression will be discussed in the later section.

7.7) Failure process and pattern discussion between different loading position

In order to check whether the failure mode and process are different or not, the overall displacement of Case 4-C (slab thickness: 18, distance between wheel and girder: 0.75m) under water submerged condition is shown in Figure 7-43. The displacement at loading position is very large, indicate the punching failure happened. The result is consistent with the case 2 (slab thickness: 18cm, distance between wheel load and girder: 0.75m). Therefore, it can be concluded that whether the slab is under dry or wet environmental crack, the punch shear failure happened eventually at the wheel load position.

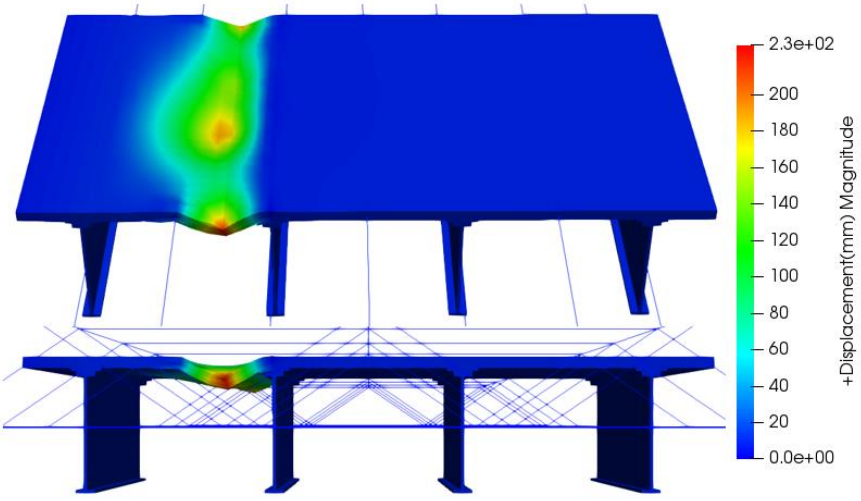

Figure 7-43 Overall displacement of case 4-C under wet environmental condition

The maximum principle strain distribution of the top and bottom surface during the deterioration process are shown in Figure 7-44 and Figure 7-45. By comparing the top and bottom surface maximum principle strain, it gives the same result the bottom side shows strain delayed strain generation. Therefore, under wet environmental condition, regardless of the position of the wheel load, strain on the top of the slab occurs earlier than bottom side when

the slab is in wet environmental condition, and inspecting only the bottom surface of the current floor slab underestimates the overall deterioration state.

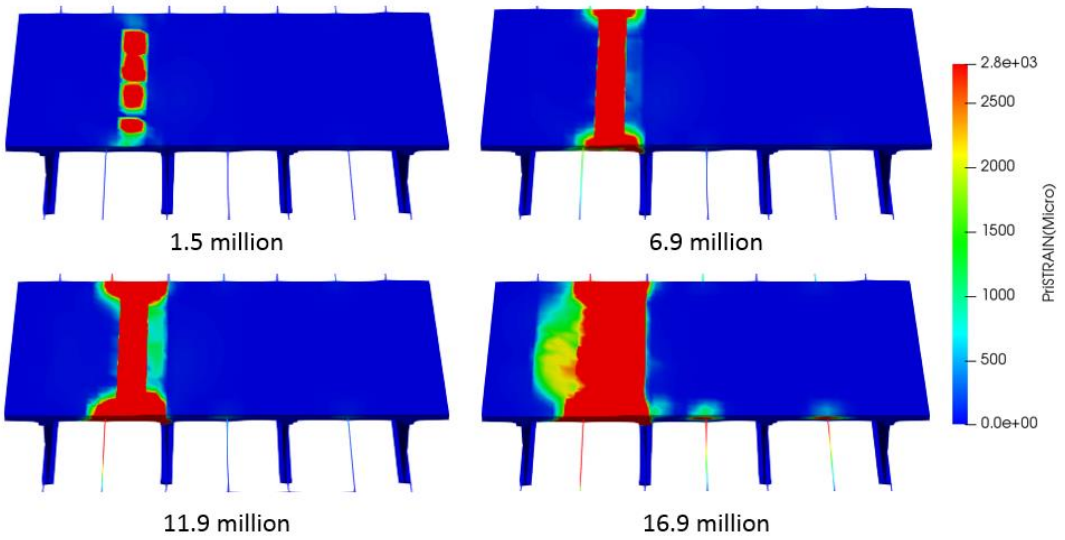

Figure 7-44 Top surface maximum principle stain distribution of case4-C transformation under wet environmental condition

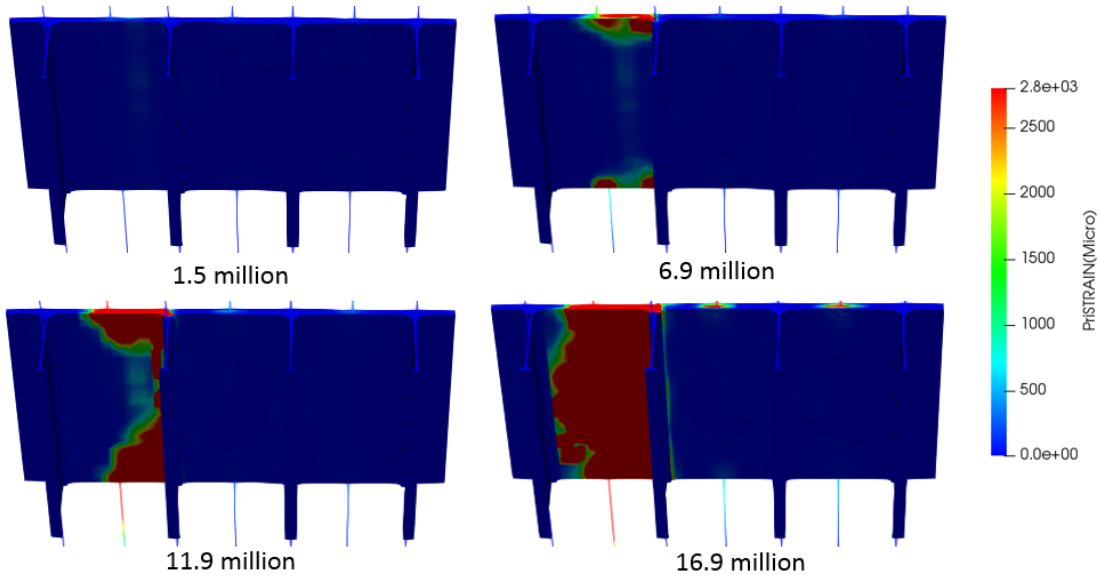

Figure 7-45 Bottom surface maximum principle stain distribution of case4-C transformation under wet environmental condition

Additionally, the cross sectional principle strain shows in Figure 7-46. Comparing with the central loading position, the loading position shows large strain, indicates that the damage occurred at the loading position. However, the result also shows large strain near the girder, indicates that in a high probability, the shear crack happened. It can be concluded that according to the different loading positon, the deterioration process is also different. Since this phenomenon can accelerate the fatigue process, therefore, the inspection should be also considered the distance between girder and wheel load. Additionally, for traditional design, the

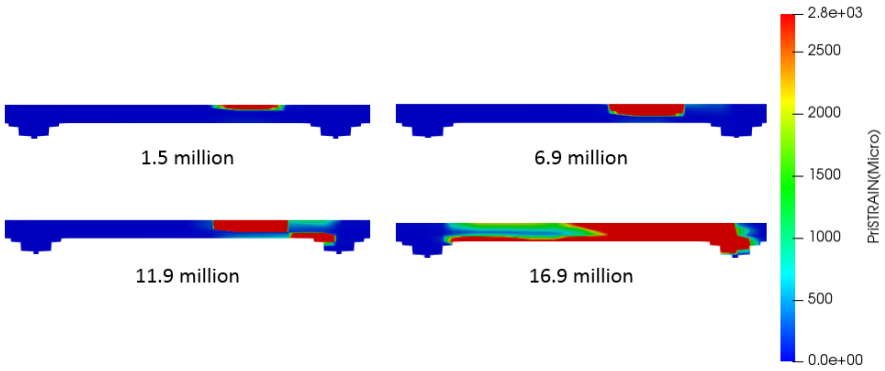

Figure 7-46 Loading applied panel cross sectional maximum principle strain distribution of Case 4-C under wet environmental condition

7.8) References

1 Fathalla, E., Tanaka, Y., & Maekawa, K. (2018). Remaining fatigue life assessment of in-service road bridge decks based upon artificial neural networks. *Engineering Structures*, *171*, 602-616.

2 Fathalla, E., Tanaka, Y., & Maekawa, K. (2019). Effect of crack orientation on fatigue life of reinforced concrete bridge decks. *Applied Sciences*, *9*(8), 1644.

3 Fathalla, E., Tanaka, Y., & Maekawa, K. (2019). Fatigue Lifetime Prediction of Newly Constructed RC Road Bridge Decks. *Journal of Advanced Concrete Technology*, *17*(12), 715-727.

4 Toshihisa Sawamatsu, Hiroshi Mitamura, & Hiroaki Nishi. (2012). A Study on Factors Deteriorating Performance of Floor Slab Waterproofing in Snowy and Cold Regions. *Monthly Report of Cold Region Civil Engineering Research Institute*, (712), 17-23.

5 Road bridge deck maintenance manual, Japan Society of Civil Engineers Steel Structure Committee Study on maintenance management evaluation of road bridge deck 2012

6 Katsuya Akabira, Hiroomi Sasaki, & Atsushi Kikuchi (2014), Case of collapsed of reinforced concrete slab due to complex deterioration. *The 8th Road Bridge Floor Symposium, Japan Society of Civil Engineers.*

Chapter 8: Full scale numerical simulation of matching actual wheel load position and non-uniform stagnant water case

8.1) Introduction

In this chapter, the wheel load position which match the actual situation are simulated. Current design didn't consider these kind of effect, therefore, this chapter will play a certain reference role for the rational bridge slab design in the future. Additionally, currently by using the GPR system, the stagnant water location can be detected. Full scale numerical simulation by considering the water location are conducted.

8.2) Result of case base on the actual lane position

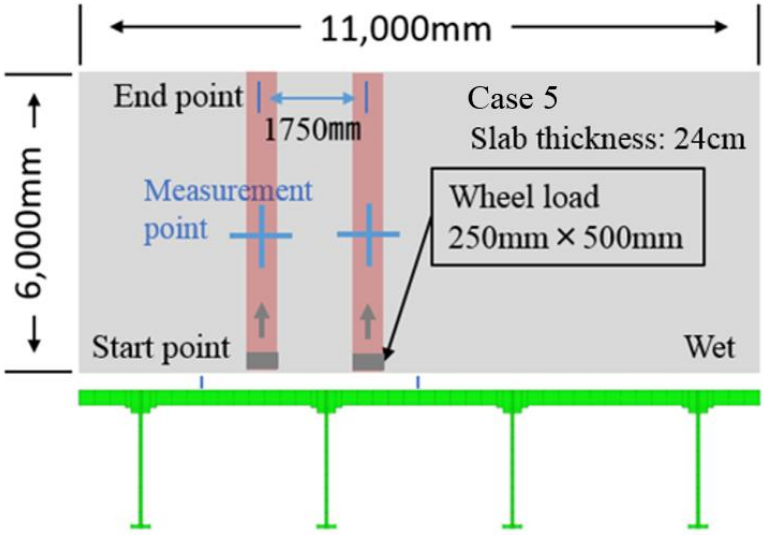

Figure 8-1 Actual wheel loading position case under wet environmental condition

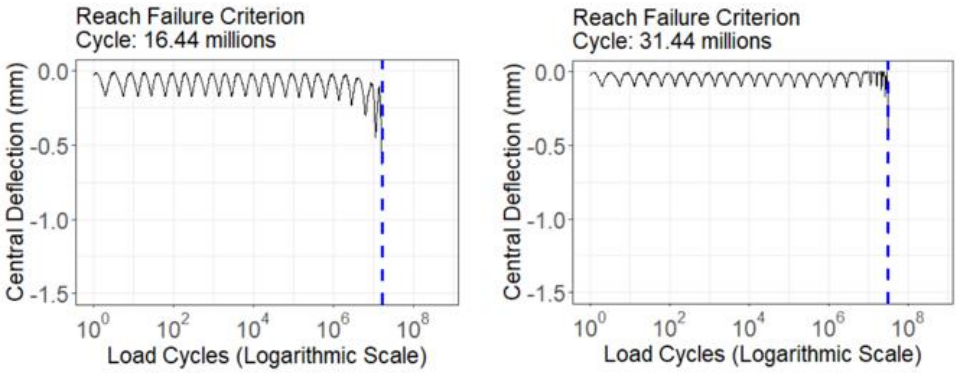

Figure 8-2 Central deflection results of actual wheel loading position case under wet environmental condition

Usually, based on the lane position, the position of wheel load on the structure is fixed at a certain range. The structure we used has two lanes and each of the lane has a width of 3.5 meters. The distance between two wheel loads are 1.75m and the traffic is assumed running at the centre of the lane. Figure 8-1 shows the wheel load position on the structure. In this case, the wheel loads are applied on different panels. The left side wheel load is 0.75m from the girder and the right wheel load is 1.00m from the girder. According to previous result, under dry condition, slab is durable and relative safe. Therefore, only the water submerged condition are discussed in this research.

The result shows in Figure 8-2. The left side wheel load shows a short fatigue cycle. Usually, if the distance between wheel loads is far from the girder, the fluctuation is larger. It can be considered that large fluctuation will cause large water pressure. Therefore, the fatigue cycle can be reached faster.

8.1) Displacement and strain distribution of actual wheel position

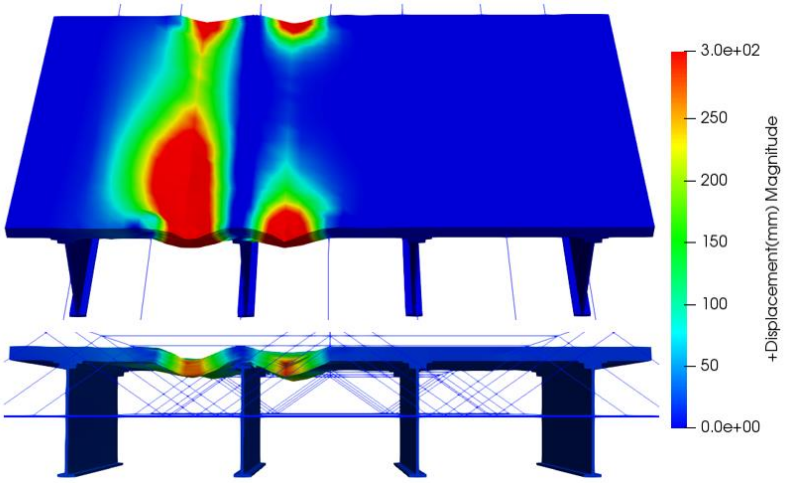

Figure 8-3 Overall displacement of actual wheel load under wet environmental condition

Figure 8-3 shows the displacement distribution. It can be seen that the punching shear failure happened in both of the wheel load position. Basically, as loading cycle increasing, the punching shear failure happened on the wheel load position.

Figure 8-4 and Figure 8-5 show top and bottom layer maximum principle strain distribution of actual loading case under wet environmental condition as loading cycle increasing. The central deflection decreasing of both side are compared in Figure 8-6. The result consistent with previous that 1) bottom surface strain distribution shows a delayed trend, 2) far distance between wheel load and girder shows fast displacement decreasing.

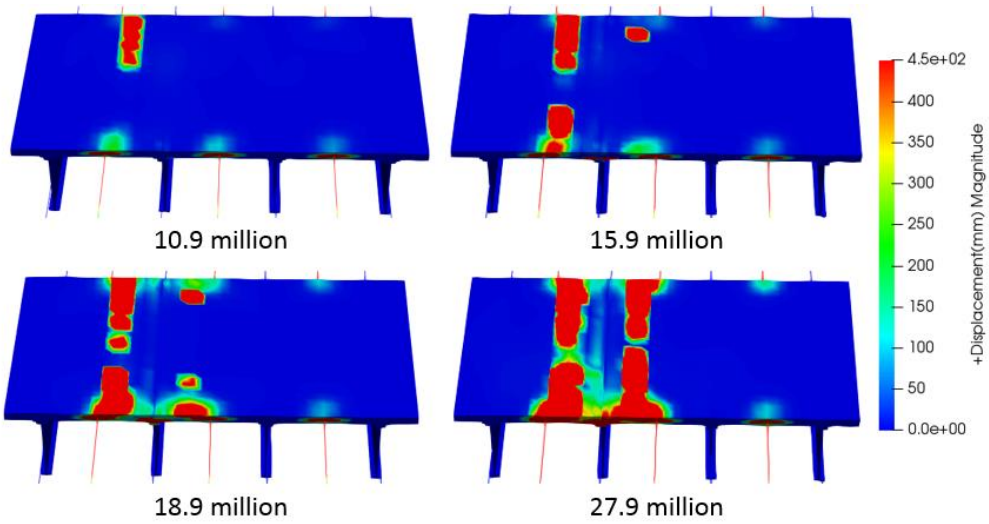

Figure 8-4 Top surface maximum principle strain distribution of actual loading position case under water submerged condition as loading cycle increasing

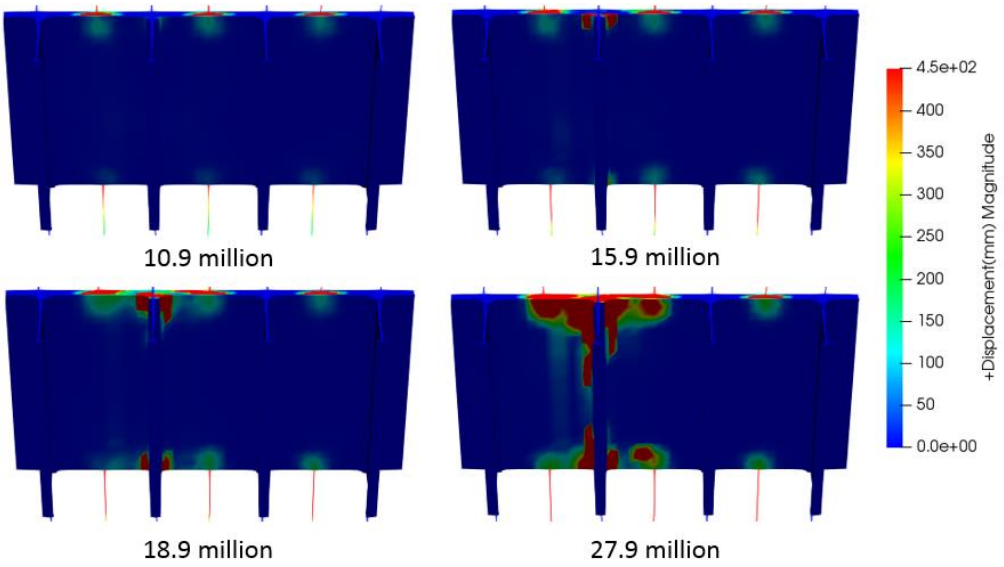

Figure 8-5 Bottom surface maximum principle strain distribution of actual loading position case under wet environmental condition as loading cycle increasing

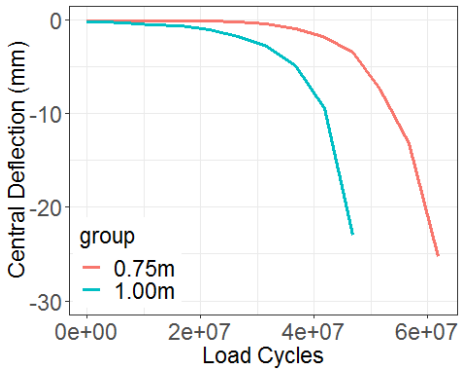

Figure 8-6 Central deflection of the actual loading position case of left and right side

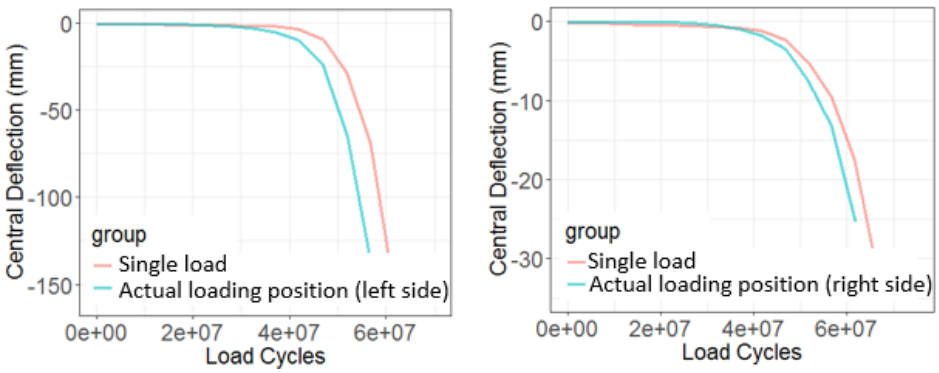

Figure 8-7 Comparison between actual loading position and single load case

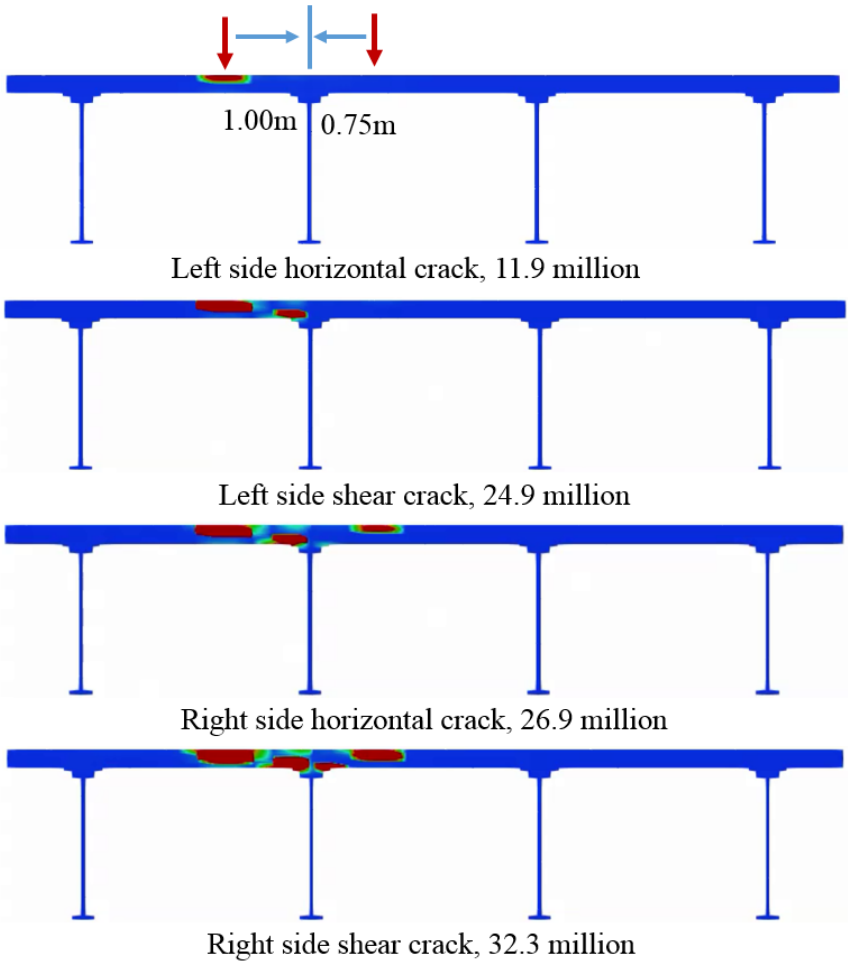

Figure 8-8 Horizontal crack and shear crack generation time

Figure 8-6 shows the central deflection comparison between left and right side actual loading cases. The result shows that the fatigue resistance is higher as the distance between wheel load and girder is closer, which is consistent with the single loading result. Additionally, Figure 8-7 shows the comparison between actual loading position and single load. Both of the deterioration of actual load are accelerated, to reach the same displacement, the fatigue cycle of actual load is less than single load case.

In the actual case, the horizontal crack and shear crack also occurred and Figure 8-8 shows the detailed information. On both side, the horizontal crack occurred first and the shear crack occurred later. However, in reality, the shear cracks of the bridge deck have not been found frequently. One of the reasons may be that compared to shear cracks, other degradations dominate the deterioration of slab, so that the bridge deck has reached its service limit before shear cracks occur. Especially in real situation, the slab is rarely under full wet environmental condition. If the slab is under non-uniform stagnant water condition, depend on the water location, the deterioration process will be complicated. Therefore, for high risk bridge slab, the detailed information should be checked in order to get precise result.

8.2) Result of non-uniform stagnant water case

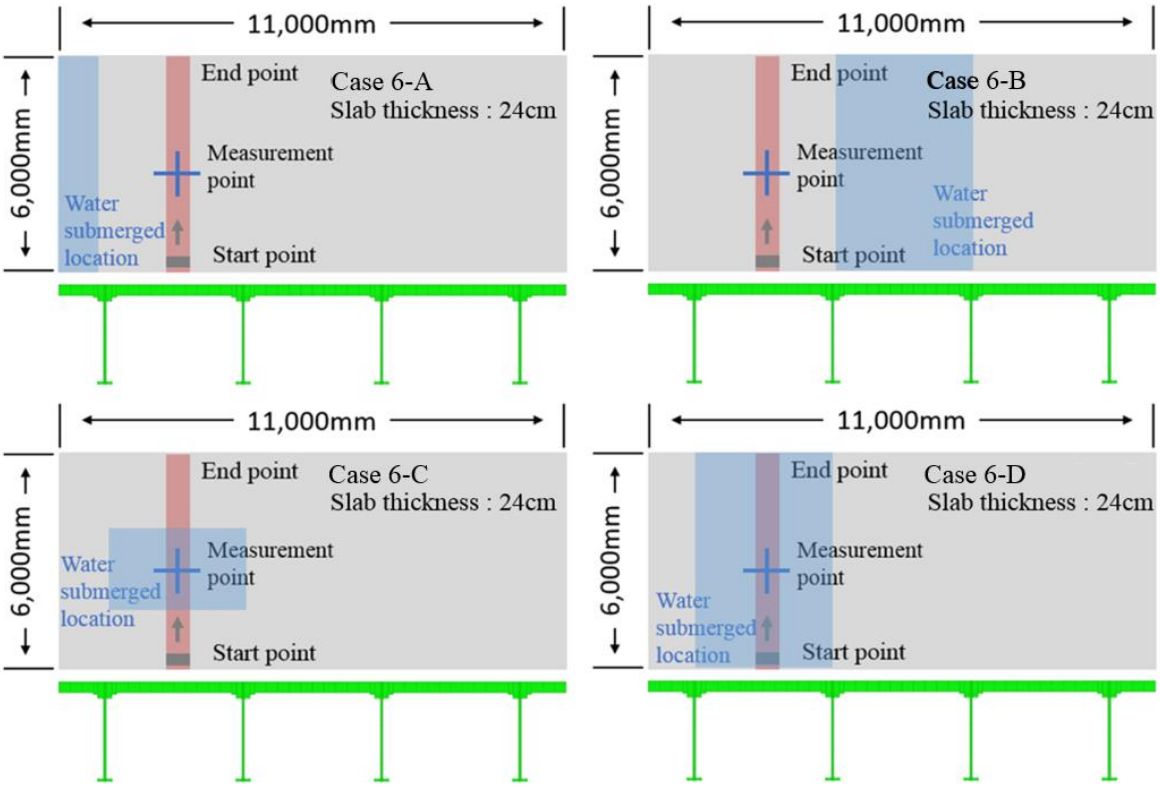

Figure 8-9 Non-uniform stagnant water submerged case

In the actual case, usually the slab is rarely under full dry and full wet case because stagnant water from rainfall may exist on reinforced concrete bridges decks due to imperfect water proofing works and insufficient maintenance. Due to different location, the fatigue cycle also may change. Therefore, the research is to be able to develop a fatigue life analysis of the bridge deck under non-uniform stagnant water submerged case. For experiment, even if the horizontal crack can be checked in an indirectly way, but it is difficult to control the environmental condition [1]. Therefore, the numerical simulation should be used to make quantitative analysis.

Previously, Eissa et al. were discussed about the effect of this under a simple plate [2]. However, the structure which are used in this research is much more complicated. Since contain three different panels, and as shown in Figure 8-9, several case are set to be compared. Case A and Case B are set to check whether the stagnant water and wheel position is applied at different panel can affect the fatigue life or not. And Case C and Case D are set to check the whether the effect of stagnant water area.

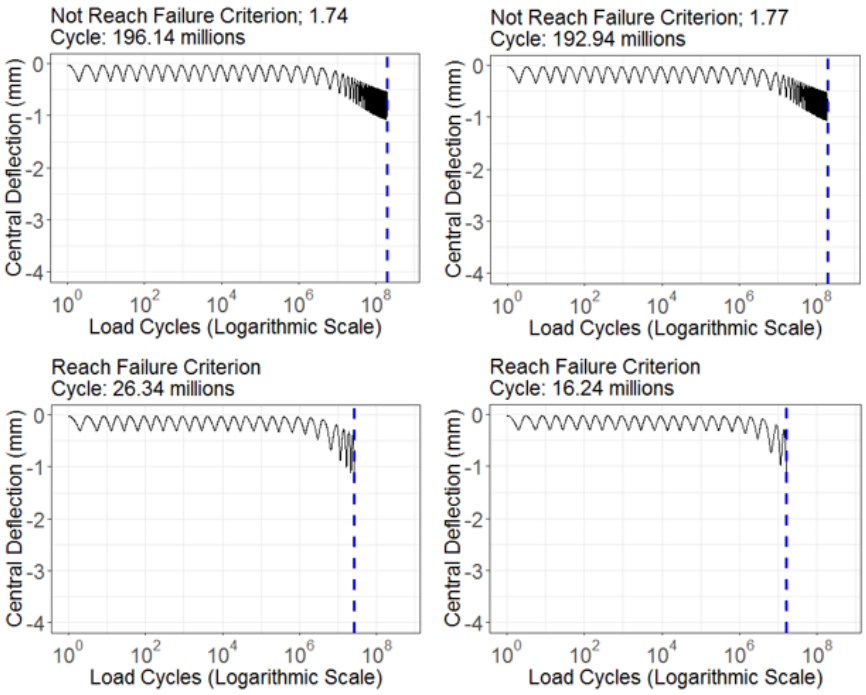

Figure 8-10 Central deflection results of non-uniform stagnant water submerged cases

The results are shown in Figure 8-10. The results of case 6-A and 6-B shows that if the wheel load and stagnant water are applied in different panel, the fatigue life is relative long, the fatigue failure criterion was not reached before all simulation steps complete. According to this result, if the panel has no wheel load, even if it is under water submerged condition, it will not affect the fatigue life. Additionally, compare with the full wet environmental cases, the partial wet condition also shows different fatigue loading cycle. Therefore, future simulation should consider not only the size, but also the location and depth of water. The horizontal crack generated condition should be checked more clearly. Additionally, complex material deterioration includes forest damage, chloride attack and ASR should also be included to improve the simulation accuracy.

8.3) References

1 Daiki Sato, Tadashi Abe & Akitaka Kiuchi (2018), Estimation of occurrence timing of horizontal crack in RC slab by fatigue test under running wheel loads, *Nihon University College of Industrial Engineering 51st Academic Lecture Performance Summary*, ISSN 2186-5647

2 Fathalla, E., Tanaka, Y., & Maekawa, K. (2019). Fatigue life of RC bridge decks affected by non-uniformly dispersed stagnant water. *Applied Sciences*, *9*(3), 607.

Chapter 9: Conclusion

9.1) Summary of the research flow

This thesis mainly contains two parts, which are survival analysis and full scale numeric simulation.

For the survival analysis, the inspection data of bridge are used to extract and quantify the risk factors which can cause the deterioration of RC slab. The survival analysis has the advantage of being able to estimate the deterioration feature in each region. Additionally, the high risk zone and the low risk zone can be clearly distinguished.

However, the survival analysis can only give a rough judgment. Even if it can give the relative deterioration rate and grasping the overall deterioration feature, but the service life cannot be predicted. Basically, the credibility and precision of survival analysis are highly depended on the on-site inspection and inspection data. If the on-site inspection cannot accurately reflect the degree of deterioration of the bridge deck, the accuracy of the survival analysis will be correspondingly reduced. In particular, if data such as vehicle weight and crack patterns cannot be recorded, the impact of such factors cannot be considered in the survival analysis. Therefore, the inspection deficiency and available range of survival analysis need to be investigated.

Here, the numerical simulation can be used to obtain the fatigue life of individual bridge slab. It is considered to have higher accuracy and freedom to set the model. So it can be used to simulate the fatigue life of the bridge deck under various environmental conditions and determine the usage limit of inspection and survival analysis by comparing the results of both. Previous studies combined these two methods and proposed a maintenance system. However, the numerical simulation is only conducted on a simple plate, which may not reflect the reality. Therefore, the full scale numerical simulation is conducted. Additionally, the Beam element is used to replace the Solid element to accelerate the simulation process.

Firstly, the result of full scale and simple plate model are compared. Then the result between full scale numerical models are compared. Through this comparison, the necessity usage of full scale model is shown and the limitation of current inspection and survival analysis are discussed. Next, the different distance between wheel load and girder are simulated and failure pattern are shown. Additionally, the case which consider the actual loading position and the partial water submerged case are also discussed. The current design didn't consider this effect, therefore, this analysis gives a good example that can be referred to rational design in the future

The conclusions of the core study of this research are as follows.

9.2) Conclusion of Chapter 3

Survival analysis, a statistical method in medical field, was applied to deal with the inspection data. Through data selection, data cleaning, data integration and the removal of highly correlated variables, the survival analysis was successfully conducted. The univariate and multivariate results were presented in this chapter and deterioration feature in eastern Japan was discussed.

1. The results show that under low traffic volume, the fatigue is not the main cause of RC slab deterioration. However, heavy winter precipitation, snowfall and the usage of de-icing salt contribute to increase risks. Therefore, the complex deterioration is the main reason for the failure of bridge slab in eastern Japan.
2. Water-related variables such as snow depth and winter precipitation increase the deterioration rate. Especially in eastern Japan, during the extended snow melting process, salt water penetrates into cracks and accelerates the deterioration process. Under this condition, if not properly protected and repaired, rebar will be corroded and slab will be seriously damaged. Correspondingly, water flow is faster for slabs with larger slopes; thus, the hazard ratio tends to be smaller. Moreover, waterproofing in eastern Japan reduces risk, indicating the importance of preventing water from penetrating the slab.
3. Using geographical coordinate information, risk scores were mapped; distinctions between high-risk and low-risk areas were shown. In eastern Japan, due to its special geographical environment, it is snowy in Japan's seaside in winter, resulting in the use of large amount of de-icing salt. Therefore, the deterioration condition and rate in this area are relatively high.

9.3) Conclusion of Chapter 4

The survival analysis was conducted by using the bridge slab inspection data in Tokyo region. The environmental characteristics of East Japan are totally different from those of the Tokyo region. As before, data selection, data cleaning and data integration were conducted. Also, unlike the eastern part of Japan, repair work is often conducted in the Tokyo region. Therefore, crack injection, steel plate bonding, replacement and other repair work were taken into consideration through the data processing and selection process. Then the univariate and multivariate analysis result were shown to compare with those of eastern Japan.

1. According to the analysis result, the risk increased by more than 30% for each additional standard unit of traffic volume, indicating that reduplicative dynamic traffic load is a major

reason for the deterioration of bridge deck slabs in the Tokyo region. Accordingly, the results reveal that slab thickness should be increased to resist traffic load. However, it was not a high risk in eastern Japan. The different deterioration characteristics in different regions were clarified.

2. Panels in different positions have different deterioration rates. Usually, the panel on the edge of the slab or near the expansion joint has high risks because of the high possibility of contact with water. In Tokyo, even panels at the centre of the slab bearing the heavy traffic loads have a less hazard ratio than those at the edge area. In addition, for both areas, the higher the flow with a greater slope, the less the hazard ratio. These results statistically prove that water plays an important role in deterioration. Therefore, waterproofing at the edge should be enhanced against severe environments.
3. Using geographical coordinate information, risk scores were mapped; distinctions between high-risk and low-risk areas were shown. In the area south of Tokyo, since the traffic volume in those areas is relatively high and most slabs in this area are relatively thin according to pre-1964 design codes, the overall risk score is high. As a result, through this quantitative multiple deterioration factors assessment, the priority of maintenance in the case of an insufficient budget will be determined by more accurate statistical analysis rather than personal subjective judgment. In short, it can be applied to optimize decision-making. Therefore, under the premise of ensuring more efficient and accurate countermeasures, financial burdens can be lessened.
4. The risk factors of bridge deck slab components were quantitatively evaluated. The results of these two typical regions can be extrapolated across Japan and used for optimal decision-making. By considering the content and quantity of risk factors, deterioration patterns can be clarified. Therefore, design, maintenance and repair can be rationalized.

9.4) Conclusion of Chapter 7

Previous numerical simulation of fatigue life only applied the load to the middle of a simple plate. However, the fatigue life will be directly affected by distance between the load and the girder. Additionally, since the actual structure is more complicated, the size, shape and boundary conditions are totally different from those of the simple plate, so are the strain and stress distribution, displacement as well as moment. Therefore, the full-scale numerical simulation is necessary.

The finite element model of bridge with 30-meter length and 11-meter width was built. Since the model contains more than 60,000 solid elements, simulation calculation will consume a lot of time. In order to accelerate the analysis process, the beam elements were used to replace parts of the solid elements. Several cases with different slab thickness and different distance

between wheel load and girder under dry and wet environmental condition are simulated by using Com3.

1. The Beam element can be used to replace the solid element to accelerate the simulation process. By calculating the second moment of the cross section area of Beam-Solid hybrid model and full solid model, the two can be completely consistent, so is the displacement of them.
2. Inconsistent result is obtained between full scale model and simple plate model because of the totally different size and boundary condition of it. Therefore, the full scale model should be used since it is close to real structure.
3. From the displacement result, it can be seen that for all cases, during the repeated loading process, the displacement of the centre part of the RC slab starts to increase, and it can be seen that the central area was collapsed at final stage at the wheel load position, indicates the full scale model can be used to simulate punching shear failure.
4. The full scale numerical simulation results show that under wet condition, the fatigue life of slab is much less than that under dry condition. The presence of water will increase the deterioration rate of slab, because the penetration of water in pavement cracks promotes the polishing effect of the cracked surface, and the crack width increases rapidly. Therefore, the prevention of water permeation is extremely important for ensuring the safety of slab, and early actions can extend the life of the RC slab.
5. According to the different environment and waterproof condition, the slab in Tokyo region can be considered under dry condition and the slab in East Japan can be regarded as under wet condition. By comparing the results of survival analysis and numerical simulation under difference slab thickness and environmental condition, the consistency of both methods are confirmed, indirectly proved the credibility of survival analysis.
6. The current inspection of the slab is mainly visual inspection of the state of the bottom side. On the one hand, since the damage is appeared on the bottom side surface and the deterioration process through long time period for dry case, current inspection and survival analysis can consider this type of deterioration. On the other hand, under wet case, it can be concluded that if there is visible deterioration, such as the cracking of bottom surface, the overall degree of deterioration may have been serious according to the maximum principle strain on the bottom surface shows a delayed trend. Additionally, the horizontal crack is occurred. Most importantly, the horizontal crack does not occur after the acceleration period, but at the initial stage of deterioration (latency period) through a short period of time. At the present time, it is not possible to determine the presence of horizontal cracks in the bottom surface of the slab, and survival time analysis cannot be considered or underestimated this type of deterioration. Future inspection should consider the distance among girder, wheel load and crack pattern. Especially, the non-destructive inspection

method (GPR) and combined with full scale numerical simulation should be conducted to acquire more accurate information for the maintenance of the bridge slab. Additionally, the waterproof layer should be functional all the time to prevent water from invading the slab.

7. The distance between the girder and wheel load can affect the fatigue life. In general, when the distance between the wheel load and girder is relatively long, the fluctuation caused by loading is also large. Since the motion can increase the internal water pressure of the RC slab, the fatigue failure can be reached early. Current design didn't consider these kind of effect, therefore, this result will play a certain reference role for the rational bridge slab design in the future.
8. However, there are some exceptions. In some cases, the closer the girder is to the wheel load, the shorter the fatigue life. It can be thought of as an effect of shear strength. The fatigue life of the RC slab depends not only on the fluctuation, but also on the shear strength. On the one hand, the fluctuation increases with the increase of the distance between wheel load and girder. On the other hand, with the decrease of distance, the shear strength between the wheel load and girder increases. Both of these effects can determine the fatigue life of the girder.

9.5) Conclusion of Chapter 8

In this chapter, the wheel load position which match the actual situation are simulated and compared with single wheel load case. Additionally, full scale numerical simulation by considering the water location are also conducted.

1. Comparing with the single wheel load, the case of actual loading position shows less fatigue cycle even if the two wheel loads applied on different panels. Therefore, it can be concluded that under multiple wheel load, the fatigue resistance of the structure is reduced.
2. Compare with the full wet environmental cases, the partial wet condition shows different fatigue loading cycle. In order to get more precise result, GPR system should be induced to detect the water location. Future inspection need to combine the distance effect between wheel load and girder as well as the stagnant water location. Currently, the simulation only considers the full dry and full wet environmental condition, therefore, the horizontal crack generated condition should be checked more clearly based on the information above. Additionally, complex material deterioration includes forest damage, chloride attack and ASR should also need to be induced to improve the simulation accuracy.

Appendix: parametric survival model

Introduction

Actually, Cox regression is only one of many survival models. Since the partial likelihood are used to estimate the regression coefficient, it is more flexible, which can be used for any case. However, as mentioned before, it cannot give a future prediction. And parametric survival model just makes up for this shortcoming. Not like Cox regression, parametric gives an assumption which the shape of hazard under a specific distribution. Therefore, the key point is to select the best distribution which is fit for the dataset.

Advantages of parametric model in survival analysis include: the distribution of survival time can be estimates. Residuals can represent the difference between observed and estimated values of time. Estimated parameters provide clinically meaningful estimates of effect [1].

In this chapter, firstly, the methodology of parametric model is introduced. Then several model which contain exponential, Weibull, log-normal and generalized distribution are selected and fitting condition of each model are evaluated. By comparing the results, log-normal and generalized model which has the best fit are selected. Additionally, the survival probability of each panel 10 year later are shown. However, according to the comparison result of non-parametric and parametric, since the data are insufficient inspection data, the hazard fluctuation are relatively high. Therefore, further data accumulation is expected.

Methodology of parametric survival model

As discussed in the previous research, the likelihood distribution for right censored data fall into two categories. In the case of individual is censored at X_i, then we have

$$\mathcal{L}_i(\beta) = S_i(X_i) \qquad \text{(app.-1)}$$

In the case of individual fails at X_i

$$\mathcal{L}_i(\beta) = f_i(X_i) = S_i(X_i)\lambda(X_i) \qquad \text{(app.-2)}$$

Therefore, the full likelihood is

$$\begin{aligned}\mathcal{L}(\beta) &= f_i(X_i) = \lambda_i(X_i)^{\delta_i} S_i(X_i) \\ &= \prod_{i=1}^{n} \left[\frac{\lambda_i(X_i)}{\sum_{j\in R(X_i)} \lambda_j(X_i)}\right]^{\delta_i} \left[\sum_{j\in R(X_j)} \lambda_j(X_i)\right]^{\delta_i} S_i(X_i) \qquad \text{(app.-3)}\end{aligned}$$

Where δ_i is the index for censoring, if the individual is censored, δ_i equal to 1, and if individual is failed, δ_i equal to 0. The first term contained almost all the information about β, while the last two term contain information about $\lambda_0(t)$.

Taking logs, and recalling the expression linking the survival function S(t) to the cumulative hazard function $\Lambda(t)$, the log-likelihood function for censored survival data can be obtained and shown in the equation below

$$logL = \sum_{i=1}^{n} \{d_i log\lambda(t_i) - \Lambda(t_i)\} \quad \text{(app.-4)}$$

Parametric survival model selection

In our research, four parametric survival model, which are exponential, Weibull, log-normal and generalized gamma distribution are selected. The exponential distribution is the simplest survival model. Weibull model, log-normal and generalized gamma distribution are commonly used distribution. The advantage of these models are their flexibility which can fit many curves.

Exponential distribution

Different kinds of proportional hazard models may be obtained by making different assumption about the baseline survival function, or equivalently, the baseline hazard function. If the baseline risk is constant over time, the exponential model is obtained. The probability density function, hazard function and accumulate hazard function are shown below.

$$f(t) = \lambda e^{-\lambda t} \quad \text{(app.-5)}$$

$$F(t) = 1 - e^{-\lambda t} \quad \text{(app.-6)}$$

$$h(t) = \lambda \quad \text{(app.-7)}$$

The exponential regression model belongs to proportional families. It is the most concise survival model in survival analysis. On the other hand, because it is simple, it does not have diversity and flexibility.

Weibull survival model

Weibull distribution is also a generalization of the simple exponential distribution. Weibull regression model is one of the most popular forms of parametric regression model that it provides estimate of baseline hazard function as well as coefficients for covariates. The

survival function, the probability density function, the hazard function and accumulation hazard function are shown below.

$$S(t) = e^{-(\lambda t)^p} \quad \text{(app.-8)}$$

$$f(t) = p\lambda(\lambda t)^{p-1} e^{-\lambda t^p} \quad \text{(app.-9)}$$

$$h(t) = p\lambda(\lambda t)^{p-1} \quad \text{(app.-10)}$$

$$H(t) = (\lambda t)^p \quad \text{(app.-1)}$$

Log-normal survival model

The log-normal distribution is a probability from a continue random variable which was transform from a normal distribution. The log-normal distribution can be applied in many fields of studies, for instant in hydrology that can be used to analyse extreme values of daily, monthly or yearly rainfall. Additionally, the maintenance of a system also can be estimated [2, 3].

The probability density function can be shown as follow

$$f(t) = \frac{1}{\sqrt{2\pi}\sigma t} exp(-\frac{1}{2}(\frac{lnt - \mu}{\sigma})) \quad \text{(app.-11)}$$

And the cumulative distribution function is

$$F(t) = \varphi[\frac{lnt - \mu}{\sigma}] \quad \text{(app.-12)}$$

Where φ is a cumulative distribution function form normal distribution.

So that, the survival function of lognormal distribution is

$$S(t) = 1 - \varphi[\frac{lnt - \mu}{\sigma}] \quad \text{(app.-13)}$$

The hazard function is as follows

$$h(t) = \frac{\frac{1}{\sqrt{2\pi}\sigma t} exp(-\frac{1}{2}(\frac{lnt - \mu}{\sigma}))}{1 - \varphi[\frac{lnt - \mu}{\sigma}]} \quad \text{(app.-14)}$$

Generalized gamma distribution

The generalized gamma distribution becomes more popular due to its flexibility. The probability density function can be defined as

$$f(t) = \frac{p\lambda(\lambda t)^{\alpha-1}e^{-(\lambda t)^p}}{\Gamma(\frac{\alpha}{p})} \quad \text{(app.-15)}$$

The survival probability of generalized gamma distribution is

$$\mathrm{S(t)} = \frac{1 - \gamma\{\frac{\alpha}{p}, (\lambda t)^p\}}{\Gamma(\frac{\alpha}{p})} \quad \text{(app.-16)}$$

Where

$$\gamma(\mathrm{s,x}) = \int_0^x t^{s-1}e^{-t}dt \quad \text{(app.-17)}$$

The hazard function is

$$\mathrm{h(t)} = \frac{p\lambda(\lambda t)^{\alpha-1}e^{-(\lambda t)^p}}{1 - \gamma\{\frac{\alpha}{p}, (\lambda t)^p\}} \quad \text{(app.-18)}$$

The generalized gamma distribution can be used to test the adequacy of commonly used gamma, Weibull and exponential distribution, since they are all nested within the generalized gamma distribution family.

Survival probability result of parametric survival model

In this research, the inspection data from Tokyo region are used to estimate each model. the reason is that the data from Tokyo region are already accumulated 40 years by every year inspections, and also the bridge slab are constructed almost at same period, therefore, the data quality is relatively higher than the other region. Additionally, the affect by construction quality is also small.

The result of survival possibility is shown in Figure app.-1 to Figure app.-5. For comparison, the black line is the result of Kaplan-Meier curve. The model adequacy can be assessed by inspecting by Kaplan-Meier curves stratified by categorical variables. The fitting result of exponential, Weibull, log-normal and generalized gamma result also are shown in the Figure. For the group of all bridge, each parametric models show similar result. It can be seen that they can roughly catch the trend of the non-parametric estimation. However, by comparison each parametric model, the result of exponential distribution seems stiff than other model.

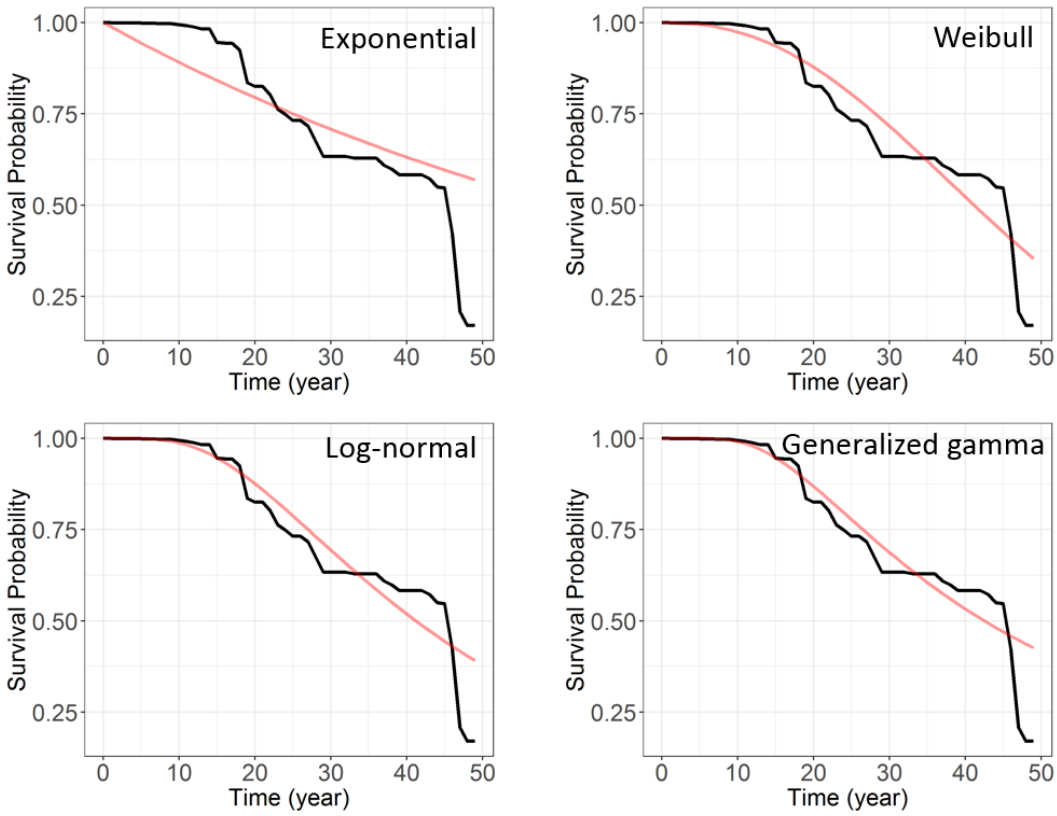

Figure app.-1 Survival probability of all bridge slab and fitting result of parametric model

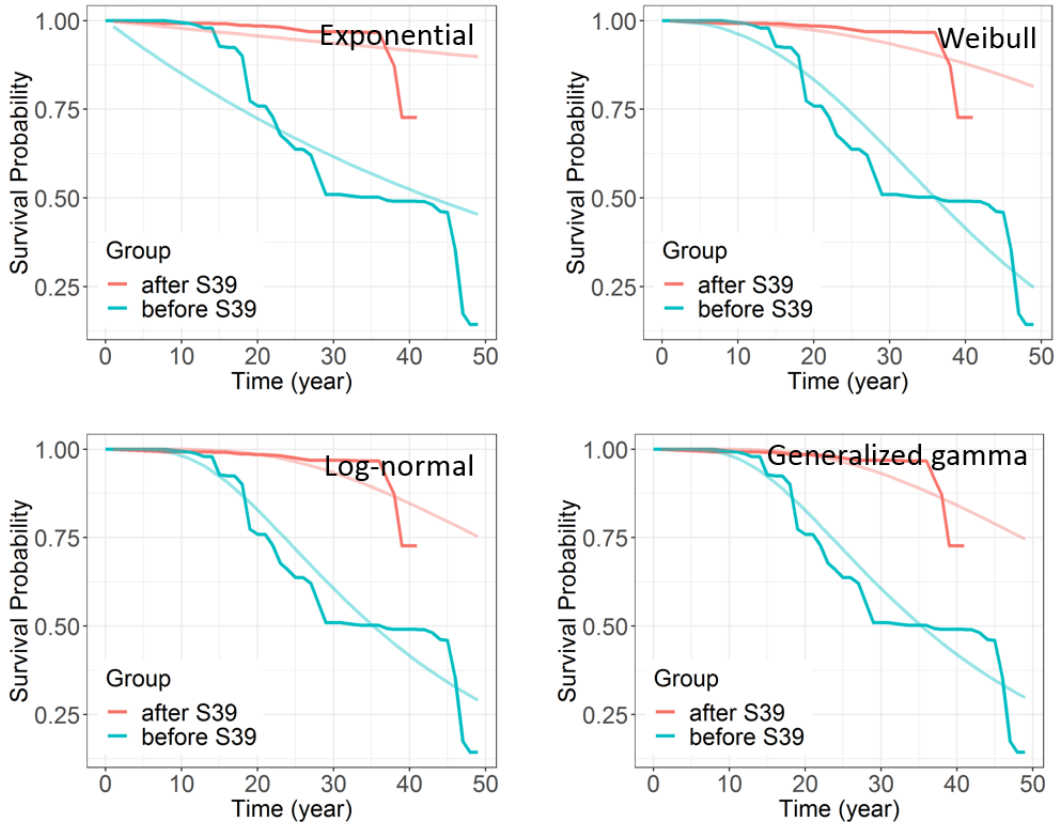

Figure app. -2 Survival probability of design code and fitting results of parametric models

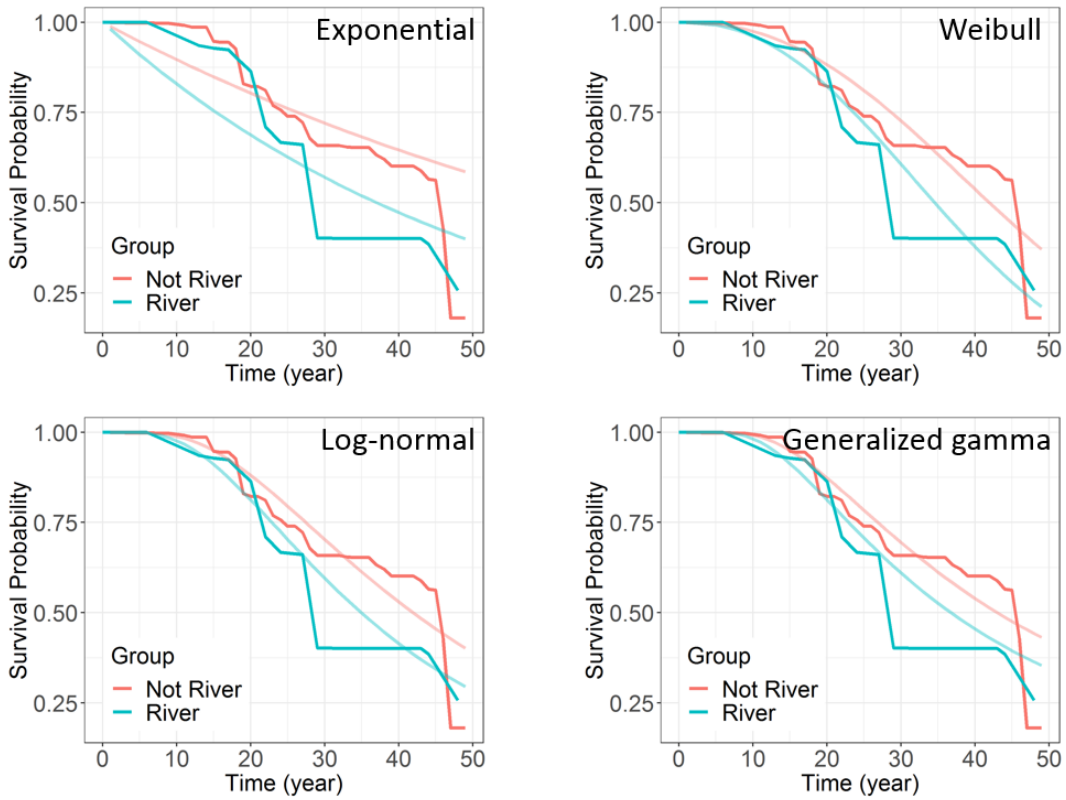

Figure app.-3 Survival probability of crossing condition and fitting results of parametric models

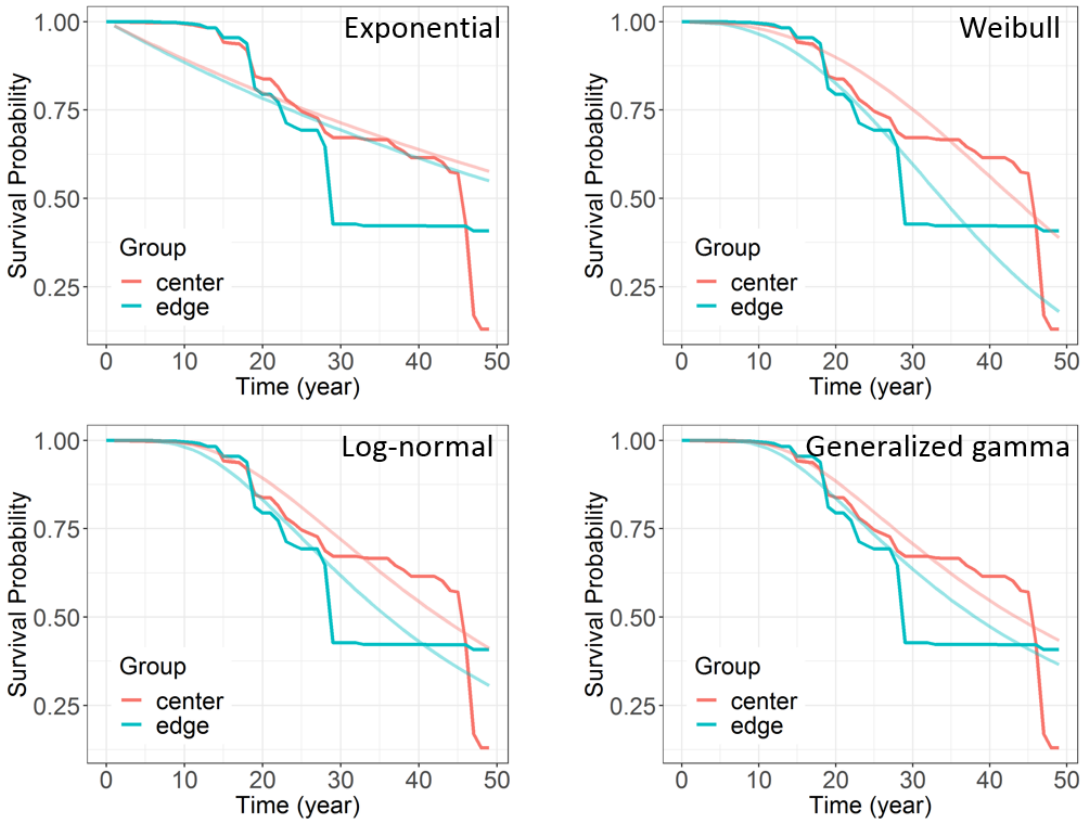

Figure app.-4 Survival probability of panel position and fitting results of parametric models

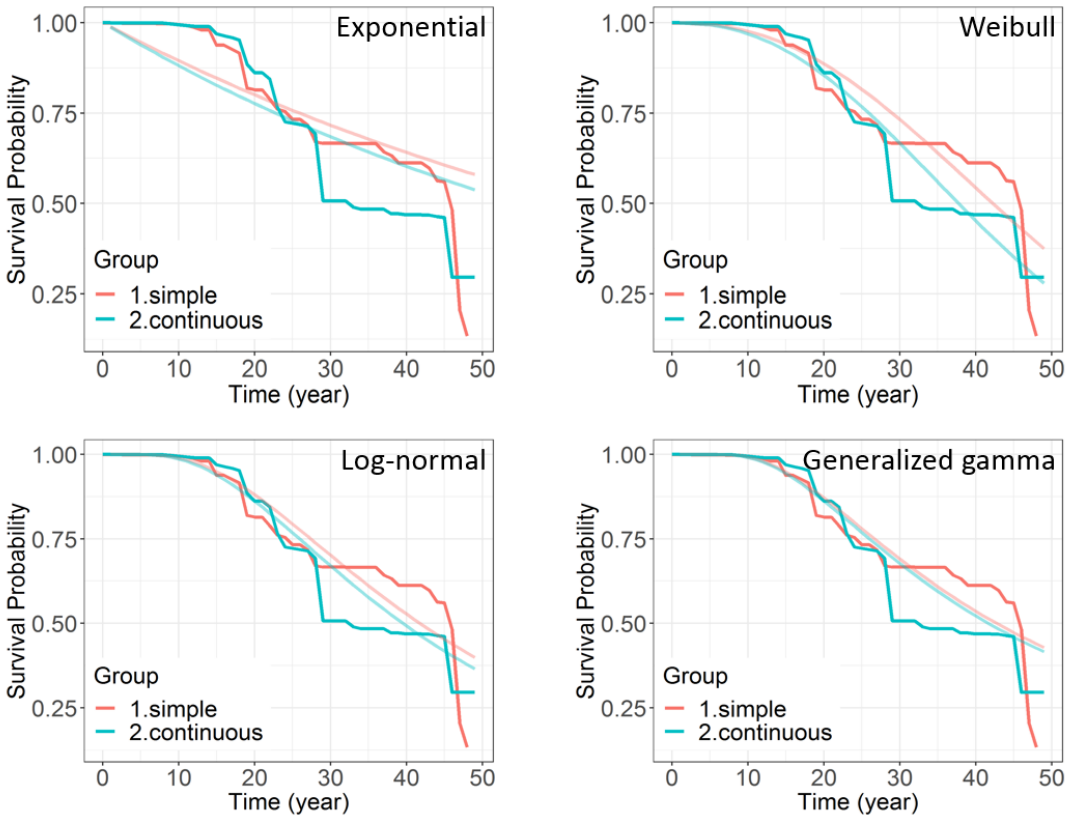

Figure app. -5 Survival probability of girder type and fitting results of parametric model

The survival probability result of design code, crossing condition, panel position and girder type are also shown in the figure. For some group like crossing condition and panel position, even though the Kaplan-Meier shows that the declination rate between groups are different, for example in the case of panel position, the survival probability of edge group is higher than centre group, but after 15 years usage, the survival probability of edge is lower than centre group. The reason is that in the first stage, there was lots of deterioration due to heavy traffic load, but over time, deterioration due to environment factors became predominant. Additionally, according to the definition of survival probability function, the population is decreasing over time. Therefore, the fluctuation is also become large. In the Figure it can be clear see a sudden drop at the survival year around 30 and 47. According to the parametric model, it gives a proportional hazard assumption, therefore survival probability of edge group is lower in all time period.

Basically, except exponential survival model, the parametric model can give a reasonable fitting, indicate that by using appropriate model, the survival probability can be estimated and future survival possibility can be calculated.

Multivariate analysis result of parametric survival model

Table app.-1 AIC and likelihood of each parametric model

Distribution	Log-likelihood	Freedom	AIC
Exponential	-40708.4	10 (1+9)	81436.8
Weibull	-37751.9	11 (2+9)	75525.8
Log-normal	-37222.0	11 (2+9)	74466.1
Gengamma	-37221.6	12 (3+9)	74467.1

Before, multivariate analysis, the AIC and likelihood estimation of each model are shown in Table app.-1. Akaike proposed AIC as an estimate of the expected log likelihood to estimate the goodness of models fitted to a given set of data. It has greatly widened the range of application of statistical methods [4, 5]. The equation is defined as

$$\mathrm{AIC} = 2\mathrm{k} - \ln(\mathrm{L}) \qquad \text{(app.-19)}$$

Where k is the number of estimated parameters in the model. And L is the maximum value of likelihood function for the model.

From the result, it can be seen that the log-normal and generalized gamma model give a similar result, which are the best fit than other survival model.

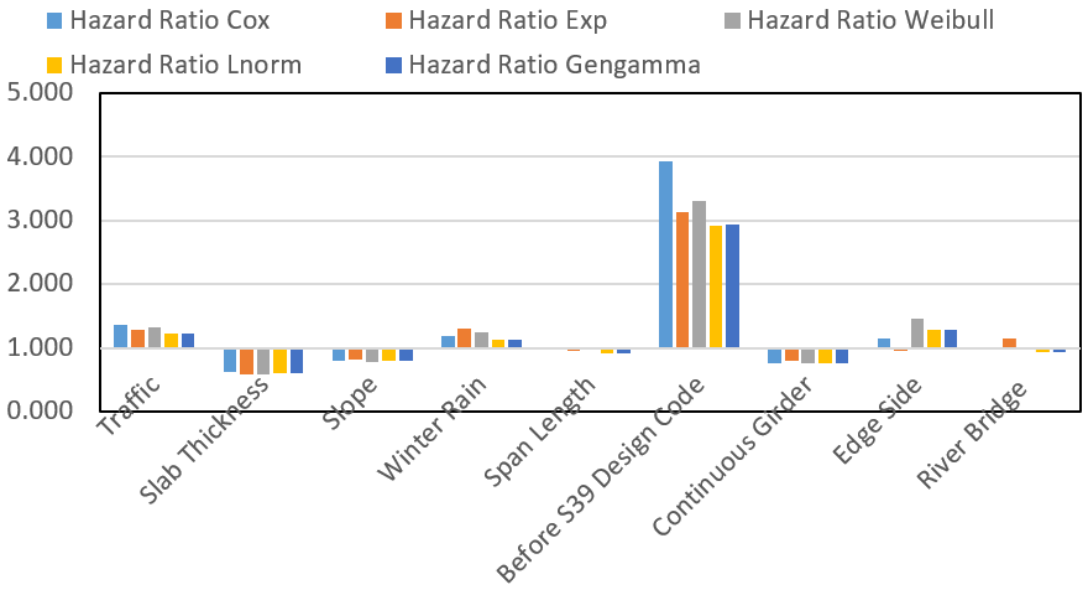

Figure app. -6 Multivariate analysis result of each parametric model

The multivariate analysis result of each parametric model is shown in Figure app.-6. The x-axis represents each group and y-axis is hazard ratio. For comparison, the result of Cox regression is also shown in the figure and the variable selection are also the same as Cox regression. It can be seen that the hazard ratio of all groups shows similar result, indicate that the applicability of parametric model for hazard ratio calculation. Also, as mentioned before, since the exponential survival model are stiff, the result of some groups are inconsistent with other survival model.

Discussion of the fitting of non-parametric model and parametric model

From the previous, the survival probability and hazard ratio of each group can be estimated by using appropriate parametric model. Especially, for the survival model like generalized gamma distribution, because of its flexibility, it can be dealing with many types of data set which has the different shape of distribution. From the comparison result of AIC, the fact that log-normal and generalized gamma distribution is the best fit are proved, but still from the survival probability, the difference is not clearly shown. The reason is because that the survival probability is integrated with the probability density function, the change of it is smoother than the hazard. Therefore, by directly comparing hazard of each group is a clearer way to show which model is better. First, from the non-parametric survival model

$$\hat{S}(t) = \prod_{t_i<t} \frac{n_i - d_i}{n_i} = \prod_{t_i<t} (1 - \frac{d_i}{n_i}) \qquad \text{(app.-20)}$$

We can get accumulate density function

$$F(t) = 1 - S(t) \qquad \text{(app.-21)}$$

Then by using the equation

$$f(t) = \frac{dF(t)}{dt} = \frac{F_{i+1}(t) - F_i(t)}{t_{i+1} - t_i} \qquad \text{(app.-22)}$$

The hazard can be calculated as follow

$$h(t) = \frac{f(t)}{S(t)} \qquad \text{(app.-1)}$$

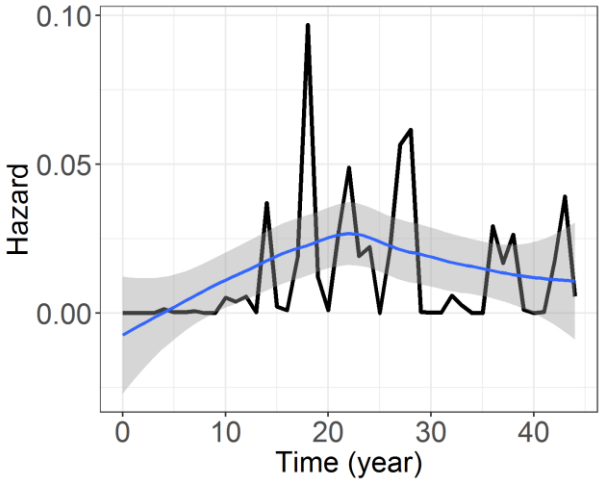

Figure app. -7 Hazard shape from non-parametric

Figure app.-7 shows the shape of hazard which obtain from non-parametric method. It can be seen that the due to insufficient data, the shape of hazard is not smoothly, indicates that further data accumulation are needed. According to the big data concept, in some cases, the distribution shape can be identified only when the data reaches million level. However, still the unimodal trend of hazard can be seen by using smooth function.

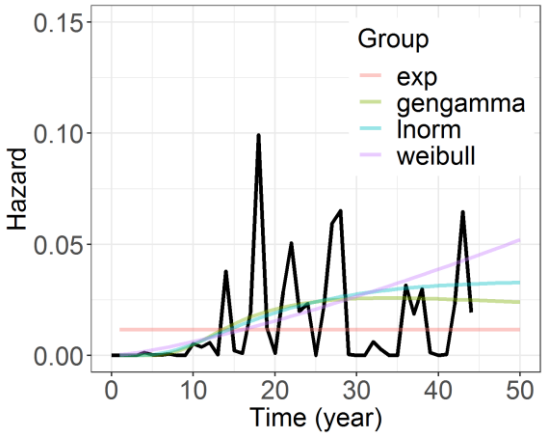

Figure app. -8 Hazard fitting result of each parametric model

The fitting result are shown in Figure app.-8. The result shows that only the log-normal and generalize gamma distribution gives unimodal distribution of hazard, indicate that these two models fit for our data. For exponential, the hazard is constant in all time period. For Weibull model, the hazard increasing all the time, therefore after 50 years, the hazard is over estimated. Figure app.-9 shows the hazard distribution of each parametric model in 2019. The exponential survival model showing constant result which does not change, therefore, the results are same in all time period. For Weibull result, according to the mean value of hazard, it can been seen that the hazard are over estimated. The meaning of hazard is instantaneous destruction rate, in Figure app.-9, the hazard indicates the event happening possibility of each slab panel in 2019.

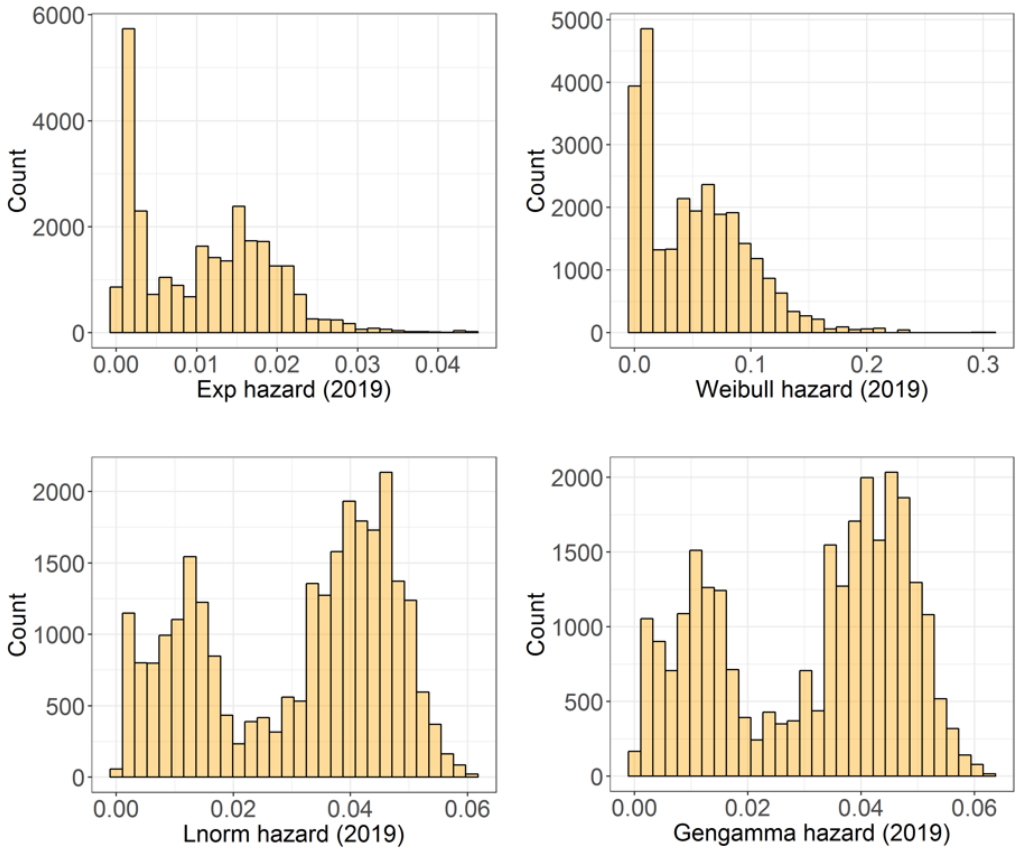

Figure app. -9 Hazard distribution of each parametric model in 2019

The benefit of parametric model is not to calculate the hazard ratio, the usage of these model is because the future status can be predicted. To compare the prediction, 4 panel are randomly selected and the hazard of each panel are shown by using 4 types of parametric model (as shown in Figure app.-10). Obviously, on one hand, the exponential and Weibull model is not good method to estimate our current data set. On the other hand, the model log-normal and generalized gamma distribution gives same result, also confirmed the credibility of the two methods.

Also, by using the regression coefficient of each variate, the variable can be set to any number and the survival probability can be compared. Figure app.-11 shows the survival probability under different traffic volume and slab thickness. This can be applied in the bridge slab designing.

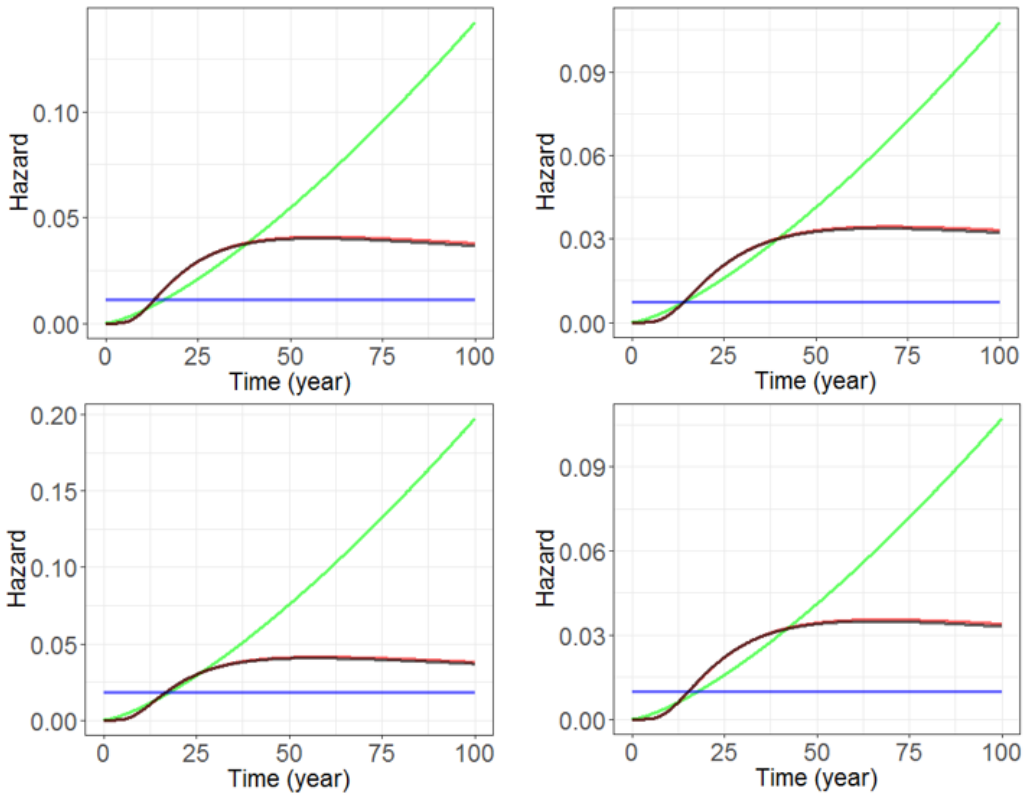

Figure app. -10 Hazard of 4 example panels

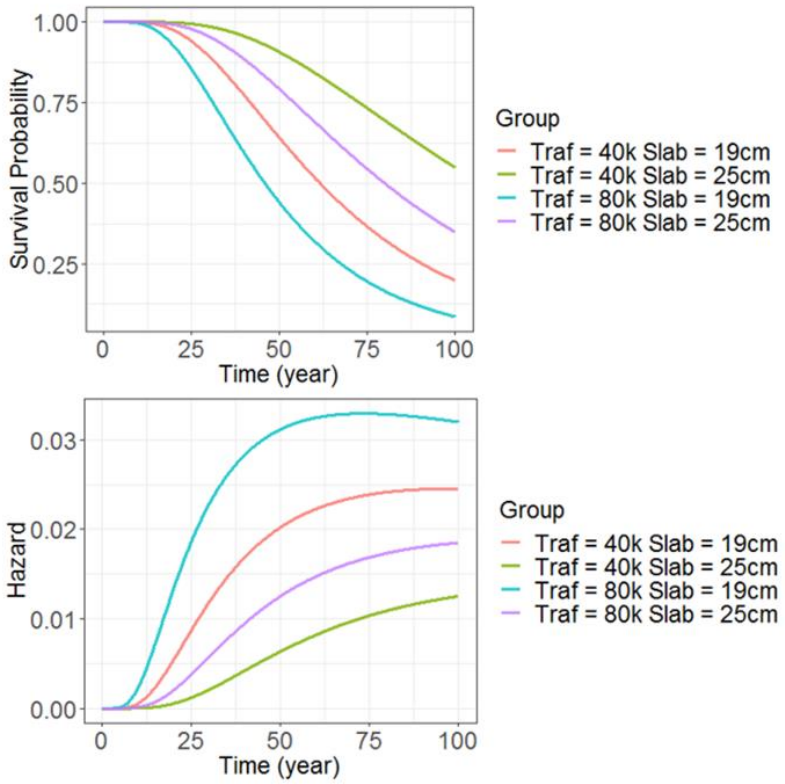

Figure app. -11 Survival probability and hazard under different traffic volume and slab thickness

Reference

1 Zhang, Z. (2016). Parametric regression model for survival data: Weibull regression model as an example. *Annals of translational medicine*, *4*(24).

2 Bain L and Engelhardt M 2000 Introduction to Probability and Mathematical Statistics (California: Duxbury Press An Imprint of Wadsworth Publishing Company)

3 Kurniasari, D., Widyarini, R., & Antonio, Y. (2019, October). Characteristics of Hazard Rate Functions of Log-Normal Distributions. In *Journal of Physics: Conference Series* (Vol. 1338, No. 1, p. 012036). IOP Publishing.

4 Akaike, H. (1998). Information theory and an extension of the maximum likelihood principle. In *Selected papers of hirotugu akaike* (pp. 199-213). Springer, New York, NY.

5 Ishiguro, M., Sakamoto, Y., & Kitagawa, G. (1997). Bootstrapping log likelihood and EIC, an extension of AIC. *Annals of the institute of Statistical Mathematics*, *49*(3), 411-434.